THE NIDOGEN-DOMAIN PROTEIN DEX-1 IS NECESSARY FOR THE *CAENORHABDITIS ELEGANS* DAUER MORPHOLOGY AND BEHAVIOR

BY

KRISTEN M FLATT

DISSERTATION

Submitted in partial fulfillment of the requirements
for the degree of Doctor of Philosophy in Neuroscience
in the Graduate College of the
University of Illinois at Urbana-Champaign, 2019

Urbana, Illinois

Doctoral Committee:

Associate Professor Nathan Schroeder, Chair and Director of Research
Professor Janice Juraska
Professor William Brieher
Assistant Professor Adrés Vidal-Gadea, Illinois State University

ABSTRACT

The ability to modify a given phenotype to adapt to the external environment (i.e. phenotypic plasticity) is a critical component of an organism's ability to survive unfavorable conditions. The free-living nematode, *Caenorhabditis elegans* is an excellent example of phenotypic plasticity. When exposed to unfavorable conditions, *C. elegans* halts reproductive development and enters an alternative developmental stage called dauer. Dauer larvae undergo extensive tissue remodeling, including changes to the outer cuticle, muscle, and nervous system. Although several morphological and behavioral traits of the dauer larvae have been described, the molecular mechanisms underlying dauer-specific tissue remodeling have remained poorly understood. This work provides evidence that the nidogen domain-containing protein DEX-1 facilitates the stage-specific tissue remodeling observed during dauer morphogenesis. DEX-1 was previously shown to function as a secreted extracellular matrix protein that regulates sensory dendrite formation during embryogenesis. However, we found an alternative developmental role for DEX-1. Specifically, we show that DEX-1 is also required for remodeling of the stem-cell like hypodermal seam cells and formation of the cuticular lateral alae. Further, we found that DEX-1 is necessary for proper dauer mobility, and may function as a component of the neuromuscular system to facilitate dauer locomotion behaviors. We show that *dex-1* is secreted from the seam cells, but functions locally in a cell-autonomous manner to facilitate dauer morphogenesis. *dex-1* expression during dauer is also regulated through DAF-16/FOXO-mediated transcriptional activation. Finally, we show that *dex-1* genetically interacts with a family of zona pellucida-domain genes to regulate seam cell remodeling and alae formation.

Taken together, this work shows that DEX-1 is an extracellular matrix component that plays a critical role in *C. elegans* tissue plasticity during dauer formation.

ACKNOWLEDGEMENTS

First and foremost, I would like to acknowledge and thank my advisor and mentor, Dr. Nathan Schroeder, for his guidance and support throughout my graduate school journey. Without the initial encouragement from Dr. Schroeder to pursue my PhD, I may have never begun, and without his unending encouragement throughout, I may have never finished. I am grateful for all of the lessons, constructive criticisms and feedback I have received (whether it seemed like it at the time, or not... I can now say that I am indeed grateful). I remember the day I became Dr. Schroeder's founding lab member. I had never worked with *C. elegans* before, and really had very little experience working in a lab, at all. Dr. Schroeder took a chance on me that day, and through years of constantly challenging me to do better, encouraging me to think critically and independently, and teaching me to persevere despite setbacks, he has taken me from an inexperienced lab technician to a Doctor of Philosophy in Neuroscience. So, thank you, Dr. Schroeder, for taking that chance and believing in me. You have helped me become the scientist and person that I am today, and I am forever grateful to have had the opportunity to work with you.

I would also like to thank my committee members, Dr. Janice Juraska, Dr. William Brieher, Dr. Tahir Saif and Dr. Andrés Vidal-Gadea for their support and advice throughout my project. Thank you all for taking the time to learn about worm biology with me. I truly appreciate all of the guidance and helpful conversations we have shared over the course of this project.

I would also like to acknowledge Scott Robinson at the Beckman Institute for being a wealth of (both useful and useless) information and for always supporting and encouraging my interest in electron microscopy. Knowing and working alongside you has truly been a highlight of my graduate career.

To all of my lab mates, both current and former, I would also like to recognize you all for your invaluable support and friendship. To name a few, Janet Wood, Stephanie Boas, Jayna Patel, and Ziduan (Paul) Han – thank you all so much for being you. Each of you have touched my life in your own unique way, and I am forever grateful to have met you. I would like to thank Becky Androwski, in particular, for being a great lab mate and becoming one of my closest friends. Thank you for listening to all of my feelings –be it over my wins or losses - and encouraging me to always work hard and move forward. Your friendship has made my grad school experience more enjoyable and honestly, kept me sane. I'm glad we were in this together.

I would also like to shout out my immense gratitude to my family, who have given me unconditional love and support in all ways imaginable throughout my graduate school journey. To my mom and dad, Michele Rolla and Derek Flatt, I cannot put into words how grateful I am for your love and support. You have both always encouraged me to pursue my dreams and have supported me, despite your reservations, throughout my PhD. To my step-parents, Jason Rolla and Melinda Flatt, thank you both as well for being my support system, even when you didn't have to be. You have all come together to support me and I couldn't have done any of this without you.

To my grandparents, Karen and Frankie Chamness, you two have been my rock. Thank you for constantly encouraging me and reminding me that I am capable of

anything. I cannot express in words how much I love and appreciate you. I absolutely would not be the person that I am today without you. Thank you for everything you have done and continue to do for me.

To my great-grandpa, Marcel Chamness, even though you aren't here to see me graduate, you always told me this day would come. I remember even as a little girl, you always told me I could achieve anything I wanted in life - that I was smart and capable and that I would be something great. I have always remembered your words of encouragement and held them close to my heart. Even though you won't be here in person, I know you are here in spirit, and I know you are proud. I love you always.

Finally, I would like to thank my boys, Brian and Aiden. Over the last several years, Brian has stood by my side and supported me through this journey. He has been there through every challenge I've faced, and continuously reminded me that failure is not always the end of the world, even when it feels like it. Brian, I cannot thank you enough for your unconditional love and support, for your kindness and understanding, and your ability to tolerate me in any phase or mood. Thank you for always, always, always making me laugh, even when I'm in a not-so-laughy mood. Thank you for challenging me to always push myself, and not let my anxiety and self-doubt get in the way of my goals. Thank you for being there for me, day-in and day-out, to tell me how awesome I am, and reminding me to be nice to myself. You have been my biggest cheerleader and I'm so happy and grateful to have you.

Aiden Douglas – you are my reason for everything I do. Since the day you were born, you have given me a sense of purpose in life, and you motivate me to be a better person every single day. You remind me daily, even when I feel like I have the world on

my shoulders, to stop and enjoy simple things – like funny YouTube videos and ice cream sandwiches. You have made me happier than I ever thought I could possibly be, just by being who you are. I am so fortunate to be your mom. Thank you for dealing with my crazy schedule, and for being understanding and forgiving when I sometimes had to work instead of playing Xbox (even though Xbox sounded way more fun). Everything I do, and everything I will do, will always be for you. I hope that one day I can play a small part of the role for you that you have played for me. I hope that my journey can motivate you to pursue your dreams, and never let anything or anyone stop you from becoming the amazing person I know you will be. I love you more than words can say, sweet boy.

To Aiden, my inspiration.

TABLE OF CONTENTS

CHAPTER 1: INTRODUCTION

This chapter has been adapted, in part, from Androwski *et al.* 2017.

1.1 OVERVIEW

Phenotypic plasticity, or the ability of an organism to modify its phenotype in response to environmental inputs, is a critical component of the organism's ability to survive in an ever-changing and often stressful environment. Many stress-induced phenotypic changes present as developmental and behavioral adaptations. For example, during seasonally induced hibernation periods, ground squirrels experience reversible, temperature-dependent changes in neuronal density of the hippocampus (Popov *et al.* 1992). Likewise, desert locusts alter their morphology between distinct 'gregarious' and 'solitarious' phases in response to changes in population density (Pener and Simpson 2009). While these examples of environmentally-induced adaptations prove to be evolutionarily beneficial for survival, inappropriate stress-induced plasticity may foster pathological consequences.

Unremitting stress is an unfortunate norm of society. Indeed, a 2018 survey by the American Psychological Associate revealed that nearly 75% of participating adults reported at least one symptom of stress in the previous month, with 45% reporting daily stressors impacting sleep quality (American Psychological Association 2018). In mammals, chronic stress can contribute to several physical and mental disorders including post-traumatic stress disorder, which is marked by a decrease in neuronal volume and loss of neuronal integrity of the hippocampus (Bremner *et al.* 1995; Lee *et al.* 2009). Likewise, chronic stress can also contribute to instances of heart disease,

which is the leading cause of death in the United States (Dimsdale 2008; Murphy *et al.* 2015). My thesis work uses the stress-resistant dauer stage of the free-living nematode, *Caenorhabditis elegans (C. elegans)* as a model system to investigate the molecular mechanisms that underlie stress-induced phenotypic plasticity and tissue remodeling.

1.2 THE *C. ELEGANS* DAUER STAGE AS A MODEL FOR PHENOTYPIC PLASTICITY

The free-living nematode *Caenorhabditis elegans* is an outstanding model in which to study developmental genetics and phenotypic plasticity. *C. elegans* is easily reared on *Escherichia coli* and can complete several generation cycles in a matter of weeks (Brenner 1974). *C. elegans* exists most commonly as populations of self-fertilizing hermaphrodites, which allows for maintenance of stable genetic lines. Male animals are also present at low percentages, and allow for genetic crosses. *C. elegans* is transparent, and the entire cell lineage, from single cell to reproductive adult, has been completely mapped (Sulston and Horvitz 1977; Sulston *et al.* 1983). Further, the complete connectome of the 302 neurons in the adult hermaphrodite is described, allowing investigations into the neuroanatomical basis of behaviors at the level of a single cell (White *et al.* 1986). *C. elegans* is also amenable to several genetic techniques including transformation, RNAi, and genome editing (Mello *et al.* 1991; Fire *et al.* 1998; Dickinson and Goldstein 2016).

Perhaps one of the most notable characteristics of *C. elegans* is its ability to alter its developmental pathway based on environmental inputs. In the presence of plentiful food and a low population density, *C. elegans* develops through four larval stages

before entering the reproductively active adult stage. However, under adverse environmental conditions, *C. elegans* can halt reproductive development and enter into a long-lived, stress-resistant developmental stage called dauer (Cassada and Russell 1975; Klass and Hirsh 1976; Golden and Riddle 1984)

1.3 THE DAUER FORMATION DECISION

The dauer formation decision and dauer tissue morphogenesis have been shown to be two completely separate processes (Liu and Ambros 1989). The decision to enter dauer is based on the ratio of population density to food availability, and modulated by temperature (Riddle *et al.* 1981; Golden and Riddle 1984; Vowels and Thomas 1992; Gottlieb and Ruvkun 1994; Gerisch *et al.* 2001; Jia *et al.* 2004). The amphids are the primary sensory organs in *C. elegans* and are comprised of 12 pairs of ciliated sensory neurons, 8 of which are directly exposed to the external environment (Perkins *et al.* 1986). Similar to sensory neurons in vertebrates, the exposed endings of the amphid neurons are ciliated (Perkins *et al.* 1986; Falk *et al.* 2015). The specific amphid neurons, ASI, ADF, and ASG are critical for regulating dauer formation by promoting reproductive development and inhibiting dauer formation (Bargmann and Horvitz 1991; Ouellet *et al.* 2008; Kim *et al.* 2009). In contrast, the amphid neurons ASK and ASJ promote dauer entry and regulate recovery from dauer (Bargmann and Horvitz 1991; Schackwitz *et al.* 1996). Investigation into the signaling pathways involved in the molecular translation of dauer-inducing environmental signals into the dauer formation decision has revealed a complex web of interactions between four distinct, yet evolutionarily conserved signal

cascades. These pathways include the TGFβ-like pathway, the insulin-like pathway, the guanylyl cyclase pathway, and the steroid hormone pathway.

The TGFβ-like pathway. The TGFβ, or Transforming Growth Factor-β, superfamily is a group of well-conserved, multifunctional cytokines that serve as a means for cell-to-cell communication in eukaryotes. Additionally, TGFβ proteins are responsible for driving several biological processes including cell proliferation, differentiation, and maintenance of cell identities (De Robertis 2008; Wu and Hill 2009). In humans, deregulation of TGFβ signaling can lead to several deleterious diseases including fetal malformations, infertility, and polycystic ovary syndrome (Josso *et al.* 2006; Lehmann *et al.* 2006, 2007; Wang *et al.* 2007). While humans have roughly 30 TGFβ members, *C. elegans* has only 5. However, the signaling pathways related to each are extremely well-conserved at the molecular and functional level. The *C. elegans* TFGβ protein responsible for modulating dauer formation, DAF-7, is homologous to human GDF11 which has been reported to play a role in the pathophysiology of aging, though this has recently come under debate (Katsimpardi *et al.* 2014; Sinha *et al.* 2014; Egerman *et al.* 2015; Smith *et al.* 2015).

C. elegans DAF-7/TGFβ is produced exclusively in the ASI amphid sensory neurons in the head (Schackwitz *et al.* 1996; Ren *et al.* 1996). The ASI sensory neurons function to modulate the dauer formation decision by sensing food availability, pheromone concentration and temperature (White and Jorgensen 2012). Although DAF-7/TGFβ is expressed solely in the ASI neurons, its downstream receptors and transcription factors are expressed in several tissues providing a means of coupling environmental signals with widespread regulation of several tissues (Patterson *et al.*

1997; Inoue and Thomas 2000; Gunther *et al.* 2000; da Graca *et al.* 2004). When food is plentiful and population density low, secreted DAF-7/TGFβ activates DAF-1/4 receptor kinases which are thought to phosphorylate downstream SMAD proteins resulting in their nuclear activation. In *C. elegans,* the activated SMADs, DAF-8 and DAF-14, antagonize a nuclear DAF-5/SNO-SKI complex, which in turn, promote energy metabolism and reproductive development (Estevez *et al.* 1993; Patterson *et al.* 1997; Inoue and Thomas 2000; Fielenbach and Antebi 2008). In contrast, during unfavorable conditions, the absence of DAF-7/TGFβ signaling from the ASI neurons allows the nuclear DAF-3/DAF-5 (SMAD/SNO-SKI) complex to promote dauer entry and negatively regulate energy consumption (Greer *et al.* 2008; Fielenbach and Antebi 2008).

The insulin-like pathway. Insulin signaling has been shown to play a role in longevity in several organisms, including *C. elegans, Drosophila*, and mice (Clancy *et al.* 2001; Tatar *et al.* 2001; Holzenberger *et al.* 2003; Baba *et al.* 2005). In humans, insulin deregulation is a key factor in the development of age-related disease, including cancer and diabetes (Saltiel and Kahn 2001; Osaki *et al.* 2004). Interestingly, recent studies have shown that the positive effects of insulin signaling on longevity may hold true for humans, as well (Couet *et al.* 1992; Facchini *et al.* 2001; Akintola and van Heemst 2015). Thus, the molecular and functional components of insulin signaling are fundamental in the process of aging and longevity, and studies have shown the molecular mechanisms to be highly conserved throughout evolution.

In *C. elegans,* the output of the DAF-7/TGFβ pathway is integrated with insulin signaling in the regulation of dauer formation. Similar to TGFβ secretion in the TGFβ-

like pathway, ample food supply promotes the release of the insulin-like protein, DAF-28, from the ASI and ASJ amphid sensory neurons. DAF-28 secretion acts to inhibit dauer arrest by activating the insulin receptor-like protein, DAF-2. Binding of DAF-28 to the DAF-2 receptor inhibits dauer formation through activation of a phosphoinositide 3-kinase (PI3K), and downstream PDK-1, AKT-1 and AKT-2 kinases (Morris *et al.* 1996; Kimura *et al.* 1997; Paradis and Ruvkun 1998; Paradis *et al.* 1999). Activation of AKT-1 leads to phosphorylation of the FOXO transcription factor DAF-16, inhibiting its function by sequestration to the cytoplasm and ubiquitin mediated degradation (Lin *et al.* 1997, 2001; Ogg *et al.* 1997; Lee *et al.* 2001; Hertweck *et al.* 2004; Li *et al.* 2007). Consequently, in favorable conditions animals undergo reproductive development. In contrast, low food supply and high pheromone concentration transcriptionally inhibit DAF-28/insulin-like protein production and allow DAF-16 to be translocated into the nucleus where it activates several genes important for stress-resistance and dauer formation.

Interestingly, recent work has suggested that the location and timing of insulin-like signaling influences the decision to promote longevity or reproductive arrest. While many studies of DAF-2 suggest that it functions in the nervous system to regulate both longevity and dauer arrest, the tissue in which DAF-16 functions may influence its downstream affects (Apfeld and Kenyon 1998; Wolkow *et al.* 2000). For instance, while DAF-16 in the nervous system appears to largely influence dauer formation, DAF-16 in the intestine primarily regulates lifespan (Libina *et al.* 2003). Further, promotion of dauer arrest via interrupted insulin-like signaling during early larval stages does not influence

the longevity of older adult animals, suggesting that the timing of DAF-16 activity is also an important factor in regulating the phenotypic consequences of insulin-like signaling.

The guanylyl cyclase pathway. The less-well known guanylyl cyclase pathway is suspected to function upstream of both the TGFβ and insulin-like signaling in the exposed ciliated endings of the amphid sensory neurons (Vowels and Thomas 1992; Thomas *et al.* 1993; Birnby *et al.* 2000; Murakami *et al.* 2001). The *daf-11* gene in *C. elegans* encodes a transmembrane guanylyl cyclase that is expressed in the ASI, ASJ and ASK amphid sensory neurons to regulate dauer formation, along with several other sensory neurons where it is involved in olfactory sensations (Schackwitz *et al.* 1996; Ren *et al.* 1996; Birnby *et al.* 2000; Li *et al.* 2003). In animals with defects in *daf-11* expression, DAF-7/TGFβ and DAF-28/insulin-like protein production in the ASI amphid neurons is significantly reduced. Interestingly, this defect in secretion can be rescued by expression of *daf-11* solely in the ASI neurons, indicating that the guanylyl cyclase pathway indeed functions upstream of the DAF-7/TGFβ and DAF-28/insulin-like pathways to regulate dauer formation (Murakami *et al.* 2001; Li *et al.* 2003). Interestingly, recent studies have also suggested a role for DAF-11 in DAF-16/FOXO mediated longevity of non-dauer adults, further intertwining DAF-11 function with the downstream DAF-2/insulin-like signaling pathway (Li *et al.* 2003; Hahm *et al.* 2009).

The steroid hormone pathway. The steroid hormone pathway functions downstream of the other three dauer formation pathways and serves to integrate their downstream effects (Riddle *et al.* 1981; Albert and Riddle 1988; Thomas *et al.* 1993; Gerisch *et al.* 2001, 2004). Indeed, promotion of DAF-7/TGFβ and DAF-28/insulin production results in the downstream synthesis of a steroid hormone called dafachronic acid by the cytochrome P450 protein DAF-9. Dafachronic acid binds to the downstream nuclear hormone receptor DAF-12*,* inhibiting dauer arrest and promoting reproductive development (Gerisch *et al.* 2001). When DAF-12 is not bound by its dafachronic acid ligand, it is bound by a DIN-1/SHARP complex. The binding of DAF-12 by DIN-1/SHARP represses DAF-12 dependent transcriptional activation thereby promoting dauer formation (Ludewig *et al.* 2004).

1.4 DAUER MORPHOLOGY AND BEHAVIOR

Dauers are specialized, non-feeding larvae capable of withstanding extended periods of adverse environmental conditions. Dauer-specific stress resistance is likely facilitated by several morphological changes that occur during dauer formation, including changes to cuticle, neurons and muscles (Cassada and Russell 1975; Golden and Riddle 1984; White *et al.* 1986). For example, dauers are thinner than the comparable non-dauer L3 stage larvae due to autophagy-mediated radial shrinkage of the animals' entire body (Meléndez *et al.* 2003). Interestingly, starvation conditions are also reported to trigger autophagy events in other eukaryotes, like mammals (Takagi *et al.* 2016). *C. elegans* larvae carrying mutations in the autophagy protein *bec-1*, an orthologue to mammalian Beclin1, fail to complete normal dauer development and have

fewer lipid stores, defects in radial constriction and lack dauer-specific SDS resistance. *bec-1* is expressed in remodeling tissues, including the hypodermis and pharynx, during dauer development (Meléndez *et al.* 2003). The autophagy-mediated radial shrinkage of the lateral seam facilitates formation of raised cuticular ridges called lateral alae. The dauer cuticle is also biochemically altered compared to that of non-dauer animals, adding to its resistant nature (Blaxter 1993). Indeed, one of the most common techniques for separating non-dauers from dauers is exposure to 1% sodium dodecyl sulfate (SDS) for 30 min (Cassada and Russell 1975). While non-dauers are killed within minutes at all tested concentrations of SDS, dauer larvae appear completely unaffected in up to 10% SDS (Flatt *et al.* 2019).

Behaviorally, dauer larvae suppress the pharyngeal pumping required for ingestion of bacterial food. While non-dauer animals live for roughly two weeks in the presence of plentiful food, *C. elegans* dauers can survive for months without feeding. In addition to the absence of feeding, dauers display additional behaviors that are unique to the dauer stage. On a Petri dish, non-dauers typically move continuously in search for food or mates. In contrast, dauers are frequently behaviorally quiescent, or immobile. Interestingly, dauers are sensitive to touch and move rapidly following physical stimulation (Cassada and Russell 1975). This dauer-specific locomotion behavior may be due to changes in neuromuscular structure during dauer (Dixon *et al.* 2008).

Perhaps the most noticeable among dauer-specific behaviors is ‘nictation’ wherein a dauer will climb elevated objects, raise its body into the air and stand on its tail. In addition to individual nictating dauers, they will occasionally form undulating swarms containing numerous dauers. Nictation is thought to serve as a dispersal

strategy; by elevating its body above the ground, *C. elegans* can reduce surface tension and increase the possibility it will be picked up by a passing arthropod. Both experimental data and the association of *C. elegans* dauers with arthropods in nature support this dispersal hypothesis (Félix and Braendle 2010; Lee *et al.* 2011). Previous work has shown that dauer-specific remodeling of sensory head neurons called the IL2s (Inner Labial 2) is necessary for initiation of nictation behavior (Lee *et al.* 2011; Schroeder *et al.* 2013). Taken together, these data provide evidence that stress-induced tissue remodeling during dauer formation is necessary for increased resistance against environmentally unfavorable conditions.

Changes to the cuticle. The cuticle, which is largely secreted by hypodermal cells, covers the outside of the animal and the lumen of the pharynx. It is composed of cross-linked collagenous and non-collagenous proteins that provide protection from the outside environment and facilitate locomotion. The cuticle comprises roughly 24% of the proteins synthesized during dauer as opposed to 9% in adult animals (Wolkow and Hall 2011). Extensive cross-linking, disulfide bond formation and increased hydrophobic amino acid content facilitate the decreased permeability of the dauer cuticle compared to other larval stages (Cassada and Russell 1975; Kramer 1997). Along with structural differences, the dauer cuticle is also biochemically distinct from non-dauers (Blaxter 1993). The surface coat, composed of negatively charged carbohydrates and heterodimeric protein complexes, is found on the exterior of the epicuticle and is important for *C. elegans'* survival (Zuckerman *et al.* 1979; Blaxter 1993). Though surface coats can be found on all stages, disruption of surface coat proteins of dauer

larvae can be increasingly detrimental. For example, mutations in surface protein gene *srf-3* results in a loss of SDS resistance in dauer larvae (Politz *et al.* 1990). Likewise, mutations in *srf-4,-8* and *-9* were determined to be pleiotropic, as these mutant animals were observed to not only have defects in their cuticle surface, but also in cell migration patterns (Blaxter 1993).Thus, many different components are required to maintain the integrity of the cuticle. However, a deeper investigation into the specific proteins that comprise the dauer cuticle is necessary to determine the precise nature of its resistant characteristics.

During dauer formation, a dauer-specific cuticular plug forms around the lips of the animal that occludes the buccal cavity – preventing the animal from ingesting toxins or food. This flap of cuticle, called the cheilostom cuticle or “bridging cuticle” is a continuous projection that forms from the body wall cuticle (Albertson and Thomson 1976; Wright and Thomson 1981; Hall *et al.* 2005). The pharyngeal epithelium largely retains its overall morphology during dauer, however, appears thinner and shrunken (Wolkow and Hall 2011). Cuticle sheets also line the interior area of the buccal cavity during all stages, but appear to be more reinforced during dauer (Hall *et al.* 2005). Electron micrographs show that the dauer cuticle contains a thick, striated layer that, along with the buccal plug, assists in maintaining its impermeability (Popham and Webster 1979).

Along with changes in thickness and composition, the cuticle also undergoes structural changes during dauer formation. Down both sides of the dauer larvae run five ridges of raised cuticle called the ‘lateral alae’. These cuticular structures are not present in L2, L3 or L4 stages, but similar structures are found on L1 larvae and adults.

Similarly to dauer, the reduction in width of the lateral cuticle is responsible for the formation of alae in the L1 larvae, however only two cuticular ridges with a large protrusion in the middle are observed in L1 (Singh and Sulston 1978; Sapio *et al.* 2005). Adult alae have three small protrusions that are often used as a marker for seam cell differentiation. The seam cells are a set of oval-shaped epithelial cells that extend in a row from the head to the tail -adjacent to the alae. The seam cells are embedded in the syncytial hypodermis and are thus often referred to as the 'lateral hypodermal cells.' During development, the seam cells divide in a stem cell-like fashion, generating an anterior daughter cell that fuses with the *hyp7* hypodermis and a posterior daughter cell that will continue to divide until its terminal differentiation in late-L4 (Sulston and Horvitz 1977). During dauer formation, the seam cells undergo autophagy-mediated shrinkage (Meléndez *et al.* 2003). The loss of cell volume in the seam is speculated to physically pull the outer layer of cuticle in radially via crosslinking reactions mediated, in part, by non-collagenous extracellular matrix proteins called cuticlins (Sapio *et al.* 2005).

The cuticlins. Originally isolated from the parasitic nematode *Ascaris lumbricoides*, 'cuticlin' was the name given to the insoluble material left over from cuticles treated with reducing agents (Fujimoto and Kanaya 1973). Cuticlins (CUTs) in *C. elegans* show similar characteristics, like resistance to detergents, collagenases and reducing agents (Sebastiano *et al.* 1991). Though not all CUT proteins are related, some that are required for dauer cuticle morphology share a conserved zona pellucida domain (Muriel *et al.* 2003). Zona pellucida (ZP) domains have been conserved throughout evolution and are often found in extracellular matrices. ZP proteins contain homologous regions

of roughly 260 amino acid residues with 8 strictly conserved cysteine residues that are speculated to form disulfide bridges and function in binding reactions (Bork and Sander 1992). In *C. elegans*, three of these ZP-domain containing cuticlin proteins are of particular interest to the dauer cuticle integrity – CUT-1, CUT-5 and CUT-6. CUT-1 was the first cuticlin to be isolated in *C. elegans* and is required for lateral alae formation. This cuticlin was shown to be expressed solely during dauer and to localize in a ribbon-like pattern running the length of the animal underneath the alae (Sebastiano *et al.* 1991). Interestingly, *cut-3*, a larval-stage cuticlin that is required for L1 alae formation, can rescue the dauer-specific *cut-1* mutant phenotypes when expressed from the *cut-1* promoter (Sapio *et al.* 2005). *cut-5* is required for alae formation in both L1 and dauer larvae and is secreted by the seam cells, under the area where alae will form, solely during these stages (Sapio *et al.* 2005).

Although CUT-1, -3, and -5 share similar structure and expression patterns, their functions are not redundant, as CUT-5 is required for alae formation even in the presence of CUT-1 or CUT-3 (Sapio *et al.* 2005). CUT-6 is involved in the determination of dauer body shape, but is not strictly required for alae formation (Muriel *et al.* 2003; Sapio *et al.* 2005). CUT-6 is expressed in the hypodermis during L1 and dauer cuticle development and localizes to the boundary between the hypodermis and lateral seam. Interestingly, RNAi knockdown of CUT-6 causes defects in lateral alae formation in dauers, but not in L1 larvae (Muriel *et al.* 2003). Though the effects of these proteins on the lateral alae vary, mutations in *cut-1*, *-5* and *-6* all result in a ‘dumpy’ dauer phenotype characterized by an enlarged body due to defects in radial constriction (Muriel *et al.* 2003; Sapio *et al.* 2005). Mutations in these cuticlin genes also affect the

permeability of the resulting dauer cuticles. Animals with mutations in *cut-1*, *cut-5* and *cut-6* all show sensitivity to SDS (sodium dodecyl sulfate) when compared to wild-type dauers (Flatt *et al.* 2019). However, radial shrinkage and lateral alae formation are not sufficient for SDS resistance, as animals containing mutations in *daf-13*, an uncloned "process" gene, form visually wild-type dauers that are sensitive to standard SDS treatments (Riddle *et al.* 1981).

Changes to the nervous system. Widespread and dramatic morphological changes occur throughout the nervous system during dauer that may mediate behavioral changes. The amphid sensory neurons are bilaterally symmetric, and eight of the twelve amphid neurons on each side extend ciliated dendrites to the tip of the nose, where they are open to the environment during both dauer and non-dauer stages (Albert and Riddle 1983). Interestingly, dauer larvae secrete an electron-dense material that is suspected to clog the amphid pores and protect the animals from desiccation (Albert and Riddle 1983). In non-dauer animals, the ASG and ASI neurons, which both function to inhibit dauer formation, send ciliated processes that protrude from the amphid channel opening, allowing for sensation of environmental signals. However, during dauer, the ciliated tips are displaced posteriorly and are effectively missing from the amphid bundle (Albert and Riddle 1983). This retraction of the sensory tips of the ASI neurons may be related to their functional inactivation during dauer arrest (Schackwitz *et al.* 1996).

The AFD amphid neurons have historically been known for temperature sensation, however recent work has uncovered a novel function for the AFDs in sensing magnetic orientation (Mori and Ohshima 1995; Vidal-Gadea *et al.* 2015; Bainbridge *et*

al. 2016). The sensory ending of the AFD neuron consists of several finger-like microvilli embedded in glial cells (Albert and Riddle 1983; Perkins *et al.* 1986; Doroquez *et al.* 2014), and dauer larvae contain approximately twice as many AFD microvilli as non-dauers (Albert and Riddle 1983). Interestingly, a mixture of starved non-dauers and dauers showed an opposite response to thermal gradients as well-fed non-dauers (Hedgecock and Russell 1975). That is, when well-fed animals were exposed to temperature gradients, they typically migrated to their eccritic temperature. However, when starved animals were exposed to a temperature gradient, they were observed to migrate away from the eccritic temperature (Mori and Ohshima 1995). Interestingly, similar switching of migration patterns were also observed in magnetotaxis experiments, with well-fed animals migrating 'up' and starved animals migrating 'down' (Vidal-Gadea *et al.* 2015). Though the exact function of the dauer-specific microvilli is not known, they may serve to more closely detect subtle changes in temperature, as temperature is a critical modulator of dauer formation and maintenance (Ailion and Thomas 2000). However, it is not known if ultrastructural changes to AFD during dauer mediate the observed changes in dauer behavior.

Separate from the amphids, the six inner-labial sensilla, two dorsal, two ventral and two lateral, each contain two ciliated neurons – the IL1 and IL2 neurons. During non-dauer development, the IL2 neurons each have a single, unbranched dendrite that extends from the cell-body to the tip of the nose, where it is exposed to the external environment, and unbranched axons that extend into the nerve ring (Ward *et al.* 1975; Albert and Riddle 1983; Schroeder *et al.* 2013). The IL1 neurons also extend single, unbranched processes to the nose, however the cilia of the IL1s terminate in the sub-

cuticle and are not exposed to the external environment (Ward *et al.* 1975). When animals are stimulated to enter dauer, the four dorsal and ventral IL2 dendrites undergo extensive dendritic arborization and increase their total dendritic length threefold (Schroeder *et al.* 2013). Interestingly, although the two lateral IL2 neurons do not branch as extensively as their quadrant counterparts, they do branch once at the distal end of the dendrite. Here, the lateral IL2 dendrites wrap around the nose and form a "crown-like" structure (Schroeder *et al.* 2013). The axons of the IL2 neurons also thicken and branch, and appear to change morphology during dauer, though it is not known whether this translates to changes in synaptic partners. In addition to dendritic remodeling, electron micrographs also show that the positions of the IL1 and IL2 sensory endings are reversed, with the cilia of the IL1s being more anterior, though still not exposed (Albert and Riddle 1983). Indeed, electron micrographs demonstrate that the IL2 cilia are approximately two-thirds shorter during dauer arrest. Ablation of the IL2 neurons results in a significant reduction in dauer-specific nictation behavior (Lee *et al.* 2011). Likewise, animals with defects in dauer-specific IL2 arborization also show decreased nictation (Schroeder *et al.* 2013). This suggests that remodeling of the IL2 neurons during dauer is necessary for initiation of dauer-specific nictation behaviors. However, how the arborization of the IL2 neurons functions to regulate nictation behavior remains to be determined.

The deirid sensory neurons are bilaterally paired, dopaminergic cells that are presumed to be involved in mechanical texture sensation (Sawin *et al.* 2000; Hills *et al.* 2004). There are anterior deirids (ADE) that are located approximated 80μm posterior of the nose, and the posterior deirids (PDE) that are located in the posterior body near the

tail, both on the ventral-lateral sides. Both the ADE and PDE neurons have ciliated sensory ending that are embedded in the lateral cuticle (Ward *et al.* 1975; Perkins *et al.* 1986). In addition, the deirids each have a socket cell and a sheath cell that function as glial cells. The ciliated ending of the ADE contains extends to the body wall cuticle and contains an electron-dense material which has also been observed in several other mechanosensory neurons (Perkins *et al.* 1986). During non-dauer stages, the ciliated tip of the ADE is oriented tangentially to the body wall cuticle and held in place by an electron dense extracellular structure called the nubbin (Wolkow and Hall 2011). During dauer, the ADE ending are substantially enlarged with a much larger region of electron-dense material than in non-dauers (Albert and Riddle 1983). Additionally, the ciliated endings of the ADE neurons are oriented parallel to the lateral alae. Interestingly, during dauer, the ADE socket cell remodels to form a cuticular 'truss-like' structure that holds the endings in place against the cuticle (Albert and Riddle 1983; Cinar and Chisholm 2004). Though the exact function of the remodeled dauer ADEs is not known, it has been proposed that the enhanced cuticle structure surrounding the enlarged sensory endings may improve touch sensitivity through the thickened dauer cuticle (Wolkow and Hall 2011).

Changes to muscle. Due to the shrinkage of several other tissues during the dauer stage, the muscles of the *C. elegans* dauer appear to occupy a much larger fraction of the body. The sarcomeres of the dauer muscles appear larger than in non-dauer animals, with a substantial increase in myofilaments (Wolkow and Hall 2013). This robust nature of the dauer myofilament lattice suggests that the strength of muscle

contraction in dauer animals may be up to 200% more powerful than that of non-dauer animals, which may contribute to the rapid locomotion behaviors observed in dauer animals following mechanical stimulation (Cassada and Russell 1975)).

Dauer muscles also display changes in mitochondrial ultrastructure (Popham and Webster 1979). Dauer mitochondria are enlarged and electron dense compared to non-dauer mitochondria. This supports the speculation that dauer mitochondria may exist in a condensed conformation which promotes oxidative phosphorylation and reduced respiratory rates (Hackenbrock *et al.* 1971; Popham and Webster 1979). Increased ATP production of the condensed dauer mitochondria may function to supply additional, rapid bursts of energy which may promote rapid dauer locomotion, compared to the steady state locomotion observed in non-dauer animals (Wolkow and Hall 2013).

In *C. elegans*, neuromuscular junctions form between muscle cells and motor neurons via extensions of muscle tissue called muscle arms (Dixon and Roy 2005). During non-dauer development, body wall muscles extend a stereotypic number of muscle arms to the nearest nerve cord during early larval stages. However, when animals are stimulated to enter dauer, the muscle cells extend additional, dauer-specific muscle arms to their respective nerve cords (Dixon *et al.* 2008). Interestingly, formation of the dauer-specific muscle arms appears to be regulated, at least in part, by the DAF-2/insulin-like signaling pathway, as *daf-2* mutant animals also show an increase in the number of muscle arms during non-dauer stages (Dixon *et al.* 2008). While the number of muscle arms increases during dauer, it is not known whether this remodeling impacts the number of neuromuscular junctions. One possible function for muscle remodeling is the promotion of dauer-specific behaviors such as rapid locomotion or nictation. During

movement on a flat, two-dimensional surface, *C. elegans* moves through a coordinated contraction and relaxation of body wall muscles to produce a sinusoidal movement. The standing behavior seen during dauer nictation may require coordination of muscles to allow for simultaneous contraction.

1.5 DEX-1 PLAYS DIVERSE ROLES DURING EMBRYOGENESIS.

The extracellular matrix (ECM) is a non-cellular component present within all tissues and organs. The ECM is important for developmental processes, as it provides cells with a physical scaffold for migration, morphogenesis, cell homeostasis and even differentiation. Although the fundamental components of the ECM are the same, each individual tissue within an organism has a unique composition that is generated throughout different stages of development, making the ECM both a static and dynamic structure. Zona pellucida (ZP) proteins are a common component of extracellular matrices throughout the animal kingdom. For example, the founding members of the zona pellucida protein family, ZP1, ZP2, and ZP3, are found in the egg coat of mammalian oocytes and are the functional component to which the zonadhesin coat of the sperm bind (Wassarman 1987; Hardy and Garbers 1995; Hinsch and Hinsch 1999). Other mammalian ZP proteins are found in the vascular lumen, kidney tubules and the tectorial membrane of the inner ear (Legan *et al.* 1997; ten Dijke *et al.* 2008; Zaucke *et al.* 2010; Yan *et al.* 2012). *C. elegans* also has extracellular matrices associated with its various cell types. Similar to ECM function in mammals, the ECM of *C. elegans* provides a scaffold for cells to develop their appropriate shapes which can critically influence their function. Interestingly, previous work has shown that the ECM protein,

DEX-1, is necessary for the proper morphology of sensory dendrites during embryogenesis (Heiman and Shaham 2009). DEX-1 shares domain homology with mammalian tectorin proteins that anchor stereocilia in the inner ear, and are required for hearing. Additionally, DEX-1 shares domain composition with human SNED1 (Sushi, nidogen and EGF domain protein 1), which has been implicated in breast cancer metastasis (Naba *et al.* 2014; Flatt *et al.* 2019). Further, recent work also indicates a role for DEX-1 in multiple embryonic apical extracellular matrices to shape the developing epithelium (Cohen *et al.* 2019).

DEX-1 is necessary for sensory dendrite morphology. In most developmental systems, neurite length is generally established via emergence of a growth cone the cell body and extending to its target position, pulling neuronal tissue that will eventually become a dendrite or axon, into existence (Wu and Cline 2003; Williams and Truman 2004). However, in *C. elegans* dendritic length of the amphid sensory neurons is established through a process called retrograde extension (Sulston *et al.* 1983; Nguyen *et al.* 1999; Heiman and Shaham 2009). In retrograde extension, the sensory endings of the dendrites are anchored to their target location and the cell body then migrates to its target location. The anchoring of dendritic tips during retrograde extension is dependent on the extracellular matrix protein, DEX-1 (Heiman and Shaham 2009). The *dex-1* gene encodes a single-pass transmembrane protein with two nidogen-like domains separated by an epidermal growth factor (EGF) – like domain, and a zonadhesin-like domain. Interestingly, nidogen is also a common component of ECM basement membranes, including neuronal basement membranes in *C. elegans* (Kim and Wadsworth 2000). In

an effort to understand how neuronal structure is modulated during embryonic development, Heiman and Shaham 2009 isolated the mutant strain *dex-1(ns42)* which truncates the protein at the *dex-1* zonadhesin domain. Their studies revealed that the dendritic tips of the amphid neurons of *dex-1(ns42)* mutants failed to remain anchored to their target location, and were instead dragged posteriorly with the cell body. Expression analysis determined that during embryogenesis *dex-1* is expressed in several non-neuronal tissues, suggesting that DEX-1 functions as a secreted protein to facilitate dendritic tip anchoring. Strikingly, it was also determined that DEX-1 mediated dendritic tip anchoring is dependent on interactions of DEX-1 with a ZP-domain ECM protein, DYF-7. Interestingly, fusion of the DEX-1 and DYF-7 proteins shares a similar domain homology to the mammalian α-tectorin protein (Heiman and Shaham 2009). In humans, tectorins form a matrix (the tectorial membrane) in the inner ear that functions to anchor stereocilia, and are required for hearing (Legan *et al.* 1997; Petit *et al.* 2001). Interestingly, a *dex-1;dyf-7* double mutant displayed a temperature-dependent synthetic lethal phenotype during early embryonic stages that was due to malformation of the excretory system, suggesting that *dex-1* can function with ZP-domain proteins in several tissues to facilitate formation of various systems (Heiman and Shaham 2009). These findings provide the first evidence of DEX-1 function as an extracellular matrix protein capable of interacting with ZP-domain proteins to facilitate developmental processes and tissue morphogenesis.

DEX-1 functions in embryonic apical extracellular matrices. In addition to the well-known stromal extracellular matrix, there exists the less well-known apical extracellular

matrices (aECMs). These aECMs line exposed epithelial surfaces, such as the stratum corneum on the outside of the skin (Feingold 2007), or the inside of tubes, such as the glycocalyx inside blood vessels (Reitsma *et al.* 2007). *C. elegans* contains several different types of aECMs. For example, most surfaces of the animals are lined by cuticle composed largely of collagen and ZP-domain cuticlin (CUT) proteins (Sebastiano *et al.* 1991; Muriel *et al.* 2003; Sapio *et al.* 2005; Page and Johnstone 2007). In contrast, the pharynx is lined by a different type of cuticle containing chitin (Zhang *et al.* 2005). During embryogenesis, the cuticles are not secreted until epidermal elongation and morphogenesis is completed, and epithelial tissue has developed a pre-cuticular matrix (Priess and Hirsh 1986). During this process, several non-CUT ZP-domain proteins play important roles in the shaping of the embryonic tissues (Kelley *et al.* 2015; Gill *et al.* 2016; Vuong-Brender *et al.* 2017).

A survey of aECM mutants with defects in excretory function identified a new allele of the previously described gene, *dex-1*. The newly isolated allele, *dex-1(cs201)* displays a much stronger phenotype than the previously isolated *dex-1(ns42)* allele, presumably through truncation of both nidogen-like domains (Cohen *et al.* 2019; Flatt *et al.* 2019). Investigation of this new allele showed that DEX-1 is required to shape several embryonic epithelial tissues, including pharynx, excretory system and epidermis. Indeed, *dex-1(cs201)* mutants display several phenotypes that phenocopy previously characterized ZP-protein mutants (Cohen *et al.* 2019; Flatt *et al.* 2019). For example, *dex-1(cs201)* mutants often arrest at the L1 larval stage due to an ingressed pharynx (Pin) phenotype. Pin mutations occlude the pharyngeal opening and prevent feeding, causing starvation. Interestingly, this defect was observed during early

embryonic development, similar to what is observed in ZP-domain *fbn-1* mutants, which also fail to maintain pharyngeal attachment during embryonic elongation (Kelley *et al.* 2015). Similar to some CUT mutants, *dex-1(cs201)* mutants also display defects in L1 body morphology and alae formation, suggesting a role for DEX-1 in maintaining structural integrity of the larval cuticle (Cohen *et al.* 2019). Embryonic expression analysis showed DEX-1 accumulation in the excretory duct and pore lumen, at the nose tip, and along the apical surface of the developing pharynx. All of these locations of *dex-1* expression coincide with regions rich in ZP-domain protein expression, consistent with previous reports that *dex-1* interacts with ZP-domain proteins to regulate tissue morphogenesis during early larval development (Heiman and Shaham 2009; Cohen *et al.* 2019).

CHAPTER 2: THE NIDOGEN-DOMAIN PROTEIN DEX-1 IS NECESSARY FOR DAUER-SPECIFIC CHARACTERISTICS

This chapter has been adapted, in part, from Flatt *et al.* 2019.

2.1 INTRODUCTION

To survive changing environments, organisms modify their phenotype (*i.e.* phenotypic plasticity). During periods of unfavorable environmental conditions, *C. elegans* halts reproductive development and enters the stress-resistant dauer stage. Dauer larvae differ from non-dauers in both morphology and behavior due to remodeling of several tissues making them an excellent model of phenotypic plasticity. Here, we examine the role of the tectorin-like adhesion protein, DEX-1 in dauer morphological development and show an alternative developmental role for DEX-1 in dauer formation and tissue morphology.

2.2 MATERIALS AND METHODS

Strains and plasmids. All strains were grown under standard conditions unless otherwise noted (Brenner 1974). The wild-type Bristol N2 strain and the following mutant strains were used: CHB27 *dex-1(ns42)* III, UP2571 *dex-1(cs201)* III; *csEx402 [dex-1p::dex-1a + unc-199p::gfp]*, CB1372 *daf-7(e1372)* III, DR129 *daf-2(e1370) unc-32(e189)* III. All mutant strains were backcrossed at least twice. *dex-1(cs201)* was generated using standard EMS mutagenesis protocols (Brenner 1974; Flibotte *et al.* 2010) and identified based on balancer mapping and whole genome sequencing (Cohen *et al.* 2019). *dex-1(ns42)* was a gift from Dr. Maxwell Heiman (Department of

Genetics, Harvard University, Boston, MA) (Heiman and Shaham 2009). The IL2 neurons were observed using JK2868 *qIs56[lag-2p::gfp]* V (Blelloch *et al.* 1999; Ouellet *et al.* 2008; Schroeder *et al.* 2013).

The plasmid pMH7 *dex-1p::dex-1* was a generous gift of Dr. Maxwell Heiman (Heiman and Shaham 2009). Additionally, translational reporter *dex-1p::sfgfp::dex-1* (pJC24) contains the 2.1 kb *dex-1* promoter and *dex-1* (isoform a) complementary (cDNA) from pMH7 (Cohen *et al.* 2019). *sfgfp* was inserted either at an internal endogenous BglII restriction site to generate a full-length fusion tagged upstream of the first nidogen domain, or inserted at the 3' end of a cDNA truncated before the transmembrane domain (Cohen *et al.* 2019). For a complete list of primers and plasmids, please see the Supplemental Table.

Animals containing extrachromosomal arrays were generated using standard microinjection techniques (Mello *et al.* 1991), and genotypes confirmed using PCR analysis and observation of co-injection markers. *dex-1(ns42)* animals were injected with 20 ng/ml of plasmid and 80 ng/ml of *unc-122p::gfp*, *unc-122p::rfp* or *sur-5::gfp* as the co-injection marker. *dex-1(cs201)* animals were injected with 30 ng/ml of pJC15 or pJC24 and 50 ng/ml of co-injection marker pHS4 (*lin-48p::mrfp*).

Domain schematics were constructed using the wormweb.org Exon-Intron Graphic Maker. Domain locations were determined using the Simple Modular Architecture Research Tool domain prediction software (Schultz *et al.* 1998). The additional low complexity area of DEX-1 with similarity to zonadhesin was assigned based on previous work (Heiman and Shaham 2009).

Dauer formation and recovery assays. Dauers were induced by one of two methods. For non-temperature-sensitive strains, we used plates containing crude dauer pheromone extracted by previously established procedures (Vowels and Thomas 1992; Schroeder and Flatt 2014). For temperature-sensitive strains with mutations in *daf-7(e1372)* or *daf-2(e1370)*, dauers were induced using the restrictive temperature of 25°C (Riddle *et al.* 1981).

For dauer formation and recovery assays, gravid hermaphrodites were incubated on EC_{90} pheromone plates (Schroeder and Flatt 2014) and allowed to lay eggs for 3-4 hours at 25ºC. Adult animals were removed from the plate and the eggs incubated at 25ºC for 72 hours. Dauer larvae were counted and divided by the total number of animals (dauer + non-dauer) on the plate. The plastic sides of plates were also checked for trapped dauers. To quantify dauer recovery, 10 dauers from each genotype were transferred to seeded NGM plates and allowed to recover at 22ºC. Animals were checked every 24 hours for recovery. Formation and recovery assays were performed in triplicate and results analyzed using an unpaired t-test in GraphPad Prism6 software.

Microscopy and rescue analysis. Unless otherwise specified, animals were mounted onto 4% agarose pads and immobilized with 0.1 or 0.01 M levamisole for dauers and non-dauer or partial dauers, respectively. In our hands, dauers frequently lay in a dorsal-ventral position following anesthesia. Therefore, to image the lateral side, dauers were immobilized by mounting on 4% agarose pads with Polybead Polystyrene 0.10 mm microspheres (Polysciences Inc., #00876) (Kim *et al.* 2013). A Zeiss AxioImager microscope equipped with DIC and fluorescence optics was used to collect images. For

radial constriction experiments, Z-stack images were taken and Z-projections were made using FIJI. Diameter measurements were taken near the center of the terminal pharyngeal bulb. Measurement data were analyzed using a one-way ANOVA with Bonferroni's multiple comparisons test using GraphPad Prism 6 software. The resulting Z-projections were used to measure body diameter. For seam cell area analysis, area was measured for V2pap, V2ppp, and V3pap and averaged to give one measurement per animal (Sulston and Horvitz 1977). Seam cell measurement data were analyzed by an unpaired t-test. For confocal microscopy of the IL2 neurons, dauers were mounted on 10% agarose pads and anesthetized with 0.1 or 0.01 M levamisole. Animals were imaged using a Zeiss LSM 880 confocal microscope.

For transmission electron microscopy of *dex-1* mutant and N2 animals, dauer larvae were induced using pheromone plates and processed for high-pressure freezing and freeze substitution modified from previously established methods (Hall *et al.* 2012; Manning and Richmond 2015). Using OP50 Escherichia coli as a substrate and 1% propylene phenoxetol in M9 buffer as an anesthetic, animals were loaded into a metal specimen carrier coated with 1-hexadecane and frozen in an HPM 010 high-pressure freezer. Freeze substitution was performed in an FS-8500 freeze substitution system using 2% OsO4 (Electron Microscopy Sciences), 0.1% uranyl acetate (Polysciences) in 2% H20, and 100% acetone. Samples were held at -90° for 110 hr, then warmed to -20° at the rate of 5° per hour (14 hr). Samples were then held at -20° for 16 hr, then warmed to 0° at the rate of 5° per hour (4 hr). Samples were washed three times in prechilled (0°) 100% acetone and incubated at 0° for 1 hr after the final wash. Samples were then warmed to room temperature and washed an additional two times with 100% acetone.

Samples were infiltrated with 1:1 Polybed812 (Polysciences) resin: acetone for 6 hr, 2:1 resin:acetone for 14 hr, and 100% resin for 72 hr. All infiltration steps were incubated on an orbital shaker at room temperature. Samples were then embedded in molds in 100% resin plus DMP-30 hardener (Polysciences) and baked at 60° for 48 hr, then 70 nm sections were cut with a diamond knife using a PowerTome PC ultramicrotome and collected onto formvar-coated copper slot grids. Samples were imaged with a Philips CM200 transmission electron microscope.

Fluorescent bead and pharyngeal pumping assays. Fluorescent bead assays were carried out using established methods (Nika *et al.* 2016). Fluorescent beads (L3280; Sigma) were added to a concentrated OP50 *E. coli* overnight culture. Fresh NGM plates were seeded with 65 ml of the bead/bacteria suspension and allowed to dry. Twenty nematodes were added to the plate and incubated at 20° for 40 min. Worms were observed for the presence of fluorescent beads in the intestinal tract. The experiment was performed twice. Pharyngeal pumping assays were modified from previous established methods (Keane and Avery 2003). *dex-1(ns42)* and wild-type dauers were transferred to seeded NGM plates and allowed to recover for 10 min. After recovery, each animal was scored individually for 2 min, and then removed from the plate. Data were analyzed by an unpaired t-test, using GraphPad Prism 6 software.

Sodium dodecyl sulfate sensitivity assays. Sodium dodecyl sulfate (SDS) dose-response assays were performed using 12-well culture dishes containing M9 buffer and specified concentrations of SDS. Dauers were exposed to SDS for 30 min and scored

as alive if movement was observed following stimulation with an eyelash. Each concentration was tested in triplicate with each experiment containing a separate wild-type (N2) control. Dose-response curves and LD_{50} values were determined by testing 20 dauers per treatment at each concentration, with three independent experiments. The LD_{50} and 95% confidence interval of each concentration was calculated using probit analysis in Minitab 18. LD_{50} values were considered significantly different if the 95% confidence intervals did not overlap. Significant difference was denoted with a single asterisk. Single concentration assays were conducted at 0.1% SDS with 20 dauers for each genotype and three independent experiments. Data were analyzed using a one proportion exact method analysis in Minitab 18 and considered significantly different if the 95% confidence intervals did not overlap. Significant difference was denoted with a single asterisk.

2.3 RESULTS

DEX-1 is required for proper dauer morphology. Wild-type *C. elegans* dauers have a distinctive morphology due to radial shrinkage that leads to a thin appearance compared with non-dauers (Figure 2.1, A and B). I found that *dex-1(ns42)* mutants produce dauers that are defective in radial shrinkage, leading to a “dumpy dauer” phenotype (Figures 2.1C and G, 2.2A). The defect in body size appears specific to the dauer stage, as comparable non-dauer *dex-1(ns42)* mutant L3s show no differences in body size compared with wild-type L3s (Figure 2.3). Radial shrinkage in dauers is correlated with the formation of longitudinal cuticular ridges on the lateral sides of the animal, called the alae (Cassada and Russell 1975). The lateral alae of *dex-1(ns24)*

mutant dauers are indistinct compared with wild-type dauers (Figure 2.1, A, C, E, and F). In addition to radial shrinkage, dauers have an ability to survive high concentrations of SDS (Cassada and Russell 1975; Androwski *et al.* 2017). Wild-type dauers survive for hours in 1% SDS (Cassada and Russell 1975). We found that while *dex-1* mutant dauers were able to survive significantly higher concentrations of SDS than wild-type non-dauer animals, they were sensitive to 1% SDS (Figure 2.2B).

The previously isolated *dex-1(ns42)* allele results in a premature stop codon in exon 9, encoding the predicted zonadhesin-like functional domain (Heiman and Shaham 2009)(Figure 2.2C). In an unrelated screen for mutants with embryonic and early larval lethality, we isolated *dex-1(cs201)*, which introduces a point mutation at the splice donor site of intron 4 (Figure 2.2C, Cohen *et al.* 2019). Analysis of *dex-1(cs201)* cDNA suggests this results in multiple transcripts with read through into intron 4, with all introducing a new stop codon 10bp into this intron (Cohen *et al.* 2019). *dex-1(cs201)* mutants have a high rate of early larval lethality (96% dead L1s, n = 170). Similar to *dex-1(ns42)*, *dex-1(cs201)* dauers are defective in radial shrinkage, alae formation, and SDS resistance (Figures 2.1, D and G, and 2.2, A and B). To confirm *dex-1* as the causative mutation regulating these phenotypes, we rescued the radial shrinkage phenotype and SDS sensitivity of both *dex-1* mutants with *dex-1* cDNA under the control of its endogenous promoter (Figure 2.2, A and D).

Dauers suppress pharyngeal pumping and have a buccal plug that prevents feeding (Cassada and Russell 1975; Popham and Webster 1979). Non-dauers will readily ingest fluorescent beads and show fluorescence throughout the digestive system (Nika *et al.* 2016). We did not find fluorescent beads in *dex-1(ns42)* mutant dauer

intestines; however, we occasionally observed them in the buccal cavity (Figure 2.4, A–C). Additionally, we found no difference in the rate of pharyngeal pumping between *dex-1(ns42)* and wild-type dauers (Figure 2.4D). These data suggest that while pharyngeal pumping is effectively suppressed, *dex-1(ns42)* dauers have low-penetrance defects in buccal plug formation. Together, these data suggest that *dex-1* mutants form partial dauers with defects in epidermal remodeling. The enhanced sensitivity of *dex-1(cs201)* to SDS compared with *dex-1(ns42)* (Figure 2.2D) combined with our molecular data suggest that *dex-1(ns42)* is a hypomorphic allele; however, due to the early larval lethality of *dex-1(cs201)*, all further experiments were done using the *dex-1(ns42)* background, unless otherwise noted.

Finally, we examined *dex-1(ns42)* dauers for the presence of dauer-specific gene expression of *lag- 2p::gfp* in the IL2 neurons during dauer (Ouellet *et al.* 2008). Similar to wild-type dauers, *dex-1(ns42)* dauers showed appropriate dauer-specific expression (Figure 2.5). We sought to determine whether the *dex-1(ns42)* mutation would affect the initial decision to enter dauer. The dauer formation decision is based on the ratio of population density to food availability during early larval development (Golden and Riddle 1984). *C. elegans* constitutively secrete a pheromone mixture that is sensed by conspecific animals and, at high levels, triggers dauer formation (Golden and Riddle 1982). Dauers can be picked from old culture plates (starved) or can be induced using purified dauer pheromone. We found no difference in the dauer morphology phenotype between starved or pheromone-induced *dex-1(ns42)* mutant dauers (Figure 2.6). The *C. elegans* insulin/IGF-like and TGFβ signaling pathways function in parallel to regulate dauer formation (Thomas *et al.* 1993; Gottlieb and

Ruvkun 1994). Reduced insulin and TGFβ signaling induced by overcrowding and scarce food promotes dauer formation (Riddle and Albert 1997). Disruption of either the insulin-receptor homolog DAF-2 or the TGFβ homolog DAF-7 results in a dauer formation constitutive (*daf-c*) phenotype. The *dex-1(ns42)* alae formation defects were not suppressed in the *daf-7(e1372)* or *daf-2(e1370)* mutant backgrounds. While non-null alleles were used in these crosses, these data may suggest that *dex-1* acts outside of the dauer formation decision to generate dauer alae (Figure 2.7).

While screening *dex-1(ns42)* for defects in the dauer formation decision, we anecdotally observed that *dex-1(ns42)* mutants appeared to form fewer dauers that wild-type animals. To quantify this, we induced dauer formation in *dex-1(ns42)* mutant and wild-type animals using either a *daf-7(e1732)* background or high pheromone concentration. We found that in both a *daf-c* and non-*daf-c* backgrounds, *dex-1(ns42)* animals formed significantly fewer dauer larvae than wild-type (Figure 2.8). This suggests that while *dex-1* may function downstream of the dauer initiation decision, *dex-1(ns42)* mutants that enter dauer may have defects in maintaining dauer diapause. We also tested whether *dex-1(ns42)* mutant dauers showed defects in recovery from dauer. To ensure that we were isolating dauer animals, we used *lag-2::gfp* and *dex-1(ns42);lag-2::gfp* double mutants, along with wild-type N2 and *dex-1(ns42)* single mutants for recovery assays. We found no difference in the rate of dauer recovery between wild-type and *dex-1(ns42)* mutant dauers in either single or double mutant backgrounds, as 100% of animals tested were recovered after 48 hours.

2.4 DISCUSSION

The dauer stage of *C. elegans* is an excellent example of a polyphenism, where distinct phenotypes are produced by the same genotype via environmental regulation (Simpson *et al.* 2011). Compared to the decision to enter dauer, little is known about the molecular mechanisms controlling remodeling of dauer morphology. DEX-1 was previously characterized for its role in embryonic neuronal development (Heiman and Shaham 2009) and the shaping of multiple embryonic epithelia (Cohen *et al.* 2019). Our data show that DEX-1 also functions during dauer morphogenesis to regulate cuticle remodeling and dauer-specific environmental resistance. Interestingly, our data suggests that *dex-1* may function outside of the dauer pathway to regulate dauer morphogenesis, but that these *dex-1(ns42)* mutant dauers may be unable to maintain the dauer stage for extended periods. This phenomenon, known as ‘transient dauer formation’ has been described as a spontaneous recovery after dauer formation (Gems *et al.* 1998). Future experiments using strict synchronization techniques may be used to determine if this defect in dauer formation is due to transient dauer formation or defects in dauer formation initiation (Vowels and Thomas 1992).

2.5 FIGURES

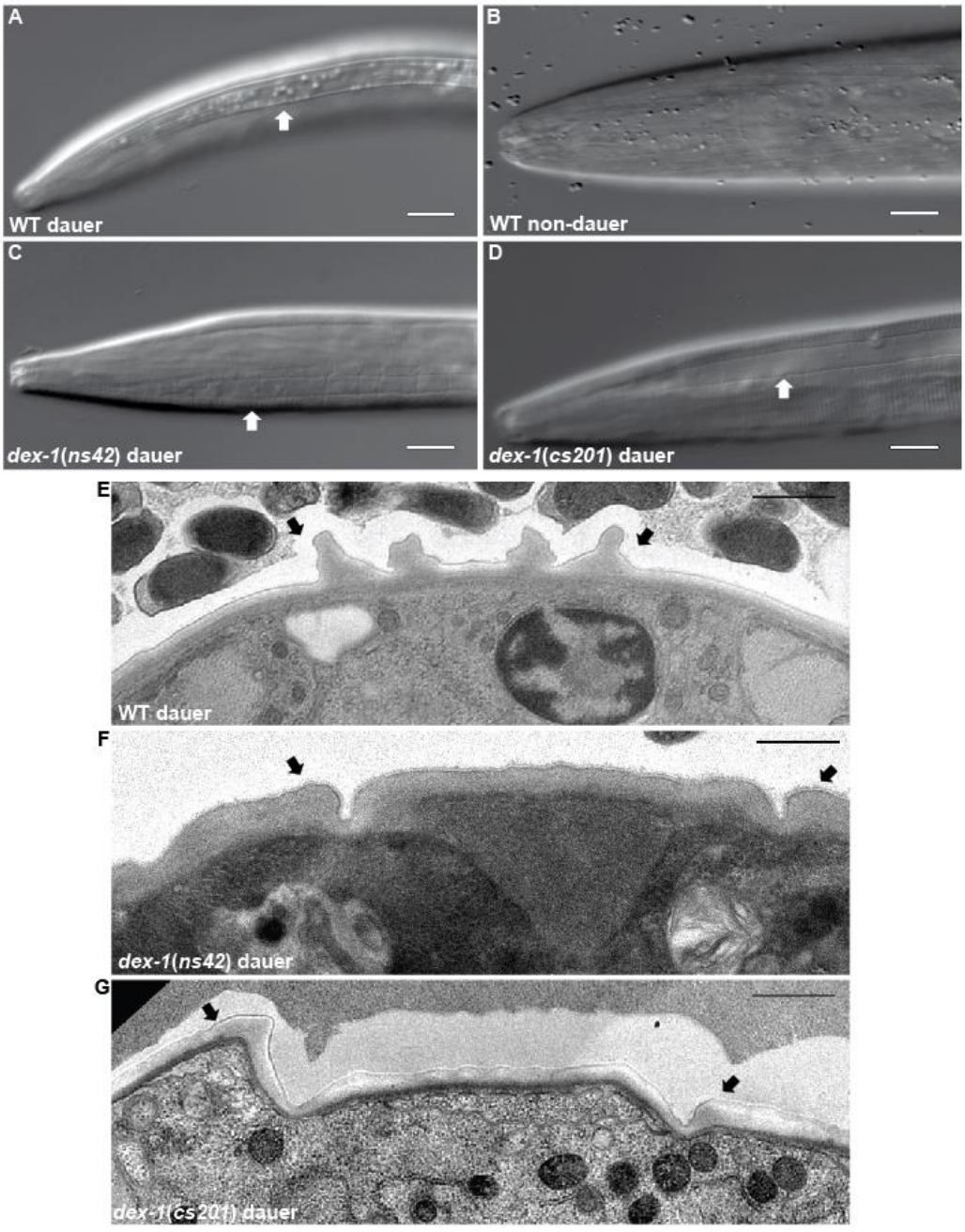

Figure 2.1: *dex-1* mutants have defects in lateral alae formation. (A) Wild-type dauers have prominent lateral alae (arrows) that are not present in the comparable non-dauer L3 stage (B). (C) *dex-1(ns42)* and (D) *dex-1(cs201)* mutant dauer alae are indistinct. All animals are lying laterally. Bar, 10 mm. (E-G) Transmission electron micrograph showing lateral alae (arrows) of a wild-type dauer (E), *dex-1(ns42)* mutant dauer (F), and a *dex-1(cs201)* mutant dauer (G). Bar, 1 mm.

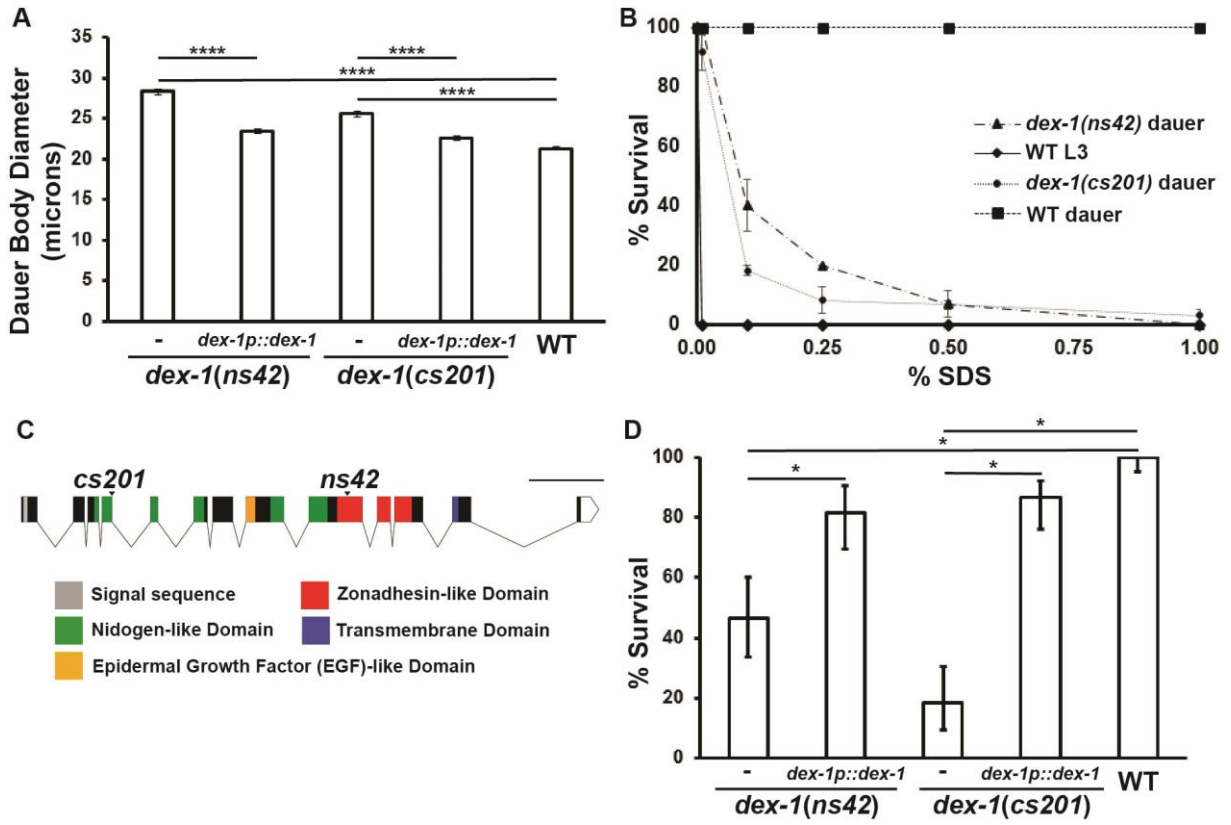

Figure 2.2: *dex-1* mutants form partial dauers. (A) *dex-1* mutant dauers are defective for dauer-specific radial shrinkage. The radial shrinkage defect can be rescued with *dex-1* cDNA driven by its endogenous promoter (n = 60 per genotype pooled from three trials). **** indicates statistical significance at P < 0.0001. Error bars indicate SEM. (B) Dose-response survival assay to SDS. *dex-1* dauers are sensitive to SDS compared to wild-type dauers, but are able to survive low levels of SDS exposure. Non-dauer animals are sensitive at all tested SDS concentrations (n = 60 per treatment and dose pooled from three independent trials). Error bars indicate SEM from three independent trials. (C) *dex-1* gene schematic. DEX-1 contains two nidogen-like domains, a single epidermal growth factor-like domain, a low-complexity domain previously predicted to have similarity to zonadhesin, and a transmembrane domain. The *cs201* mutant allele is a point mutation at the exon 4 splice donor. The previously isolated *ns42* mutation truncates the DEX-1 protein in its predicted zonadhesin-like domain. Bar, 1 kb. (D) Percent survival of dauers at 0.1% SDS. The *dex-1* SDS sensitivity phenotype is partially rescued by the endogenous *dex-1* promoter and DEX-1 cDNA (pMH7) (n = 60 per genotype pooled from three independent trials). Error bars indicate 95% confidence intervals. Non-overlapping confidence intervals were considered significantly different (*).

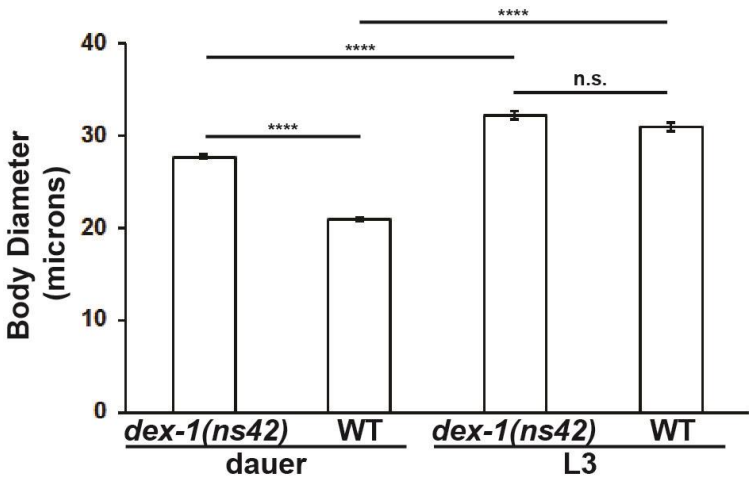

Figure 2.3: The radial shrinkage phenotype observed in *dex-1* mutants is dauer-specific. *dex-1(ns42)* dauers are defective for radial shrinkage and have a larger body diameter than wild-type dauers. However, *dex-1(ns42)* non-dauer L3 animals are not significantly larger than wild-type L3s. Error bars, SEM. (n=20, α = 0.05, p-value indicated by ****<0.0001, n.s. = not significant.)

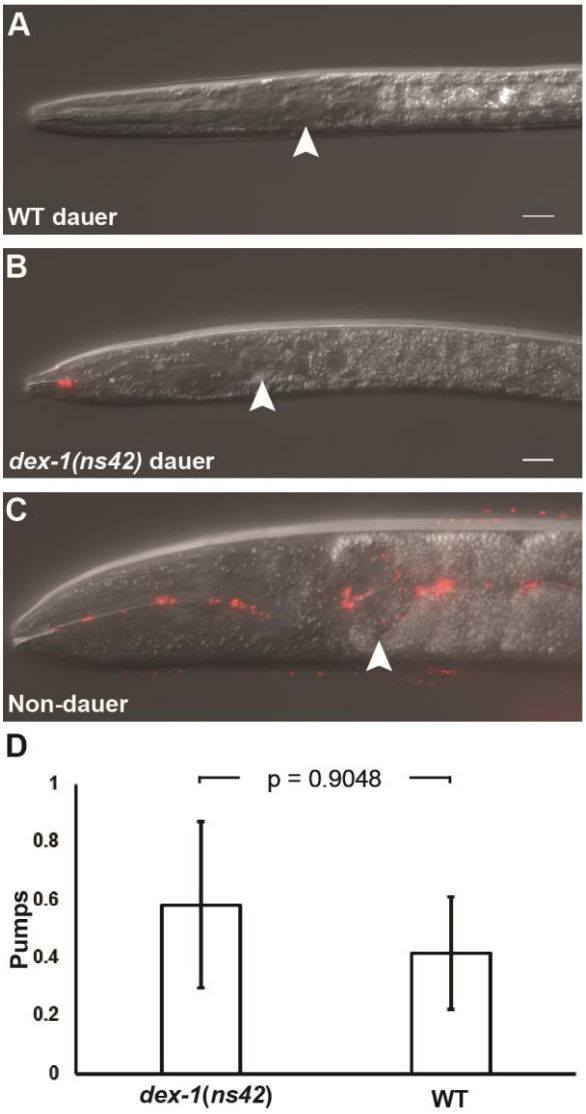

Figure 2.4: *dex-1(ns42)* dauers have defects in buccal plug formation. Dorsoventral view of a wild-type dauer (A) and lateral views of a *dex-1(ns42)* dauer (B) and non-dauer L3 (C) following a fluorescent bead feeding assay. We did not observe fluorescence in the intestines of wild-type (A) or *dex-1(ns42)* mutant (B) dauers. However, fluorescence was occasionally observed in the buccal cavity of *dex-1(ns42)* dauers (B). (C) Fluorescent beads were observed throughout the digestive tract of non-dauer animals. Arrowheads point to the terminal bulb. Scale bar, 10µm. (D) Pharyngeal pumping is effectively suppressed in *dex-1(ns42)* dauers over a two minute observation period. Error bars, SEM. n = 12.

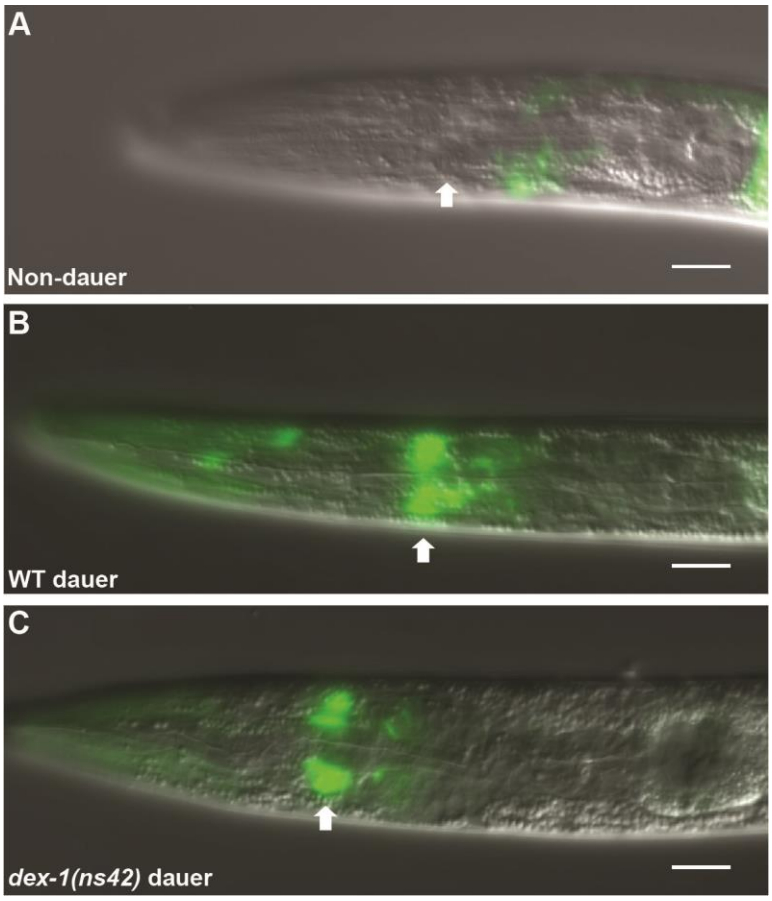

Figure 2.5: *dex-1(ns42)* dauers exhibit dauer specific expression of *lag-2p::gfp* in the IL2 neurons. Expression of *lag-2p::gfp* in the IL2 neurons is specific to the dauer stage. *lag-2p::gfp* is absent in non-dauer IL2 cell bodies (A) (arrow) but is expressed brightly in both wild-type (B) and *dex-1(ns42)* dauers (arrows). Scale bar, 10μm.

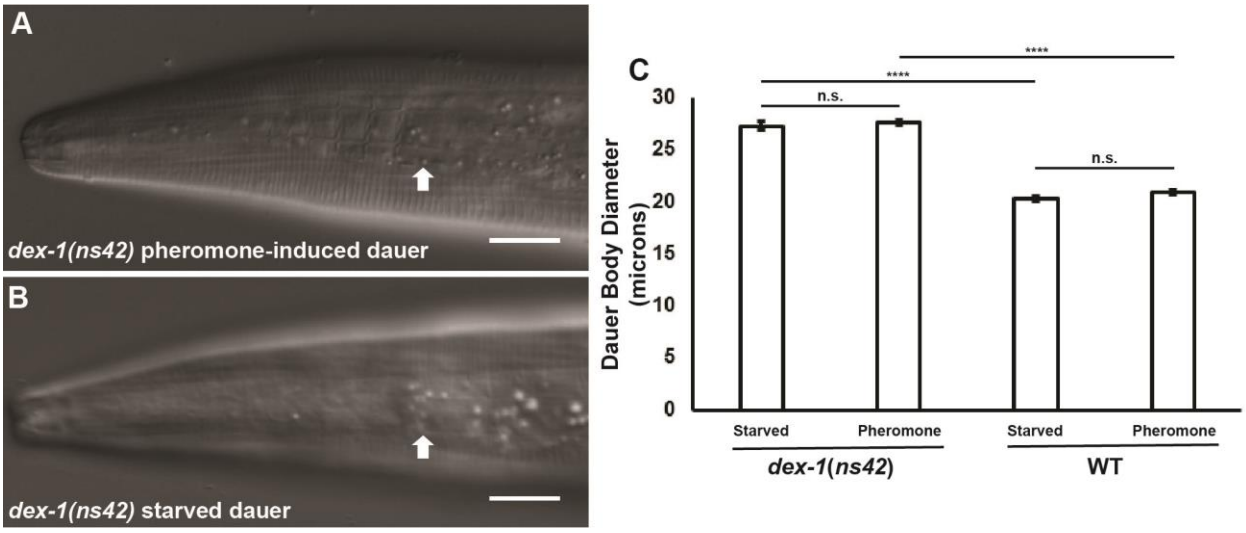

Figure 2.6: Dauers isolated from either starved or pheromone-induced populations are morphologically similar. *dex-1(ns42)* dauers taken from pheromone (A) and starved (B) plates both display indistinct lateral alae (arrows). Scale bars, 10μm. (C) Body diameter measurements for *dex-1(ns42)* and wild-type dauers showed no statistically significant differences between starved and pheromone-induced populations. Both starved and pheromone induced *dex-1(ns42)* dauers displayed defects in radial constriction compared to wild-type dauers. Error bars, SEM. (n = 20, α=0.05, p-value indicated by ****<0.0001, n.s. = not significant.)

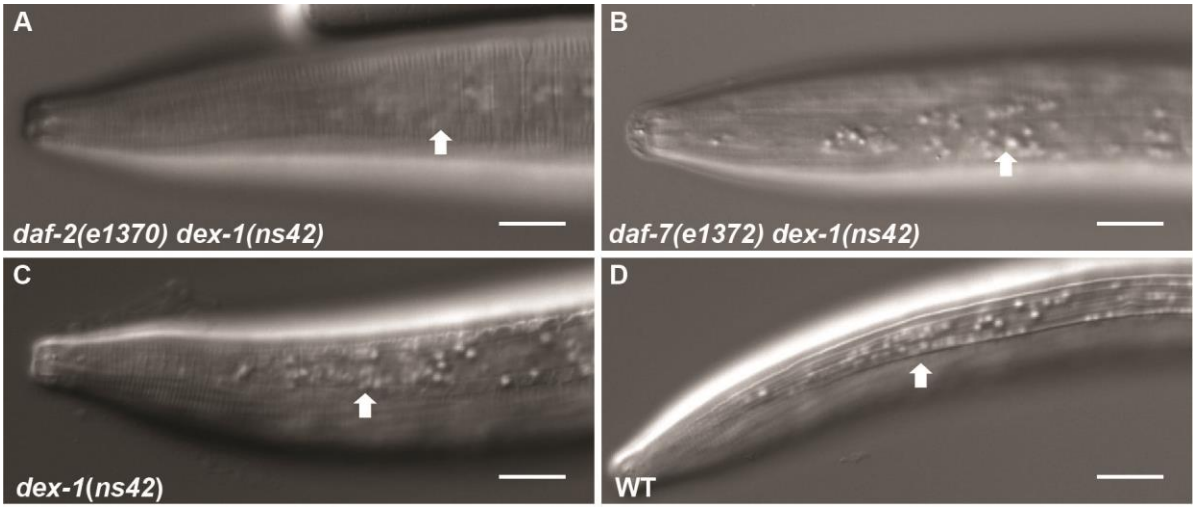

Figure 2.7: *dex-1* functions outside of the dauer decision pathway. (A-D) Lateral view micrographs of (A) *daf-2(e1370) dex-1(ns42)*, (B) *daf-7(e1372) dex-1(ns42)*, (C) *dex-1(ns42)*, and (D) wild-type dauers. *daf-c* mutations in the dauer decision pathway did not suppress the *dex-1(ns42)* alae phenotype. Arrows point to the lateral alae. Scale bar, 10μm.

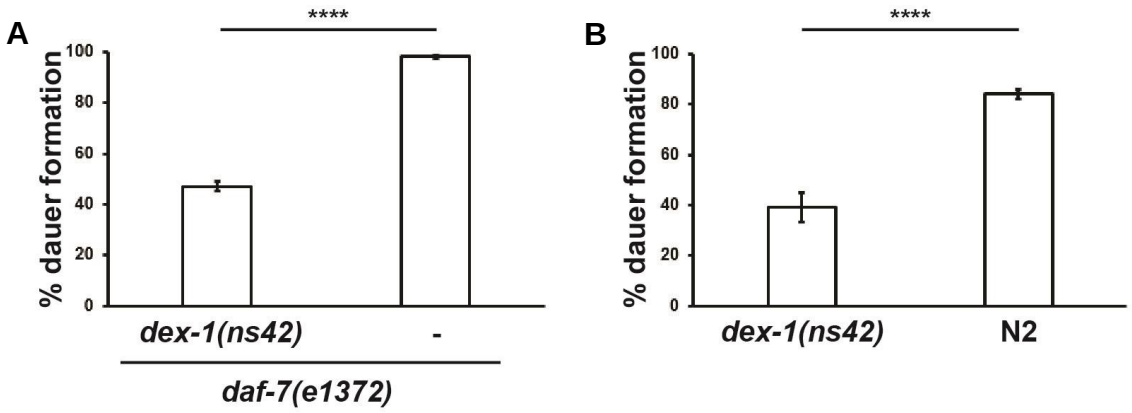

Figure 2.8: *dex-1* mutants form fewer dauers in both *daf-c* and non-*daf-c* backgrounds. Quantification of dauer formation showed that *dex-1(ns42)* mutants form fewer dauers in both the dauer constitutive *daf-7(e1372)* (A) and wild-type (B) backgrounds. (n=6, α=0.05, p-value indicated by **** where $P < 0.0001$). Error bars indicate SEM.

CHAPTER 3: DEX-1 IS SECRETED, BUT ACTS LOCALLY TO REGULATE SEAM CELL REMODELING DURING DAUER MORPHOGENESIS

This chapter is adapted, in part, from Flatt *et al.* 2019.

3.1 INTRODUCTION

Dauer-specific radial shrinkage and alae formation are regulated by a set of lateral hypodermal seam cells called the seam cells (Singh and Sulston 1978; Meléndez *et al.* 2003). Seam cell function and remodeling are critical for proper dauer morphology and increased environmental resistance. The seam cells also have stem cell-like properties. During non-dauer development, the seam cells undergo asymmetrical divisions at larval molts to produce an anterior differentiated cell and a posterior seam cell (Sulston and Horvitz 1977). Alternatively, if the animal enters dauer diapause, the seam cells shrink and stop dividing (Meléndez *et al.* 2003; Karp and Ambros 2012). Here, we show that DEX-1 is upregulated in the seam cells during dauer formations and functions to facilitate seam cell remodeling as a secreted protein that localizes in or near the dauer alae.

3.2 MATERIALS AND METHODS

Strains and plasmids. All strains were grown under standard conditions unless otherwise noted (Brenner 1974). The wild-type Bristol N2 strain and CHB27 *dex1(ns42)* III. The transgenic line JR667 *wIs51 [SCMp::GFP+unc-119(+)]* was used to observed the seam cell nuclei and ST65 *ncIs13[ajm1::gfp]* was used to observe the apical

junctions of the seam cells (Köppen *et al.* 2001). Both were provided by the CGC. All mutant strains were backcrossed at least twice.

The *dex-1(ns42)* mutant strain and the following plasmids were generous gifts from Dr. Maxwell Heiman (Department of Genetics, Harvard University, Boston, MA): pMH7 *dex-1p::dex-1*, pMH8 *pha-4p:: dex-1*, pMH111 *dex-1p(5.7 kb)::gfp* (Heiman and Shaham 2009). The *sur-5::gfp* construct used for mosaic analysis was a generous gift from Dr. Trent Gu (Gu *et al.* 1998; Yochem *et al.* 1998). Plasmids were constructed using Gibson Assembly (E2611S; New England Biolabs, Beverly, MA) and restriction enzyme cloning (for a complete list of primers and plasmids, please see the Supplemental Table). The seam cell-specific expression plasmid was built by replacing the *dex-1* promoter from pMH7 with a 1.21 kb *cut-5* promoter region. The hypodermal-specific *dex-1* plasmid was constructed by replacing the *dex-1* promoter in pMH7 with the *cut-6* promoter (Muriel *et al.* 2003; Sapio *et al.* 2005). Additionally, translational reporters *dex-1p::sfgfp::dex-1* (pJC24) and *dex-1p::dex-1(ecto)::sfgfp* (pJC15) contain the 2.1 kb *dex-1* promoter and *dex-1* (isoform a) complementary (cDNA) from pMH7 (Cohen *et al.* 2019). *sfgfp* was inserted either at an internal endogenous BglII restriction site to generate a full length fusion tagged upstream of the first nidogen domain, or inserted at the 3' end of a cDNA truncated before the transmembrane domain. See Cohen *et al.* 2019 for further cloning details.

Animals containing extrachromosomal arrays were generated using standard microinjection techniques (Mello *et al.* 1991), and genotypes confirmed using PCR analysis and observation of co-injection markers. *dex-1(ns42)* animals were injected with 20 ng/ml of plasmid and 80 ng/ml of *unc-122p::gfp*, *unc-122p::rfp* or *sur-5::gfp* as

the co-injection marker. *dex-1(cs201)* animals were injected with 30 ng/ml of pJC15 or pJC24 and 50 ng/ml of co-injection marker pHS4 (*lin-48p::mrfp*).

Microscopy. Unless otherwise specified, animals were mounted onto 4% agarose pads and immobilized with 0.1 or 0.01 M levamisole for dauers and non-dauer or partial dauers, respectively. In our hands, dauers frequently lay in a dorsal-ventral position following anesthesia. Therefore, to image the lateral side, dauers were immobilized by mounting on 4% agarose pads with Polybead Polystyrene 0.10 mm microspheres (Polysciences Inc., #00876) (Kim *et al.* 2013). A Zeiss AxioImager microscope equipped with DIC and fluorescence optics was used to collect images. For radial constriction experiments, Z-stack images were taken and Z-projections were made using FIJI. Diameter measurements were taken near the center of the terminal pharyngeal bulb. Measurement data were analyzed using a one-way ANOVA with Bonferroni's multiple comparisons test using GraphPad Prism 6 software. The resulting Z-projections were used to measure body diameter. For seam cell area analysis, area was measured for V2pap, V2ppp, and V3pap and averaged to give one measurement per animal (Sulston and Horvitz 1977). Seam cell measurement data were analyzed by an unpaired t-test.

Sodium dodecyl sulfate sensitivity assays. Single concentration assays were conducted at 0.1% SDS with 20 dauers for each genotype and three independent experiments. Data were analyzed using a one proportion exact method analysis in Minitab 18 and considered significantly different if the 95% confidence intervals did not overlap. Significant difference was denoted with a single asterisk.

***dex-1* expression analysis.** Ten animals were measured for each genotype. Mosaic analysis was conducted using *dex-1(ns42)* dauer animals expressing extrachromosomal *dex-1p::dex-1* and *sur5::gfp* (Yochem *et al.* 1998). Lateral view micrographs were taken of transgenic animals and seam cells were scored for the presence of *sur-5::gfp* in the nucleus. Areas of lateral alae adjacent to seam cell nuclei positive for *sur-5::gfp* expression were scored as either full, partial, or no rescue. Seam cells not expressing *sur-5::gfp* were also counted and the adjacent alae scored. Twelve animals were observed for mosaicism, with one set of seam cells being scored for each animal.

3.3 RESULTS

DEX-1 functions as a tightly localized, secreted protein to facilitate seam cell remodeling and lateral alae formation. *dex-1* is expressed at high levels during embryogenesis to regulate sensory dendrite formation and subsequently downregulated throughout development (Heiman and Shaham 2009). However, previous microarray data suggested that *dex-1* is also upregulated during dauer (Liu *et al.* 2004). Dauer-specific radial shrinkage and subsequent lateral alae formation are facilitated by shrinkage of the seam cells (Singh and Sulston 1978; Meléndez *et al.* 2003). Using the *ajm-1::gfp* apical junction marker (Köppen *et al.* 2001), we found that *dex-1(ns42)* mutant dauer seam cells are larger and have jagged, rectangular edges, unlike the smooth, elongated seam cells of wild-type dauers (Figure 3.1). These data suggest that DEX-1 is required for seam cell remodeling. To determine the location of *dex-1*

expression, we generated transgenic animals expressing green fluorescent protein (GFP) driven by a 5.7 kb 5' *dex-1* upstream promoter. We observed bright fluorescence in the seam cells and glia socket cells of the anterior and posterior deirid neurons starting in the pre-dauer L2 (L2d) stage. Expression of *dex-1p::gfp* in the seam cells and deirid socket cells persisted throughout dauer (Figure 3.2). We also observed *dex-1p::gfp* expression in unidentified pharyngeal cells during all larval stages (Figure 3.2C). To determine the subcellular localization of DEX-1 during dauer remodeling, we expressed *dex-1* cDNA (isoform A) tagged with super-folder GFP (sfGFP) under the control of its endogenous promoter. This *dex-1p::sfgfp::dex-1* construct rescued the SDS phenotype in *dex-1(ns42)* mutant dauers, suggesting it is functional (Figure 3.3A). During dauer, we observed sfGFP along the length of the animal above seam cells in a mosaic pattern alternating between alae with diffuse sfGFP expression immediately under the outer ridges and alae with bright and punctate expression immediately below the lateral ridge (Figure 3.3B). Interestingly, regions with diffuse GFP expression correlated with proper radial constriction and intact lateral alae, whereas regions with bright, punctate expression did not undergo proper dauer shrinkage and lacked alae (Figure 3.3B). The mosaicism in alae formation was observed in both wild-type and *dex-1(ns42)* dauers expressing the *dex-1p::sfgfp::dex-1* construct, indicative of dominant negative effects of the transgene.

DEX-1 contains a putative transmembrane domain, but was previously suggested to be secreted through cleavage of the large extracellular domain (Heiman and Shaham 2009). To test if DEX-1 can function as a secreted protein during dauer, we expressed a *dex-1p::dex-1(ecto)::sfgfp* construct that truncates the C-terminal

transmembrane domain. Consistent with a role as a secreted protein, the truncated DEX-1 construct rescued the SDS resistance (Figure 3.3A), radial shrinkage, and alae formation phenotypes (Figure 3.4, A and B). To further examine where DEX-1 acts to regulate seam cell remodeling, we expressed *dex-1* cDNA under the control of cell-specific promoters. First, we expressed *dex-1* in the seam cells using the *cut-5* promoter. *cut-5* was previously shown to be expressed specifically in the seam cells during L1 and dauer (Sapio *et al.* 2005). Seam cell-specific expression of *dex-1* rescued the *dex-1(ns42)* radial shrinkage in a mosaic pattern similar to that seen with the full-length *sfgfp::dex-1* construct (Figure 3.4C). Expression of *dex-1* under a pharyngeal promoter failed to rescue the *dex-1* seam cell phenotype, suggesting that *dex-1* expression is necessary near the seam cells (Figure 3.4, B and D). The basolateral membranes of the seam cells are surrounded by a syncytial hypodermis. We hypothesized that the close proximity of the surrounding hypodermis to the seam cells would be sufficient for secreted DEX-1 to function during seam cell remodeling. We therefore expressed *dex-1* under the control of a *cut-6* promoter that was previously shown to drive expression in the hypodermis, but not in the seam cells, during dauer (Muriel *et al.* 2003). While *dex-1* expression in the surrounding hypodermis failed to rescue the *dex-1* dauer-specific alae phenotype (Figure 3.4E), hypodermal expression of *dex-1* resulted in partial rescue of the radial shrinkage phenotype, suggesting a limited ability for DEX-1 to translocate *in vivo* (Figure 3.4B)

Finally, to verify that DEX-1 is functioning in a cell-autonomous manner, we performed a mosaic analysis using *dex-1p::dex-1* and *sur-5::gfp* as the co-injection marker (Yochem *et al.* 1998). We found that in cells expressing *sur-5::gfp*: 56% showed

full rescue of the lateral alae, 29% showed at least partial alae rescue, and 16% showed no alae rescue (n = 12 animals, 191 cells). We did not observe alae rescue in cells that did not express nuclear *sur-5::gfp* (Figure 3.4F). Together, these data indicate that *dex-1* acts cell-autonomously to regulate seam cell remodeling during dauer.

In addition to their role in cuticle remodeling during dauer formation, the seam cells also have stem cell-like properties. During non-dauer development, seam cells divide at larval molts to produce a seam cell daughter and a differentiated daughter cell (Sulston and Horvitz 1977). During dauer, the seam cells enter a quiescent state and only resume division following recovery from dauer. To determine if *dex-1* is required for maintaining seam cell quiescence during dauer, we used a seam cell nuclei marker to examine the number of seam cell nuclei in wild-type and *dex-1(ns42)* backgrounds. Interestingly, we found the *dex-1* mutant dauers have a slight, but statistically significant, increase in the number of seam cell nuclei compared with wild-type dauers (*dex-1* $\bar{x}$ = 16.63 ± 0.09928, WT $\bar{x}$ = 15.95 ± 0.1715, p = 0.0010, n = 40). This could suggest that *dex-1* plays a role in maintaining the seam cell quiescence during dauer.

3.4 DISCUSSION

Our data show that DEX-1 functions during dauer-specific remodeling of the stem cell-like seam cells. We demonstrate that DEX-1 is secreted, but acts locally in a cell-autonomous manner to regulate seam cell remodeling during dauer morphogenesis. DEX-1 is similar in sequence to the human ECM protein SNED1 (Sushi, Nidogen, EGF-like domains 1). High levels of SNED1 expression promote invasiveness during breast cancer metastasis (Naba *et al.* 2014), suggesting a possible mechanical role in tissue

remodeling. Interestingly, results from our full-length translational DEX-1 reporter indicate that seam cell remodeling can also be perturbed by a dominant negative effect of DEX-1 overexpression. Seam cells with bright, aggregated sfGFP::DEX-1 expression were correlated with indistinct lateral alae and large body diameter, whereas diffuse sfGFP::DEX-1 correlated with intact alae. We hypothesize that this could be the result of increased interaction of DEX-1 protein with either itself or other ZP proteins in the ECM, leading to protein aggregates that disrupt alae formation.

Our data indicate that DEX-1 acts in a cell-autonomous manner directly beneath the edges of the lateral alae. Although expression of *dex-1* in the hypodermis was sufficient to partially rescue dauer-specific radial shrinkage, hypodermal expression failed to rescue the lateral alae phenotype. We therefore propose DEX-1 may act as a secreted protein during dauer with restricted localization to the cuticle or extracellular matrix (ECM) immediately above the apical membrane of the seam cells. During embryogenesis, DEX-1 is secreted and localized to the dendritic tips (Heiman and Shaham 2009). DEX-1 may serve to couple physical interactions between the remodeled cuticular ECM and seam cell shape. Failure of these tissues to properly compact and thicken due to a loss of DEX-1 could lead to an overall weakening of the cuticle, and thus result in the SDS sensitivity observed in *dex-1* mutant dauers. Furthermore, we found that *dex-1* dauers have significantly more seam cells than wild-type dauers, suggesting ectopic divisions during dauer diapause. In mammalian cell lines, stem cell shape regulates differentiation (McBeath *et al.* 2004; Kilian *et al.* 2010). For example, mesenchymal stem cells will differentiate into adipocytes or osteoblasts depending on whether the cell is round or flat, respectively (McBeath *et al.* 2004). We

speculate that the shrinkage observed during dauer may be important for maintenance of seam cell quiescence. Previous research demonstrated a role for autophagy in dauer-specific seam cell remodeling (Meléndez *et al.* 2003). It will be interesting to determine if dauer-specific changes to autophagy are influenced by DEX-1–mediated mechanical forces.

3.5 FIGURES

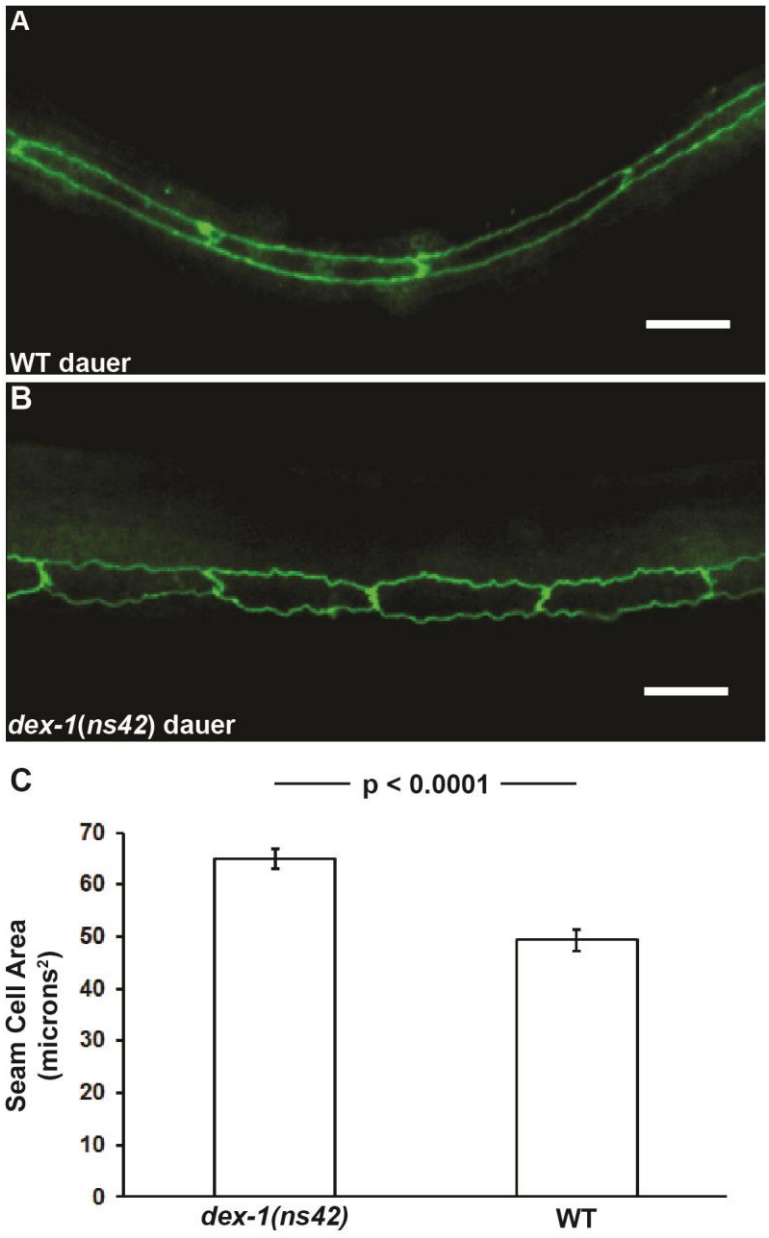

Figure 3.1: *dex-1* mutant dauers have defects in seam cell shrinkage. Lateral view micrographs of (A) wild-type (WT) and (B) *dex-1(ns42)* dauers expressing the apical junction marker *ncIs13* [*ajm-1::gfp*]. The seam cells of wild-type dauers are elongated and smooth, while *dex-1(ns42)* mutant seam cells are wider with jagged edges. Bar, 10µm. (C) Quantification of seam cell area as measured with the *ajm-1::gfp* reporter. Data were analyzed by an unpaired *t*-test (*dex-1(ns42)* dauer n = 14, WT dauer n = 15). Error bars indicate SEM.

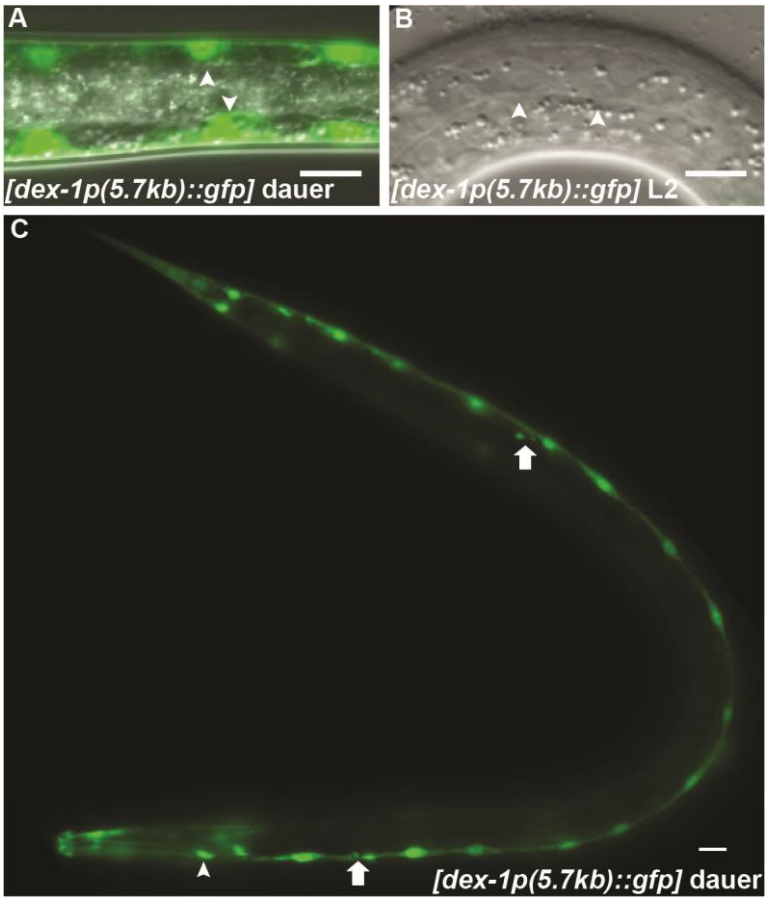

Figure 3.2: *dex-1* is expressed in the seam cells during dauer. (A) Dorsoventral view of a dauer animals expressing *dex-1p::gfp* from a 5.7 kb promoter. (B) GFP is seen in the seam cells (arrowheads) during dauer and is not expressed during L3. Bar, 10µm. (C) Lateral view of a dauer animals expressing *dex-1p::gfp* from a 5.7 kb *dex-1* promoter region. IN addition to the seam cells along the length of the animals, *dex-1* is expressed in the socket glial cells of the anterior and posterior deirid neurons (arrows) during dauer, and in unidentified pharyngeal cells (arrowhead) during all larval stages. Bar, 10µm.

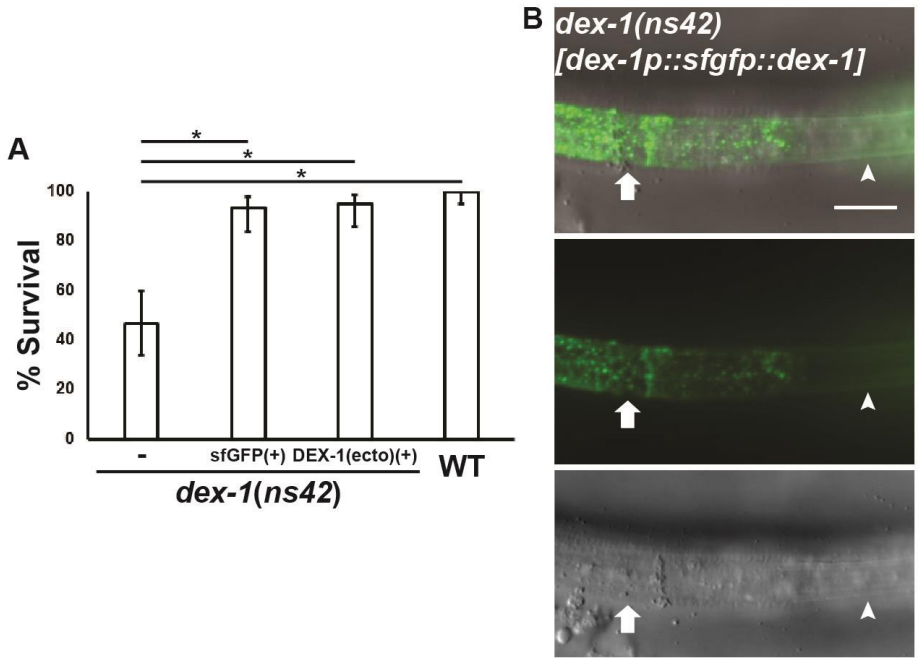

Figure 3.3: DEX-1 is localized to the outer ridges of the lateral alae. (A) Functional full-length *dex-p::sfgfp::dex-1* and truncated *dex-1p::dex-1(ecto)::sfgfp* constructs rescue the *dex-1(ns42)* SDS sensitivity phenotype to wild-type levels. Error bars indicate 95% confidence intervals. Non overlapping confidence intervals were considered significantly different (*) (n=60 per genotype pooled from three independent trials). (B) Lateral view overlay (top), fluorescence (middle) and DIC (bottom) micrographs of a *dex-1(ns42)* dauer expressing a full-length *dex-1p::sfgfp::dex-1* construct. The full-length *dex-1p::sfgfp::dex-1* construct rescues the lateral alae phenotype in a mosaic pattern. *dex-1::sfgfp::dex-1* localizes in a diffuse pattern to the areas immediately below the outer ridges of rescued, intact lateral alae (arrowheads). In contrast, in areas where lateral alae are not rescued, DEX-1 expression is bright and punctate and localizes throughout the lateral ridge (arrows). Bar, 10µm.

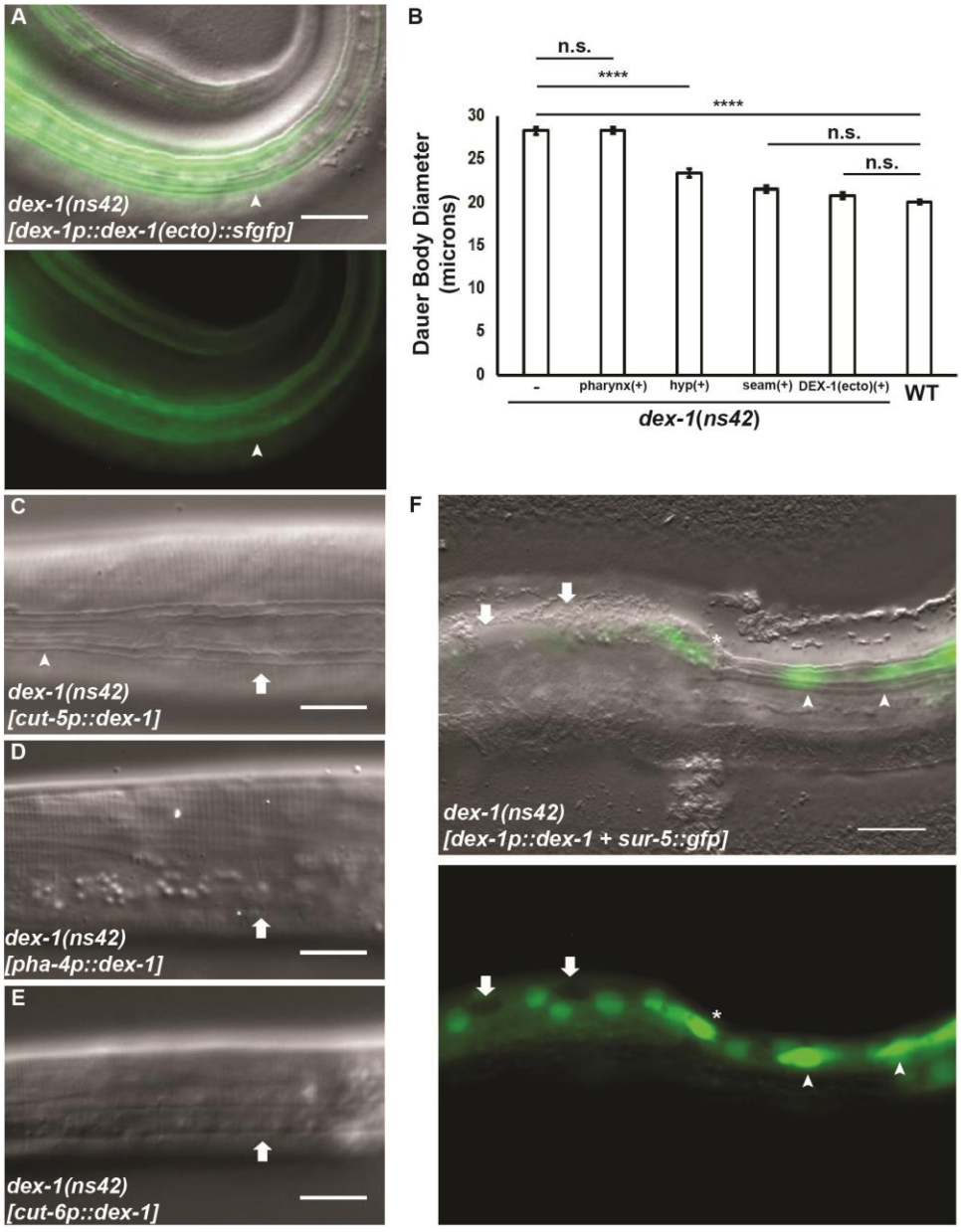

Figure 3.4: DEX-1 functions as a secreted protein in a tightly localized manner. (A) Lateral view DIC overlay (top) and fluorescence (bottom) images of a *dex-1(ns42)* dauer expressing *dex-1p::dex-1(ecto)::sfgfp,* which lacks the C-terminal transmembrane domain. *dex-1p::dex-1(ecto)::sfgfp* localizes to the outer edges of the lateral ridge and completely rescues the *dex-1(ns42)* alae phenotype (arrowheads). (B) Cell-specific rescue of body diameter in *dex-1(ns42)* suggests DEX-1 functions cell-autonomously. Error bars, SEM. **** indicates statistical significance at $P < 0.0001$ (n =15). (C) *dex-1* expression from the *cut-5* promoter rescues the *dex-1(ns42)* alae formation phenotype in a mosaic pattern. Arrowhead points to areas with rescued alae, arrow points to areas with partially rescued alae. *dex-1* expression from a (D) *pha-4* pharyngeal and (E) *cut-6* hypodermal promoter fail to rescue alae formation in *dex-1(ns42)* dauers. Arrows point to the indistinct lateral alae. (F) DIC overlay (top) and fluorescence (bottom) image of a *dex-1(ns42)* dauer expressing a *dex-1p::dex-1* construct with *sur-5::gfp*. *sur- 5::gfp* expression in seam cell nuclei was correlated with rescue of the lateral alae (arrowheads), while the absence of *sur-5::gfp* correlated with indistinct lateral alae and a larger body diameter (arrows). Occasionally, *sur-5::gfp* was expressed in seam cell nuclei that did not show lateral alae rescue (*). Bar, 10 mm.

CHAPTER 4: DEX-1 INFLUENCES DAUER-SPECIFIC BEHAVIORS

This chapter is adapted, in part, from Flatt *et al.* 2019.

4.1 INTRODUCTION

Dauer larvae exhibit distinct locomotion behaviors compared to non-dauer animals (Cassada and Russell 1975; Gaglia and Kenyon 2009). While non-dauers exhibit bouts of spontaneous locomotion in search of food or potential mates, dauer larvae are often found to be behaviorally quiescent. Interestingly, dauer larvae are capable of immediate and rapid locomotion following mechanical stimulation. This rapid locomotion response is likely due to dauer-specific tissue remodeling. For example, dauer larvae undergo radial shrinkage of the entire body, resulting in formation of raised cuticular ridges called the lateral alae. Though the function of the dauer lateral alae is not well understood, it is hypothesized that they aid in dauer-specific locomotion over various terrains. Additionally, dauer larvae undergo remodeling of the muscular systems, including increases to myofilament lattices and changes in mitochondrial conformations to promote short, but powerful bouts of locomotion (Hackenbrock *et al.* 1971; Popham and Webster 1979). Here we show that dauer locomotion is not entirely dependent on lateral alae formation, and that defects in the neuromuscular system of *dex-1* mutant dauers may impact their ability to perform the rapid locomotion behaviors observed in wild-type dauers.

4.2 MATERIALS AND METHODS

Strains and plasmids. All strains were grown under standard conditions unless otherwise noted (Brenner 1974). The wild-type Bristol N2 strain and the CHB27 *dex1(ns42)* III and UP2571 *dex-1(cs201)* III mutant strains were used for behavioral analysis. All mutant strains were backcrossed at least twice. *dex-1(ns42)* was a generous gift of Dr. Maxwell Heiman (Department of Genetics, Harvard University, Boston, MA) (Heiman and Shaham 2009). *dex-1(cs201)* was generated using standard EMS mutagenesis protocols (Brenner 1974; Flibotte *et al.* 2010) and identified based on balancer mapping and whole genome sequencing (Cohen *et al.* 2019). The IL2 neurons were observed using PT2660 *myIs13[klp-6p::gfp+pBx]* III and PT2762 *myIs14[klp-6p::gfp+pBx]* V (Blelloch *et al.* 1999; Ouellet *et al.* 2008; Schroeder *et al.* 2013). The deirid neurons were observed using TG2435 *vtIs1[dat-1p::gfp +rol-6(su1006)]* V (Nass *et al.* 2002). Muscle arms and the nerve cords were observed using RP247 *trIs30[him-4p::yfp+hmr-1b::DsRed2+unc-129nsp::DsRed2]* (Dixon and Roy 2005).

The seam cell-specific expression plasmid was constructed using Gibson Assembly (E2611S; New England Biolabs, Beverly, MA). To do this, we replaced the endogenous *dex-1* promoter in the pMH7 plasmid with a 1.2 kb *cut-5* promoter region (for a complete list of primers and plasmids, please see the Supplemental Table). Animals containing extrachromosomal arrays were generated using standard microinjection techniques (Mello *et al.* 1991), and genotypes confirmed using PCR analysis and observation of co-injection markers. *dex-1(ns42)* animals were injected with 20 ng/ml of plasmid and 80 ng/ml of *unc-122p::gfp*.

Microscopy and muscle arm analysis. For light microscopy, animals were mounted onto 4% agarose pads and immobilized with 0.1 or 0.01 M levamisole for dauers and non-dauer or partial dauers, respectively. In our hands, dauers frequently lay in a dorsal-ventral position following anesthesia. Therefore, to image the lateral side, dauers were immobilized by mounting on 4% agarose pads with Polybead Polystyrene 0.10 mm microspheres (Polysciences Inc., #00876) (Kim *et al.* 2013). A Zeiss AxioImager microscope equipped with DIC and fluorescence optics was used to collect images. To determine the average width of wild-type muscle arms, we measured the width of muscle arms from muscle cells #9, 11, 13, 15 and 17 as described by Dixon and Roy 2005. Measurements from 3 individual wild-type animals were averaged to determine a standard average muscle arm width of 0.98µm. For all following experiments, muscle arms greater than 2µm in width were considered abnormal. For mutant muscle arm analysis, muscle arms from muscle cells #9, 11 and 13 as described by Dixon and Roy 2005 were measured at the estimated mid-point. The calculated number of abnormal muscle arms was divided by the total number of muscle arms and multiplied by 100, giving a single measurement for each animal. Muscle arm data were analyzed using an unpaired t-test in GraphPad Prism 6 software.

For transmission electron microscopy, dauer larvae were induced using pheromone plates and processed for high-pressure freezing and freeze substitution modified from previously established methods (Hall *et al.* 2012; Manning and Richmond 2015). Using OP50 *Escherichia coli* as a substrate and 1% propylene phenoxetol in M9 buffer as an anesthetic, animals were loaded into a metal specimen carrier coated with 1-hexadecane and frozen in an HPM 010 high-pressure freezer. Freeze substitution

was performed in an FS-8500 freeze substitution system using 2% OsO4 (Electron Microscopy Sciences), 0.1% uranyl acetate (Polysciences) in 2% H20, and 100% acetone. Samples were held at -90º for 110 hr, then warmed to -20 at the rate of 5º per hour (14 hr). Samples were then held at -20º for 16 hr, then warmed to 0º at the rate of 5º per hour (4 hr). Samples were washed three times in pre-chilled (0º) 100% acetone and incubated at 0º for 1 hr after the final wash. Samples were then warmed to room temperature and washed an additional two times with 100% acetone. Samples were infiltrated with 1:1 Polybed812 (Polysciences) resin: acetone for 6 hr, 2:1 resin:acetone for 14 hr, and 100% resin for 72 hr. All infiltration steps were incubated on an orbital shaker at room temperature. Samples were then embedded in molds in 100% resin plus DMP-30 hardener (Polysciences) and baked at 60º for 48 hr, then 70 nm sections were cut with a diamond knife using a PowerTome PC ultramicrotome and collected onto formvar-coated copper slot grids. Samples were imaged with a Philips CM200 transmission electron microscope.

Dauer formation. Dauers were induced using plates containing high concentrations (EC_{90}) of crude dauer pheromone extracted by previously established procedures (Vowels and Thomas 1992; Schroeder and Flatt 2014).

Locomotion assays. For movement assays, animals were transferred to unseeded NGM plates and allowed to sit at room temperature for 10 min before being assayed. Animals were stimulated near the anus with an eyelash and the number of body bends was scored. Counting was stopped if the animal did not complete another body bend

within 5 sec of stopping, or if the animal reversed direction. Each animal was scored twice and then removed from the plate. Counts were averaged and then analyzed using a nonparametric Kruskal–Wallis test with Dunn's multiple comparisons test, or Mann–Whitney U test, using GraphPad Prism 6 software.

4.3 RESULTS

DEX-1 plays a role in dauer-specific locomotion behaviors. Morphological changes during dauer are accompanied by changes in behavior. Wild-type dauer animals are often quiescent, but move rapidly when mechanically stimulated (Cassada and Russell 1975). Anecdotally, we noticed a higher percentage of quiescent *dex-1* dauers than wild-type dauers. To quantify this behavior, we developed a behavioral assay to measure movement following mechanical stimulation (see Materials and Methods). Although both *dex-1* mutant and wild-type dauers initially respond to mechanical stimulation, the *dex-1* mutant dauers have significantly reduced locomotion and display slightly uncoordinated body movements (Figure 4.1A). This locomotion defect was dauer-specific, as non-dauer *dex-1* animals moved at wild-type levels following mechanical stimulation (Figure 4.1B). In addition to seam cell remodeling, the IL2 and deirid sensory neurons remodel during dauer formation (Albert and Riddle 1983; Schroeder *et al.* 2013). The IL2s regulate dauer-specific behaviors (Lee *et al.* 2011; Schroeder *et al.* 2013), while the deirids respond to specific mechanical cues (Sawin *et al.* 2000). We therefore examined these neuron classes using fluorescent reporters; however, we observed no obvious difference in neuronal structure between *dex-1(ns42)* and wild-type (Figure 4.1, C and D). Given that *dex-1* was primarily expressed in the

seam cells during dauer, we tested if seam cell-specific expression could rescue the behavioral phenotype. Surprisingly, although seam cell-specific expression of *dex-1* rescued radial shrinkage and alae formation defect in a mosaic pattern, seam cell-specific *dex-1* expression completely rescued the *dex-1(ns42)* dauer locomotion defects (Figure 4.1A). The ability of seam cell-specific expression of *dex-1* to completely rescue the dauer-specific locomotion defects, independent of radial shrinkage and alae formation, may suggest a role for DEX-1 in locomotion-specific neuronal circuits during dauer.

C. elegans locomotion is regulated by the motor neurons found in the ventral nerve cord (VNC). The somas of all motor neurons are located in the VNC and a subset send commissures to the dorsal side that run along the dorsal hypodermal ridge and form the dorsal nerve cord (DNC) which innervates the dorsal muscles. Interestingly, a previous RNAi screen revealed that a knockdown of DEX-1 resulted in failure of motor neuron commissures to reach the DNC (Schmitz *et al.* 2007). To determine if these effects were observable during dauer, we used transmission electron microscopy to observe the dorsal nerve cords of *dex-1(cs201)* and wild-type dauers. We found that while wild-type dauers had intact DNC commissure bundles, the DNC of *dex-1(cs201)* mutant dauers appeared defasciculated (Figure 4.2). Further, the dorsal hypodermal ridge appeared enlarged in *dex-1(cs201)* dauers compared to wild-type (Figure 4.2). This may suggest a role for DEX-1 in maintaining the integrity of the dorsal nerve cord, and the surrounding tissues.

The motor neurons facilitate locomotion in *C. elegans* through innervation of muscle cells via projections of muscle tissue called muscle arms (Dixon and Roy 2005)

(Figure 4.2). *C. elegans* typically extend a characteristic number of muscle arms during non-dauer development. However, previous work shows that dauer animals send additional, dauer-specific muscle arms to make connections with the nerve cord (Dixon *et al.* 2008). We hypothesized that these additional muscle arms may contribute to the rapid locomotion observed during dauer and that defects in *dex-1* may result in defects in neuromuscular connections between muscle arms and the nerve cords. Using the muscle arm reporter *trIs30[him-4p::yfp+hmr-1b::DsRed2+unc-129nsp::DsRed2]*, we determined that the average muscle arm width in a wild-type animal is roughly 1µm (See Materials and Methods). We then measured muscle arm width in *dex-1(cs201)* mutant dauers and found a statistically significant increase in the number of membranous muscle arms compared to wild-type dauers (Figure 4.3). This suggests that DEX-1 may play a role in muscle arm formation and locomotion behaviors. To determine if these defects in muscle arm formation were dauer-specific, we used the same quantification methods to investigate the comparable L3 stage. Surprisingly, we found that *dex-1(cs201)* non-dauer L3 animals also have a slight, yet statistically significant increase in abnormal muscle arms (Figure 4.4). However, the *dex-1(cs201)* L3 locomotion behaviors were unaffected (Figure 4.4).

While many morphological aspects of dauer formation are reversible upon recovery from dauer, the dauer-specific muscle arms are retained into adulthood (Dixon *et al.* 2008). Using our muscle arm marker, we observed the muscle arms in *dex-1(cs201)* and wild-type post-dauer adults and found that the *dex-1* mutants, again, showed an increased number of abnormal muscle arms compared to wild-type post-dauer adults (Figure 4.5A). To test whether these defects impaired post-dauer adult

locomotion, we used our previously developed locomotion assay (Flatt *et al.* 2019). Surprisingly, we found no differences in locomotion behaviors between *dex-1(cs201)* mutant or wild-type post-dauer adults (Figure 4.5C). Likewise, we observed similar results in both muscle arm morphology and locomotion between *dex-1(cs201)* and wild-type well-fed adults that had not gone through dauer (Figure 4.5, B and D). Taken together, these data suggest that while muscle arms by nature may be important for locomotion (Dixon *et al.* 2008), muscle arm morphology may not be consequential to non-dauer locomotion.

While investigating electron micrographs of *dex-1(cs201)* mutant and wild-type dauers, we anecdotally observed that the mitochondria of the *dex-1* mutants appear darkened with abnormal membranes and indistinct cristae, which are signs of mitochondrial distress and degeneration (Dagda *et al.* 2009) (Figure 4.2). Interestingly, similar signs of mitochondrial degradation were observed in the Duchenne's muscular dystrophy model, *dys-1*, albeit in non-dauer stages (Hughes et al., 2019). While the mitochondrial defects observed in *dex-1* mutant dauers are anecdotal observations, they may suggest a role for *dex-1* in maintaining tissue integrity during dauer. Future work is needed to determine if these *dex-1* mutant mitochondrial defects are exclusive to the dauer stage, and what role these defects may play in *dex-1* dauer locomotion defects.

4.4 DISCUSSION

Here we show that *dex-1* mutant dauers are sluggish and slightly uncoordinated following mechanical stimulation in contrast to the rapid locomotion observed in wild-

type dauers. We originally hypothesized that this dauer-specific defect in *dex-1* mutants could be due to the indistinct lateral alae observed on *dex-1* mutant dauers. However, our seam cell-specific rescue of *dex-1* resulted in a mosaic pattern of alae formation while completely rescuing the locomotion behavior. One explanation may be that DEX-1 acts cell-non autonomously to mediate dauer behaviors. Alternatively, our seam cell-specific promoter could drive undetectable expression in the neuromuscular system.

Previous RNA interference data showed that knockdown of *dex-1* results in low penetrance defects in motor neuron commissure formation (Schmitz *et al.* 2007). Indeed, our investigation into the ultrastructure of the *dex-1* mutant dauer neuromuscular system suggests that while wild-type dauers exhibit an intact DNC, the DNC of *dex-1* mutant dauers appears defasciculated which may influence the *dex-1* mutant dauers uncoordinated behaviors. Future experiments will aim to determine whether these defects in nerve cord structure are dauer specific, and how DEX-1 facilitates proper dorsal nerve cord organization.

Dauer larvae also exhibit changes in somatic muscle structure compared to non-dauers (Dixon *et al.* 2008). Nerve cords make connections with muscle cells via extensions of muscle tissue called muscle arms (Dixon and Roy 2005). Non-dauer animals develop a stereotypical number of muscle arms during early larval development. However, when animals are stimulated to enter dauer, they extend additional, dauer specific muscle arms to their respective nerve cords. While the function of these dauer-specific muscle arms is not known, it has been speculated that they may influence dauer-specific locomotion behaviors (Cassada and Russell 1975; Dixon *et al.* 2008). We show here that *dex-1* mutant dauers appear to have defects in

muscle arm morphology compared to wild-type dauers which we speculate may negatively impact *dex-1* mutant dauer locomotion. Interestingly, previous work has shown that muscle arms will extend to meet their respective nerve cords regardless of the nerve cord location (Hedgecock *et al.* 1990)(Figure 4.2). We hypothesized that defects in muscle arm formation may be a result of positional compensation due to defasciculation of the nerve cord in *dex-1* mutant dauer animals. Animals with defects in muscle arms are also often described as uncoordinated, suggesting that muscle arm morphology is important for proper locomotion (Dixon and Roy 2005). We therefore speculated that the defects in muscle arm morphology may negatively influence dauer locomotion. However, although we did observe statistically significant differences in muscle arm morphology between *dex-1* mutant and wild-type dauers, our investigation into whether these defects influenced dauer locomotion behaviors were inconclusive. While we observed abnormal muscle arms in all stages tested, we only observed locomotion defects in the dauer stage. This suggests that muscle arm morphology may not influence muscle arm function.

Finally, while investigating the ultrastructure of *dex-1* mutant dauers, we observed that the mitochondria of *dex-1* mutant dauers appeared dark and segmented compared to wild-type dauers. While mitochondria take on a condensed, electron dense conformation during dauer due to changes in respiratory rates and energy expenditure (Hackenbrock *et al.* 1971; Popham and Webster 1979), segmentation and membrane breakdown, which were also observed in *dex-1* mutant dauers, are signs of mitochondrial degeneration (Dagda *et al.* 2009). Interestingly, similar defects were observed in the *C. elegans* DMD mutant, *dys-1* (Hughes *et al.* 2019). DMD is a muscle-

wasting disease, which results in loss of locomotion due to muscle and mitochondrial degeneration (Goldstein and McNally 2010). Though our observations in the *dex-1(cs201)* mutant dauers were anecdotal, it is worth noting that loss of mitochondrial function may play a role in *dex-1* dauer locomotion defects. If this is the case, it will be interesting to determine how the degenerated dauer mitochondria recover to facilitate post-dauer adult locomotion.

4.5 FIGURES

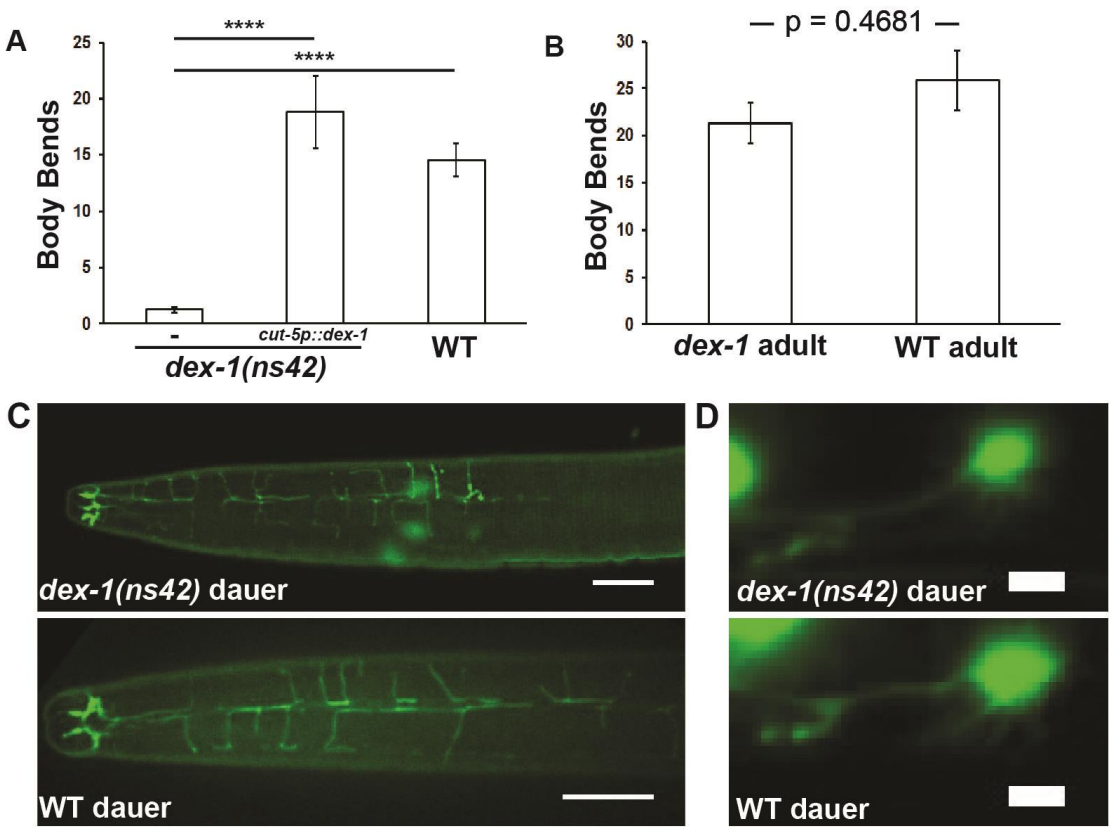

Figure 4.1: *dex-1(ns42)* dauers have defects in locomotion. (A) *dex-1(ns42)* dauers are less responsive when mechanically stimulated compared to wild-type dauers. Seam cell-specific expression of *dex-1* rescues the locomotion phenotype to wild-type levels. **** indicates statistical significance at P < 0.0001 (n =40). (B) The locomotion defect in *dex-1(ns42)* dauers is dauer-specific, as non-dauer *dex-1(ns42)* adults move at wild-type levels when mechanically stimulated (n =40). Error bars indicate SEM. (C) Dorsoventral confocal images of the inner labial 2 (IL2) neurons in *dex-1(ns42)* (top) and wild-type (bottom) dauers. Bar, 10 mm. (D) Lateral view micrographs of the anterior deirid (ADE) neurons in *dex-1(ns42)* (top) and wild-type (bottom) dauers. We did not observe any structural differences in either the IL2 or deirid neurons. Bar, 1 mm.

Figure 4.2: *dex-1(cs201)* appear to have defects in nerve cord organization and mitochondrial structure. Electron micrographs showing cross-sections of the dorsal nerve cords (false colored pink) in a *dex-1(cs201)* mutant (top) and wild-type (bottom) dauer. The nerve cord of the *dex-1(cs201)* dauer appears defasciculated compared to the wild-type dauer. A muscle cell (false colored blue) extends a muscle arm to the defasciculated nerve cord in the *dex-1(cs201)* mutant dauer. Additionally, the dorsal hypodermal ridge (false colored green) of the *dex-1(cs201)* mutant dauer is enlarged. The mitochondria (*) of the *dex-1(cs201)* mutant dauer also show signs of degeneration which were not observed in wild-type dauers. Scale bar, 500nm

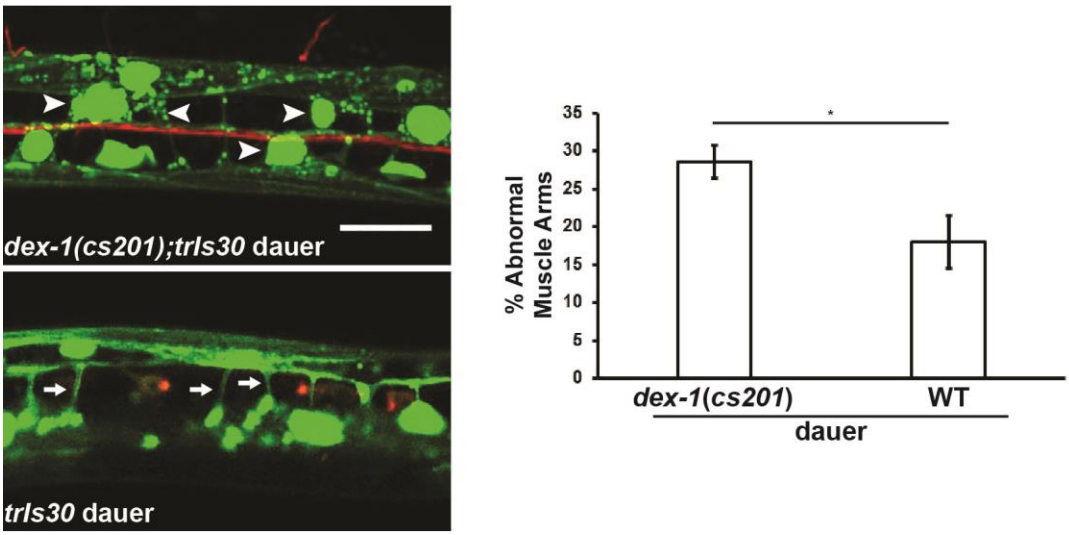

Figure 4.3: *dex-1(cs201)* mutant dauers have abnormal muscle arms. Dorsoventral view micrographs of a *dex-1(cs201)* dauer (top) and a wild type dauer (bottom) expressing the *trIs30[him-4p::yfp+hmr-1b::DsRed2+unc-129nsp::DsRed2]* reporter. The muscle arms of *dex-1(cs201)* mutant dauers appeared membranous (arrowheads) compared to those in wild-type dauers (arrows). Scale bar, 10µm. Quantification of muscle arm defects revealed that *dex-1(cs201)* dauers have a high percentage of abnormal muscle arms than wild-type dauers. (n = 10). Error bars indicate SEM. * indicates significance at $P < 0.05$.

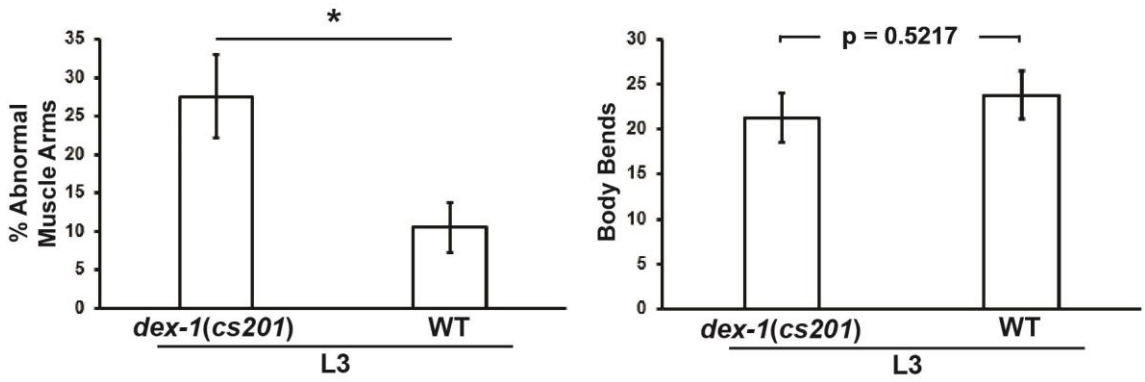

Figure 4.4: *dex-1(cs201)* L3 larvae have abnormal muscle arms and wild-type locomotion behaviors. Non-dauer L3 larvae show a slight but significant increase in abnormal muscle arms compared to wild-type L3s. (n=10). * indicates statistical significance at $P < 0.05$. However, locomotion behaviors are not affected, as *dex-1(cs201)* L3s moved at wild-type levels following mechanical stimulation. (n=25). Error bars, SEM.

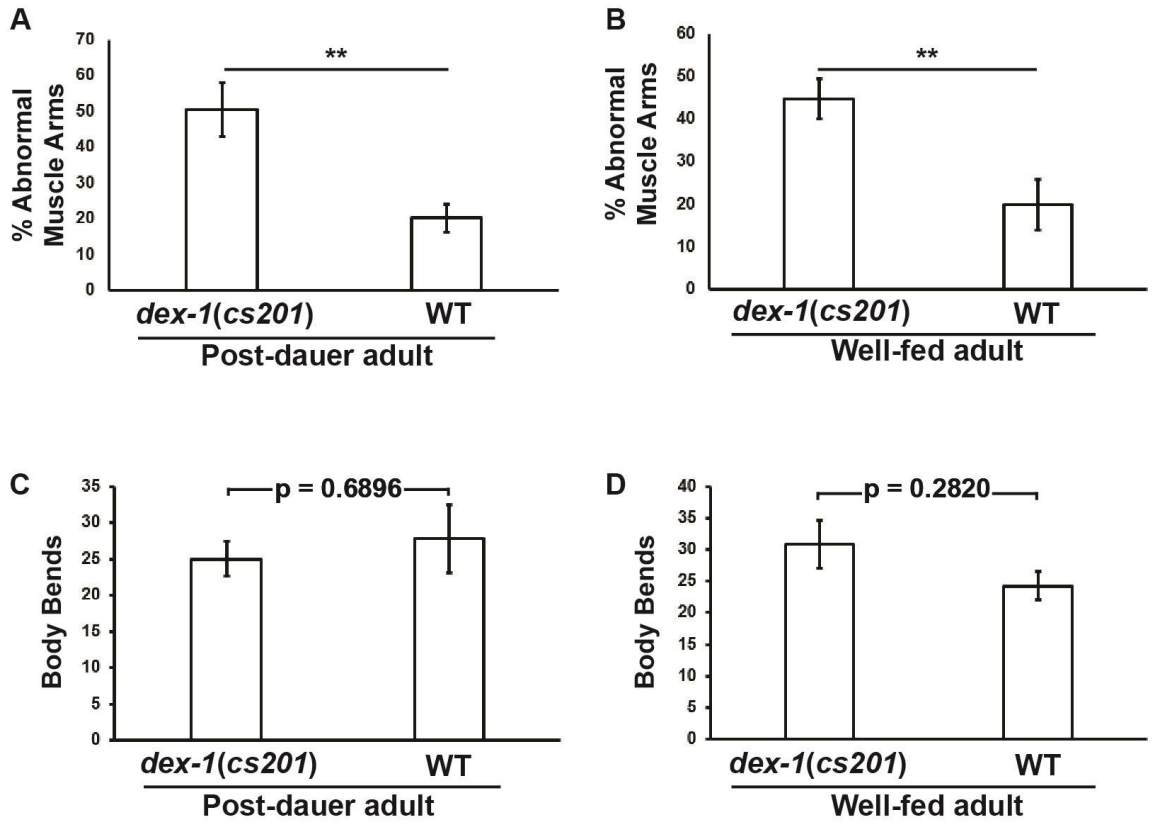

Figure 4.5: Abnormal muscle arm defects do not affect adult locomotion behavior. (A and B) Both post-dauer and well-fed *dex-1(cs201)* adult animals have an increased number of abnormal muscle arms compared to wild-type adults. (C and D) The abnormal muscle arms observed in *dex-1(cs201)* adult animals do not affect locomotion behaviors. (n = 25). Error bars represent SEM. ** indicates significance at $P < 0.01$.

CHAPTER 5: DEX-1 IS REGULATED BY THE FOXO TRANSCRIPTION FACTOR DAF-16 DURING DAUER FORMATION

This chapter is adapted, in part, from Flatt *et al.* 2019.

5.1 INTRODUCTION

The decision to enter dauer typically results in an all-or-none phenotype where dauers have every dauer morphological characteristic. However, mutations in some genes necessary for dauer formation result in an intermediate dauer phenotype, called partial dauers, in which the animals will display some, but not all, dauer characteristics (Albert and Riddle 1988). For example, when food availability is restricted, reduced insulin signaling promotes dauer formation via the sole *C. elegans* ortholog of human FOXO transcription factor, DAF-16 (Lin *et al.* 1997; Ogg *et al.* 1997; Lee *et al.* 2001). Mutations in *daf-16* result in animals incapable of forming true dauers under natural, dauer-inducing conditions. However, when exposed to high dauer pheromone concentrations, *daf-16* mutants can enter into a transient 'partial dauer' stage in which the animals arrest following a pre-dauer L2 stage, but exhibit defects in some dauer-specific characteristics (Vowels and Thomas 1992; Gottlieb and Ruvkun 1994). During reproductive development, DAF-16 is excluded from the nucleus and remains in the cytosol. However, when animals are stimulated to enter dauer, DAF-16 is translocated into the nucleus where it regulates several aspects of dauer formation. Here, we show that *dex-1* expression during dauer is regulated by the transcription factor DAF-16.

5.2 MATERIALS AND METHODS

Strains and plasmids. All strains were grown under standard conditions unless otherwise noted (Brenner 1974). The wild-type Bristol N2 strain, CHB27 *dex1(ns42)* III, and DR27 *daf-16(m27)* III were used for seam cell analyses. All mutant strains were backcrossed at least twice. The *dex-1(ns42)* mutant strain and the pMH111 *dex-1p(5.7 kb)::gfp* and pMH125 *dex-1p(2.1 kb):: gfp* plasmids were a generous gift from Dr. Maxwell Heiman (Department of Genetics, Harvard University, Boston, MA) (Heiman and Shaham 2009). The insulin response sequence was deleted from pMH111 using the Q5 Site Directed Mutagenesis Kit (E05525; New England Biolabs). For a complete list of primers and plasmids, please see the Supplemental Table. Animals containing extrachromosomal arrays were generated using standard microinjection techniques (Mello *et al.* 1991), and genotypes confirmed using PCR analysis and observation of co-injection markers. Adult animals were injected with 20 ng/ml of plasmid and 80 ng/ml of *unc-122p::gfp* as the co-injection marker.

Dauer formation. Dauers were induced using plates containing high concentrations (EC_{90}) of crude dauer pheromone extracted by previously established procedures (Vowels and Thomas 1992; Schroeder and Flatt 2014).

***dex-1* expression analysis.** To analyze *dex-1p::gfp* expression in the seam, images of dauer animals were taken using identical fluorescence settings and exposure times (10ms). The fluorescence intensities of the V2pap, V2ppp, and V3pap seam cells were measured using established methods (McCloy *et al.* 2014). Each cell was outlined and

the area, integrated density, and mean gray value were measured. Measurements were also taken for areas without fluorescence surrounding the cell. The total corrected cell fluorescence [TCCF=integrated density^2 (area of selected cell X mean fluorescence of background reading)] was calculated for each cell. The intensities of the three cells from each worm were averaged such that each nematode comprised a single data point. Variability in copy number between *dex-1p::gfp* and *daf-16(m27); dex-1p::gfp* was controlled by using the same transgene in both wild-type and *daf-16(m27)* backgrounds. Multiple independent lines were examined. To control for potential variation in copy number between the *dex-1p(IRSΔ)::gfp* strain and *dex-1p::gfp*, we examined multiple independent lines. The data were analyzed using one-way ANOVA and Bonferroni's multiple comparisons test. Ten animals were measured for each genotype.

5.3 RESULTS

***dex-1* expression is regulated by the DAF-16 transcription factor.** To understand how *dex-1* expression is regulated, we examined the upstream region of *dex-1* for potential regulatory sites. Previous chromatin immunoprecipitation sequencing data identified a putative DAF-16 binding site ~3 kb up-stream of the *dex-1* coding region (Figure 5.1A) (Celniker *et al.* 2009). DAF-16 is the sole *C. elegans* ortholog of the human Forkhead Box O-type transcription factor and a major regulator of the dauer decision (Lin *et al.* 1997; Ogg *et al.* 1997). To examine whether this region affects expression of *dex-1*, we first expressed GFP from a truncated 2.1 kb *dex-1* promoter that does not include the putative DAF-16 binding site. Unlike the 5.7 kb *dex-1p::gfp* promoter fusion, which resulted in GFP expression in the seam cells exclusively during

dauer (Figure 3.2, A and B), the shorter *dex-1* promoter drove GFP expression in the seam cells during all larval stages (Figure 5.1B). This suggests that *dex-1* is repressed during non-dauer stages and activated by DAF-16 during dauer. To further examine if DAF-16 is regulating *dex-1* expression during dauer, we examined the expression of the 5.7 kb *dex-1p::gfp* reporter in a *daf-16(m27)* mutant background. While mutations in daf-16 result in animals incapable of forming dauers, under high-pheromone concentrations, *daf-16(m27)* mutants can enter into a partial dauer state with some dauer morphological characteristics (Vowels and Thomas 1992; Gottlieb and Ruvkun 1994). *daf-16(m27)* partial dauers are identifiable by body morphology and the presence of indistinct lateral alae (Vowels and Thomas 1992). We found that the fluorescence intensity of *dex-1p::gfp* was significantly reduced in *daf-16(m27)* partial dauers compared to wild type, suggesting that DAF-16 regulates *dex-1* seam cell expression during dauer (Figure 5.1, C and D).

FOXO/DAF-16 binds to canonical DAF-16 binding elements and insulin response sequences (IRS) (Paradis and Ruvkun 1998; Obsil and Obsilova 2008). Within the chromatin immunoprecipitation sequencing–identified region (Celniker *et al.* 2009), we identified a putative IRS binding site (Figure 5.1A). To determine whether the identified DAF-16 IRS site directly regulates *dex-1* expression, we deleted the IRS sequence in the 5.7 kb *dex-1* promoter region used to drive GFP. We found that deleting the IRS sequence results in reduced GFP expression in the seam cells during dauer, similar to the levels observed in *daf-16* partial dauers (Figure 5.1, C and D). Taken together, these results indicate the 2.1 kb region proximal to the *dex-1* start codon drives expression in the seam cells, and that an unidentified element within the 3.6 kb region

upstream from the 2.1 kb activation site represses expression outside of dauer. This repression is counteracted by DAF-16 binding to the IRS during dauer formation.

5.4 DISCUSSION

Dissection of the genetic pathways regulating the decision to enter dauer has revealed insights into TGF-β, insulin, and hormone signaling (Thomas *et al.* 1993; Gottlieb and Ruvkun 1994; Riddle and Albert 1997). The FOXO transcription factor DAF-16 is a well-known regulator of the dauer formation decision by acting downstream of the insulin/IGF-1 receptor DAF-2 (Gottlieb and Ruvkun 1994; Ogg *et al.* 1997). Dauer-inducing environmental conditions lead to a translocation of DAF-16 to the nucleus, where it activates dauer formation pathways (Lee *et al.* 2001; Fielenbach and Antebi 2008). We found that *dex-1* expression during dauer is regulated by DAF-16. Based on our results, we propose that DEX-1 is repressed during non-dauer postembryonic stages and DAF- 16 serves to activate *dex-1* expression via an upstream non-canonical insulin response sequence. One hypothesis is that genetic repression of *dex-1* expression by *daf-12* during non-dauer stages is alleviated by DAF-16 translocation during dauer. Previous chromatin immunoprecipitation-sequencing also identified a putative DAF-12 binding site in the upstream region of *dex-1* in nearly the same location as our identified DAF-16 IRS binding site (Celniker *et al.* 2009; Snyder *et al.* 2011). During non-dauer stages, the nuclear hormone receptor DAF-12 is bound by DAF-9 and promotes reproductive development through activation of gene expression (Gerisch *et al.* 2004). In our working hypothesis, while DAF-9-bound DAF-12 would not directly repress *dex-1* expression, DAF-12 binding in this region may indirectly ‘block’

expression of *dex-1* during non-dauer stages. When conditions become unfavorable, DAF-9 production is down regulated, and DAF-12 is bound by the DIN-1/SHARP complex (Ludewig *et al.* 2004). This change in binding partner represses DAF-12 transcriptional activation and promotes dauer entry. Interestingly, DIN-1/SHARP-bound DAF-12 promotes translocation of DAF-16 from the cytoplasm to the nucleus during dauer formation (Hochbaum *et al.* 2011). Thus, it may be that DAF-12 acts to both repress and activate *dex-1* expression during dauer formation. Future work is necessary to characterize this putative DAF-12 binding site and determine what role it may play in dauer morphogenesis.

5.5 FIGURE

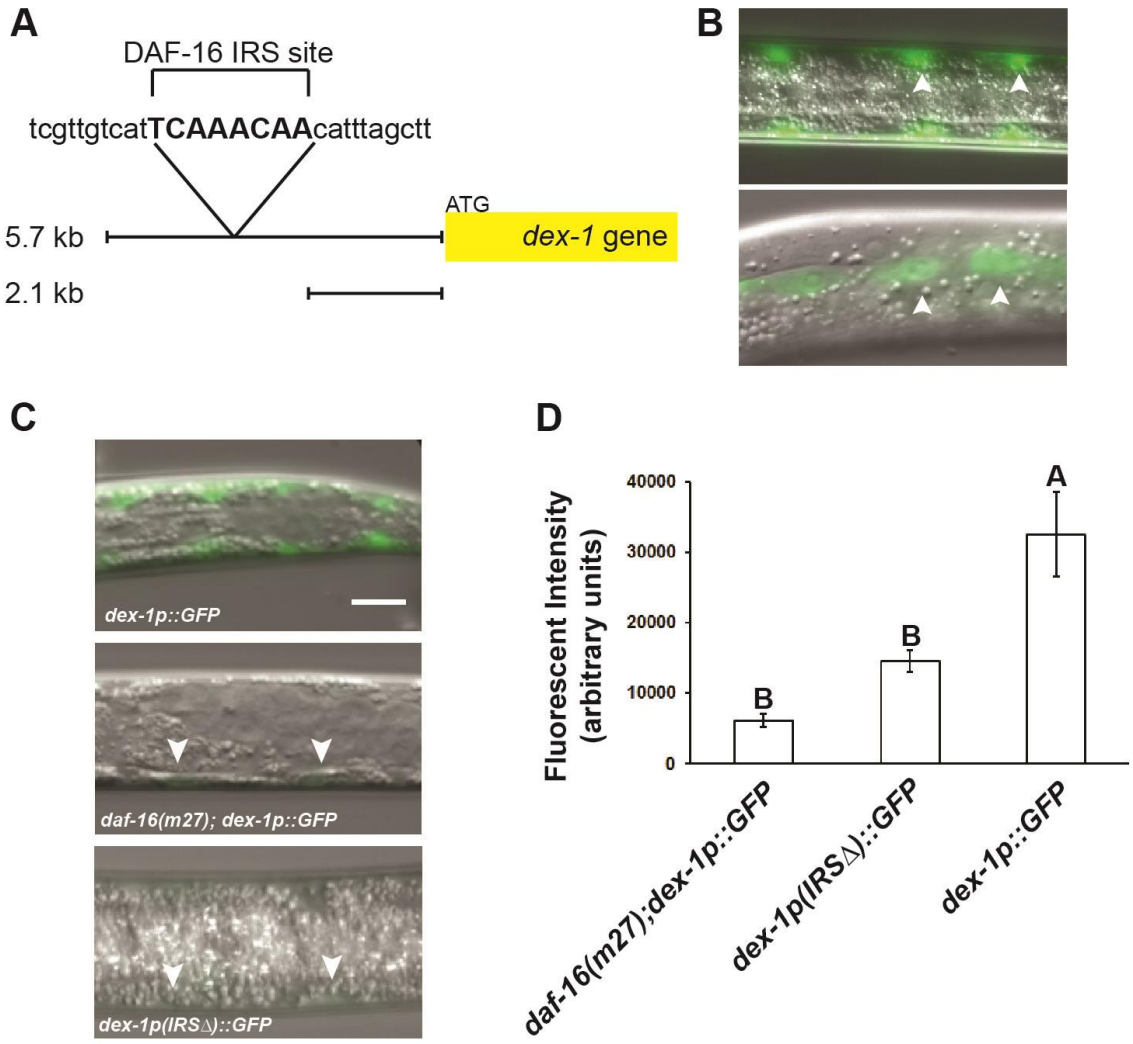

Figure 5.1: *dex-1* expression in the seam cells is regulated by DAF-16. (A) We identified a putative DAF-16 IRS binding site (in capitals) 3 kb upstream from the *dex-1* ATG start site. (B) Expression of *dex-1p::gfp* from a truncated 2.1 kb *dex-1* promoter drives fluorescence in the seam cells (arrowheads) in both dauer (top) and non-dauer (bottom) stages. Bar, 10 mm. (C) Dorsoventral view micrographs of GFP expression from the 5.7 kb *dex-1* promoter in a wild-type background (top) produces bright fluorescence in the seam cells during dauer (also see Figure 5A). Fluorescence intensity is reduced in a *daf-16(m27)* partial dauer mutant background (middle). Deletion of the DAF-16 IRS sequence (bottom) from the 5.7 kb promoter region also significantly reduces GFP expression in the seam cells during dauer. Arrowheads indicate seam cells. Bar, 10 mm. (D) Quantification of GFP expression driven by the 5.7 kb *dex-1* promoter in dauers. ** and *** indicate statistical significance at $P < 0.01$ and $P < 0.001$, respectively. Error bars indicate SEM.

CHAPTER 6: *DEX-1* GENETICALLY INTERACTS WITH ZONA PELLUCIDA-DOMAIN PROTEINS TO FACILITATE DAUER MORPHOGENESIS

This chapter is adapted, in part, from Flatt *et al.* 2019.

6.1 INTRODUCTION

DEX-1 was previously shown to function with the zona pellucida (ZP) domain-containing protein, DYF-7, to mediate dendrite extension during embryogenesis (Heiman and Shaham 2009). Our data suggest that DEX-1 acts along with additional ZP-domain proteins to regulate seam cell remodeling. Combined with previous data demonstrating a role for DEX-1 in sensory dendrite adhesion (Heiman and Shaham 2009), and recent data showing roles for DEX-1 in epithelial shaping in the embryo (Cohen *et al.* 2019), our data suggest that DEX-1 is an extracellular matrix (ECM) component that plays a role in modulating cell shape of several cell types throughout development.

6.2 MATERIALS AND METHODS

Strains and plasmids. All strains were grown under standard conditions unless otherwise noted (Brenner 1974). The wild-type Bristol N2 strain and the following mutant strains were used: FX01126 *cut-1(tm1126)* II, CHB27 *dex-1(ns42)* III, CB1372 *daf-7(e1372)* III, RB1574 *cut-6 (ok1919)* III, CB1372 *daf-7(e1372)* III, RB1629 *cut-5(ok2005)* X, SP1735 *dyf-7(m537)* X. All mutant strains were backcrossed at least twice.

dex-1(ns42) was a gift from Dr. Maxwell Heiman (Department of Genetics, Harvard University, Boston, MA) (Heiman and Shaham 2009). *cut-1(tm1126)* was provided by the Mitani Consortium (Department of Physiology, Tokyo Women's Medical University School of Medicine, Japan). ST65 *ncIs13[ajm- 1::gfp]* was used to observe the apical junctions of the seam cells (Köppen *et al.* 2001) and was provided by the CGC. The IL2 neurons were observed using PT2660 *myIs13[klp-6p::gfp+pBx]* III; PT2762 *myIs14[klp- 6p::gfp+pBx]* V and (Peden and Barr 2005; Schroeder *et al.* 2013).

Domain schematics were constructed using the wormweb.org Exon-Intron Graphic Maker. Domain locations were determined using the Simple Modular Architecture Research Tool domain prediction software (Schultz *et al.* 1998).

Dauer formation. Dauers were induced by one of two methods. For non-temperature-sensitive strains, we used plates containing crude dauer pheromone extracted by previously established procedures (Vowels and Thomas 1992; Schroeder and Flatt 2014). For temperature-sensitive strains with mutations in *daf-7(e1372)*, dauers were induced using the restrictive temperature of 25ºC (Riddle *et al.* 1981).

EMS Mutagenesis and Suppressor Screen. Synchronized populations of L4 animals were treated with ethyl methanesulfonate (EMS) using previously described procedures (Michaelson 2000). Briefly, L4 animals were incubated in 100mM EMS at 22ºC for 4 hours. Surviving animals were then isolated onto fresh, seeded NGM plates and allowed to recover. Recovered adults were allowed to lay eggs for 24 hours before being transferred to a fresh, seeded NGM plate. This was repeated twice. F1 eggs were

grown at the permissive temperature (15ºC) to adulthood and then shifted to 25ºC for 72 hours to induce F2 dauer formation. F2 populations were washed from the plate and treated with 1% SDS for 30 minutes. Suppressor mutants were recovered on seeded NGM plates at 15ºC.

Microscopy. Unless otherwise specified, animals were mounted onto 4% agarose pads and immobilized with 0.1 or 0.01 M levamisole for dauers and non-dauer or partial dauers, respectively. In our hands, dauers frequently lay in a dorsal-ventral position following anesthesia. Therefore, to image the lateral side, dauers were immobilized by mounting on 4% agarose pads with Polybead Polystyrene 0.10 mm microspheres (Polysciences Inc., #00876) (Kim *et al.* 2013). A Zeiss AxioImager microscope equipped with DIC and fluorescence optics was used to collect images.

Sodium dodecyl sulfate sensitivity assays. Sodium dodecyl sulfate (SDS) dose-response assays were performed using 12-well culture dishes containing M9 buffer and specified concentrations of SDS. Dauers were exposed to SDS for 30 minutes and scored as alive if movement was observed following stimulation with an eyelash pick. Each concentration was tested in triplicate with each experiment containing a separate wild-type (N2) control. Dose-response curves and LD50 values were determined by testing 20 dauers per treatment at each concentration, with three independent experiments. The LD50 and 95% confidence interval of each concentration was calculated using probit analysis in Minitab 18. LD50 values were considered significantly different if the 95% confidence intervals did not overlap. Significant difference was

denoted with a single asterisk. Single concentration assays were conducted at 0.1% SDS with 20 dauers for each genotype and three independent experiments. Data were analyzed using a one proportion exact method analysis in Minitab 18 and considered significantly different if the 95% confidence intervals did not overlap. Significant difference was denoted with a single asterisk.

6.3 RESULTS

Genetic interactions between *dex-1* and other extracellular matrix proteins may facilitate seam cell remodeling during dauer formation. DEX-1 acts with the ZP-domain protein DYF-7 to regulate primary dendrite extension during embryogenesis (Heiman and Shaham 2009). We therefore examined the *dyf-7(m537)* mutant for defects in dauer morphogenesis. Unlike *dex-1* mutants, *dyf-7* mutants are unable to enter dauer under typical dauer-inducing environmental conditions (Starich *et al.*), and so we examined *dyf-7* mutants in a *daf-c* mutant background. We observed that *daf-7;dyf-7* double mutants had normal dauer-specific radial shrinkage and IL2 dendrite arborization (Figure 6.1).

The cuticlin (CUT) proteins are a family of ZP-domain proteins originally isolated from nematode cuticles (Sebastiano *et al.* 1991). *cut-1* and *cut-5* are expressed in the seam cells, while *cut-6* is expressed in the surrounding hypodermis (Muriel *et al.* 2003; Sapio *et al.* 2005). Similar to *dex-1*, disruption of *cut-1*, *cut-5*, and *cut-6* results in dauers with incomplete radial shrinkage and defective alae formation (Sebastiano *et al.* 1991; Muriel *et al.* 2003; Sapio *et al.* 2005). We asked whether these defects in CUT mutant larvae were due to seam cell remodeling. We found that, similar to *dex-1(ns42)*, the

seam cells of the CUT mutant dauers were enlarged with jagged edges (Figure 6.2). Also similar to *dex-1(ns42)* mutants, we found that *cut-1(tm1126)* and *cut- 5(ok2005)* dauers were more sensitive to SDS compared with wild-type dauers (Figure 6.3, Table 6.1). Interestingly, while *cut-6(ok1919)* mutant dauers were resistant to the standard 1% SDS treatment (Muriel *et al.* 2003), we found that the *cut-6* mutant dauers were substantially more sensitive to SDS than wild-type dauers (Figure 6.3, Table 6.1). Taken together, these data indicate similar roles for DEX-1 and CUTs during dauer remodeling.

We hypothesized that, similar to its interaction with DYF-7 during embryogenesis, DEX-1 may genetically interact with the CUT proteins during dauer. We therefore examined double mutants of *dex-1(ns42)* with *cut-1(tm1126)*, *cut-5(ok2005)*, and *cut-6(ok1919)*. It is worth noting that, while the *cut* mutations are all deletion alleles (Figure 6.4), these data should be interpreted with caution as *dex-1(ns42)* is a hypomorphic allele. The *dex-1; cut-1* double mutant did not enhance SDS sensitivity beyond the *dex-1* single mutant, suggesting that they may act in the same pathway to regulate dauer remodeling (Figure 6.3, Table 6.1). The *dex-1; cut-5* double mutant was synthetically lethal during embryogenesis or early L1. This is similar to the *dex-1(ns42); dyf-7* double mutant (Heiman and Shaham 2009) and the severe loss-of- function mutant *dex-1(cs201)* (Cohen *et al.* 2019), suggesting that in addition to roles in dauer remodeling, CUT-5 has additional roles during early development. Interestingly, the *dex-1 cut-6* double mutant was intermediate in SDS sensitivity between the *dex-1* and *cut-6* single mutant (Figure 6.3, Table 6.1). We further tested the *cut* mutant phenotypes by generating double mutants between each of the *cut* mutants (Figure 6.3, Table 6.1).

The *cut-1; cut-5* double mutant showed a significant reduction of SDS resistance compared to single mutants alone. Interestingly, the *cut-1; cut-6* double mutants retained the *cut-6* SDS sensitivity phenotype. The *cut-6; cut-5* dauers showed a drastic increase in sensitivity to SDS compared to single mutants. In addition, the *cut-6; cut-5* double mutant showed a severe dumpy phenotype in all developmental stages. These results suggest that CUT-5 and CUT-6, like DEX-1 (Cohen *et al.* 2019), also play broader roles during development.

To identify potential biochemical interactors of *dex-1*, we performed a mutagenesis screen and selected for mutants that suppressed the *dex-1* mutant dauer SDS defect. To do this, we first mutagenized *dex-1(ns42);daf-7(e1735)* L4 animals using standard EMS protocols (Michaelson 2000). We then treated the mutagenized animals with 1% SDS for 30 minutes to isolate animals with suppressed SDS sensitivity. Using this method, we isolated 6 potential suppressor mutants of *dex-1* that were able to withstand 1% SDS treatment. Interestingly, while the SDS sensitivity of the recovered suppressor mutants was mitigated, the radial shrinkage defects were not. This agrees with previous reports that radial shrinkage and alae formation are not necessary for SDS resistance during dauer (Riddle *et al.* 1981).

6.4 DISCUSSION

Here we show that DEX-1 acts along with ZP-domain proteins to control dauer tissue remodeling. While the CUT mutants are all deletion alleles that disrupt the ZP domains and, therefore, likely functional null (Figure 6.4), the *dex-1(ns42)* allele is a nonsense mutation late in the coding region (Heiman and Shaham 2009). Our isolation

of the larval lethal *dex-1(cs201)* allele suggests that *dex-1(ns42)* is hypomorphic. Therefore, our *dex-1* genetic interaction experiments should be interpreted with caution. In addition to this complication, our double-mutant experiments do not provide a clear interaction pathway. For example, our results suggest that deletion of *cut-6* abrogates loss of *cut-1*. One possible explanation is a compensatory mechanism in the ECM, where loss of one ECM protein leads to increased expression of other structural components. This was previously shown in cases of osteogenesis imperfecta, where mutations in type I collagen led to increases in levels of thrombospondin and fibronectin (Fedarko *et al.* 2009). Alternatively, while we did not observe any obvious defects in the dauer formation decision in any of the double mutants, it is possible that slight differences in the ability to form dauers bias our observations toward individuals with only mild remodeling defects.

It has been proposed that biochemical compaction of the CUTs in the extracellular space between the seam and the hypodermis causes radial constriction, and thus forms the lateral alae via a “CUT tether” (Sapio *et al.* 2005).We add to this by proposing that DEX-1 is another seam-specific epidermal matrix component that, along with ZP CUTs, facilitates apical constriction of the seam and formation of dauer alae (Figure 6.5). Our data indicate that DEX-1 acts in a cell- autonomous manner directly beneath the edges of the lateral alae. Although expression of *dex-1* in the hypodermis was sufficient to partially rescue dauer-specific radial shrinkage, hypodermal expression failed to rescue the lateral alae phenotype. We therefore propose DEX-1 may act as a secreted protein during dauer with restricted localization to the cuticle or ECM immediately above the apical membrane of the seam cells. During embryogenesis,

DEX-1 is secreted and localized to the dendritic tips (Heiman and Shaham 2009). DEX-1 may serve to couple physical interactions between the remodeled cuticular ECM and seam cell shape. Failure of these tissues to properly compact and thicken due to a loss of DEX-1 could lead to an overall weakening of the cuticle, and thus result in the SDS sensitivity observed in *dex-1* mutant dauers. Interestingly, results from our suppressor screen suggest that the SDS sensitivity phenotype is likely due to defects in the structural integrity of the cuticle and not radial shrinkage or alae formation. While the SDS sensitivity of our isolated suppressor mutants was restored to wild-type levels at 1% SDS concentration, the suppressor mutants retained the *dex-1* mutant dauer body morphology. Interestingly, previous reports show that while the uncloned 'process' mutant *daf-13* forms dauers that wild-type for radial shrinkage and alae formation, they are sensitive to standard SDS treatments (Riddle *et al.* 1981). This suggests that dauer SDS resistance is acquired independently of seam cell remodeling and alae formation. In the future, it will be interesting to map these *dex-1* suppressor mutants to determine the biochemical interactors of DEX-1 during dauer.

6.5 FIGURES AND TABLE

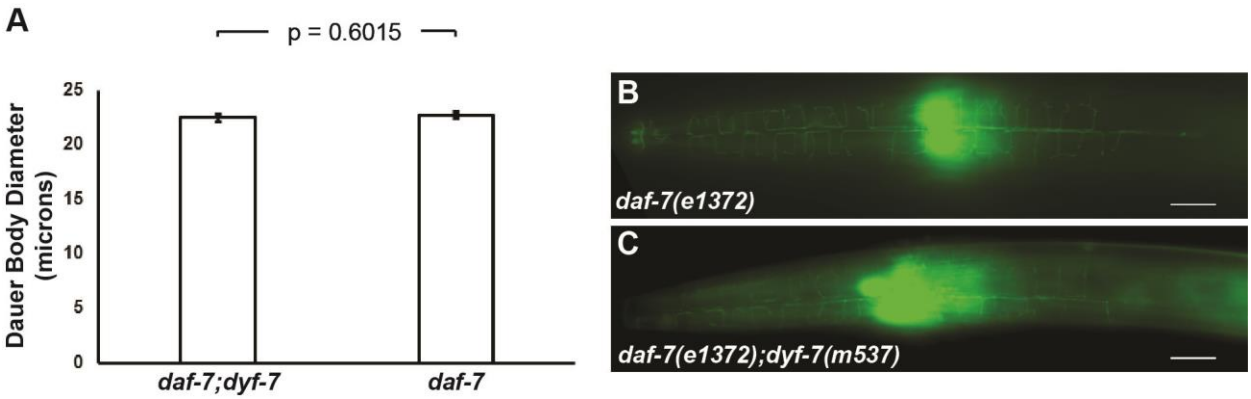

Figure 6.1: *dyf-7(m537)* dauers are wild-type for dauer-specific radial constriction and IL2 remodeling. (A) *daf-7(e1372);dyf-7(m537)* dauers undergo radial constriction similar to *daf-7(e1372)* dauers. Error bars, SEM. (n = 15). (B and C) We observed no apparent defects in IL2 remodeling between (B) *daf-7(e1372)* and (C) *daf-7(e1372);dyf-7(m537)* dauers. Scale bar, 10μm.

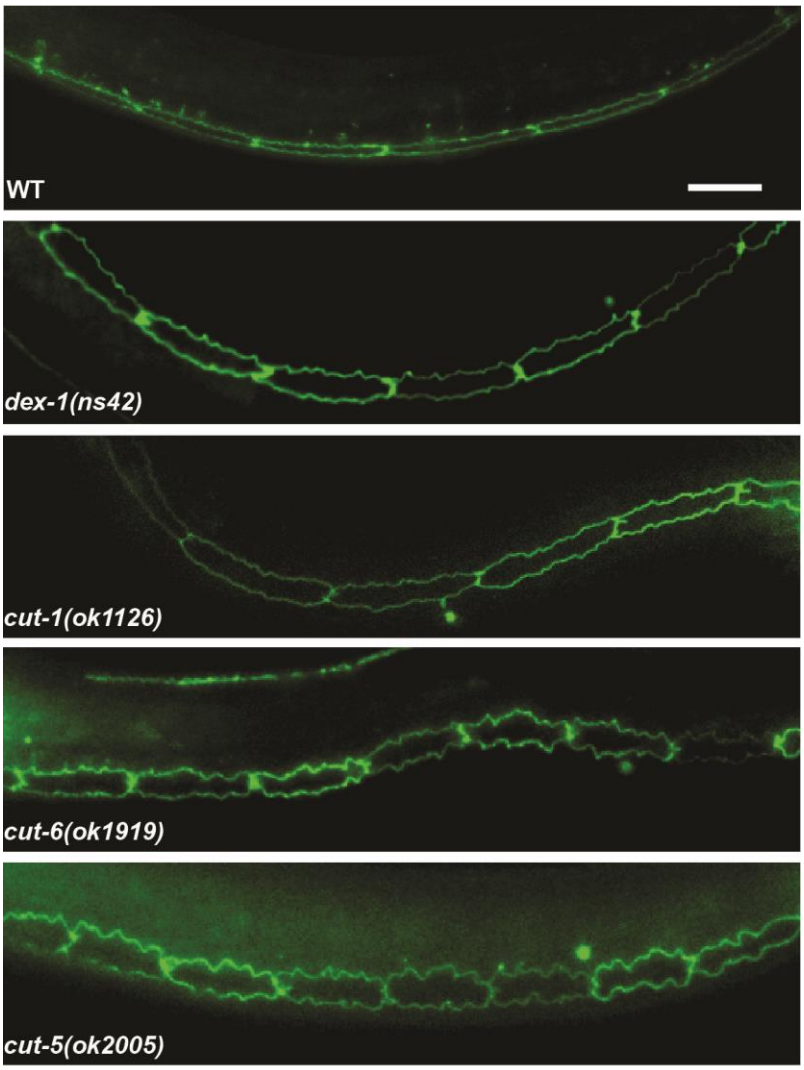

Figure 6.2: Cuticlin mutants phenocopy the *dex-1* mutant seam cell phenotype during dauer. Lateral view of wild-type, *dex-1(ns42)*, and cuticlin mutant dauers expressing the apical junction marker *ajm-1::gfp*. The seam cells in cuticlin mutants are jagged and wider, closely resembling those of *dex-1(ns42)* mutant dauers. Bar, 10 mm.

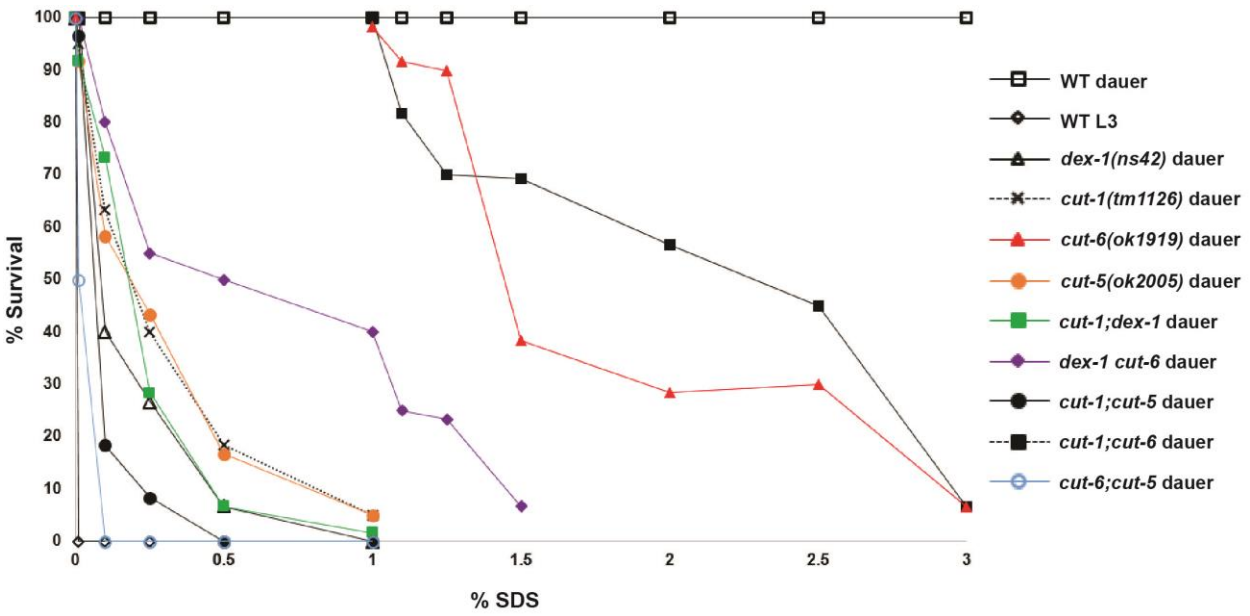

Figure 6.3: Dose response curve for wild-type, single- and double-mutant animals. Wild-type dauers were resistant to high concentrations of SDS, while non-dauer animals were sensitive to all tested concentrations. *dex-1(ns42)* and CUT mutant dauers showed intermediate SDS sensitivity phenotypes. Double mutants of *dex-1(ns42)* with CUT mutant dauers and double CUT-mutant dauers were also tested at varying concentrations of SDS.

Table 6.1. % SDS concentration necessary to kill 50% of animals tested for each genotype.

Strain	LD_{50}[a]
Wild-type dauer	>10% ± —
Wild-type L3	<0.01 ± —
dex-1(ns42)	0.15 ± 0.03
cut-1(tm1126)	0.28 ± 0.05
cut-6(ok1919)	2.02 ± 0.15
cut-5(ok2005)	0.25 ± 0.06
cut-1; dex-1	0.20 ± 0.03
dex-1 cut-6	0.71 ± 0.10
dex-1; cut-5	—[b]
cut-1; cut-5	0.08 ± 0.02
cut-1; cut-6	1.85 ± 0.10
cut-6; cut-5	0.01 ± —[c]

In all cases "-" indicates no variation. For WT dauer and L3 the LD50 was above or below the limits of the doses tested, respectively. For b (dex-1; cut-5), the LD50 was not determined due to the early larval lethality.

For c, (cut-6; cut-5) survival was exactly 50% at the lowest dose (0.01%) and there were no survivors at higher concentrations. Thus, no 95% CI is available using the Probit analysis.

[a] 50% lethal dose ± 95% confidence interval as determined by probit analysis. Genotypes with nonoverlapping confidence intervals are considered statistically different.

[b] Synthetic lethal at L1.

[c] Synthetic dumpy at all stages.

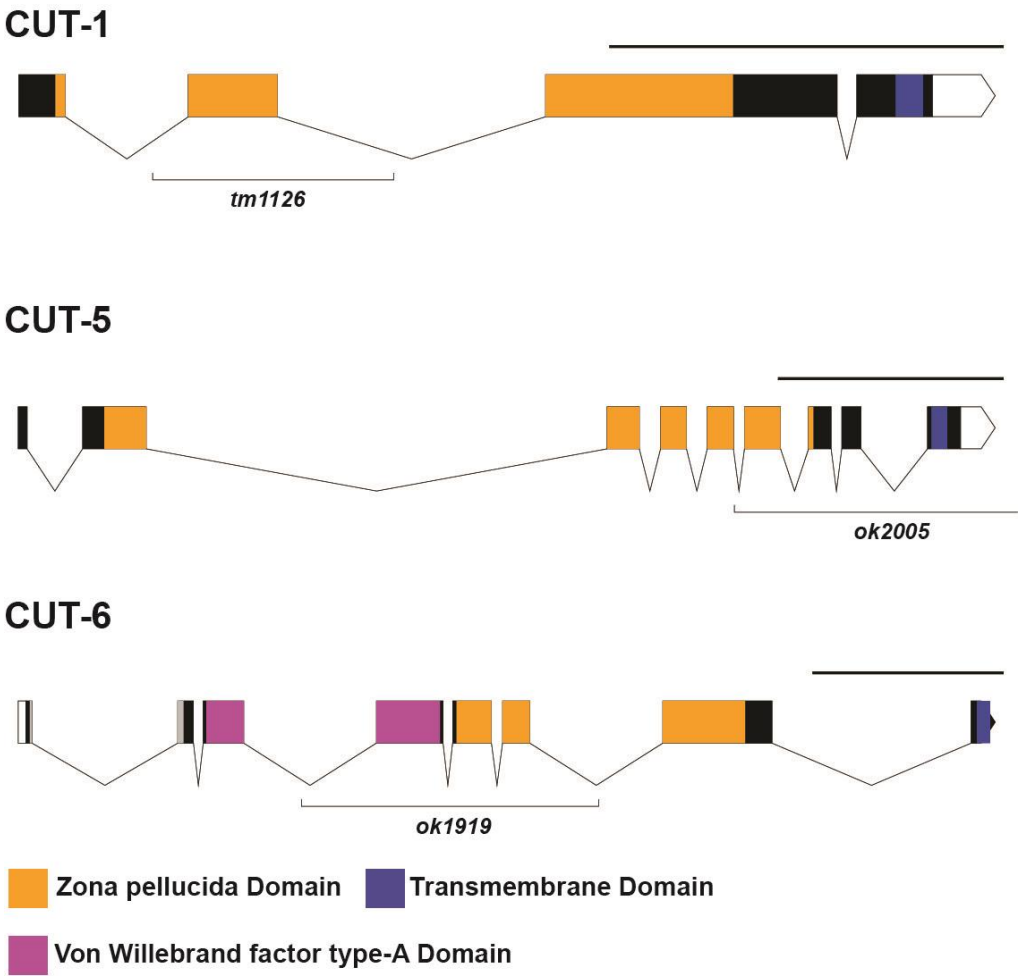

Figure 6.4: Gene schematics of cuticlins. CUT proteins share similar domains. CUT-1, CUT-5 and CUT-6 all contain zona pellucida domains and C-terminal transmembrane domains. CUT-6 alone also contains a Von Willebrand factor type-A domain near its N-terminal. The deletion mutations *cut-1(tm1126)*, *cut-5(ok2005)*, and *cut-6(ok1919)* all truncate parts of their respective ZP domains, likely resulting in functional nulls. The *cut-5(ok2005)* deletion extends 453 bases past the stop codon. Scale bars, 1kb.

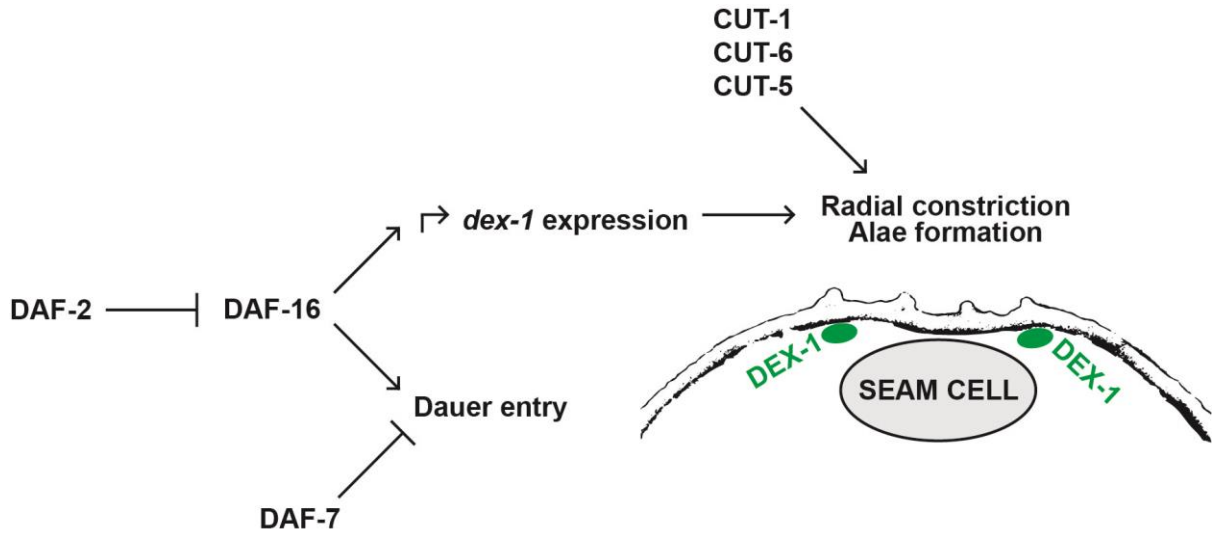

Figure 6.5: DEX-1 may function outside of the dauer decision pathway to facilitate dauer alae formation. A model diagram showing our proposed genetic pathway for *dex-1* transcriptional regulation. We show that during dauer, *dex-1(ns42)* is not suppressed by *daf-c* mutants and that *dex-1* is transcriptionally activated by DAF-16. We also show that DEX-1 functions as a secreted protein localized to the apical extracellular matrix that, along with the cuticlin proteins, facilitates dauer-specific radial constriction and alae formation.

REFERENCES

Ailion M., and J. H. Thomas, 2000 Dauer formation induced by high temperatures in *Caenorhabditis elegans*. Genetics 156: 1047–1067.

Akintola A. A., and D. van Heemst, 2015 Insulin, aging, and the brain: mechanisms and implications. Front. Endocrinol. (Lausanne). 6: 13. https://doi.org/10.3389/fendo.2015.00013

Albert P. S., and D. L. Riddle, 1983 Developmental alterations in sensory neuroanatomy of the *Caenorhabditis elegans* dauer larva. J. Comp. Neurol. 219: 461–81. https://doi.org/10.1002/cne.902190407

Albert P. S., and D. L. Riddle, 1988 Mutants of *Caenorhabditis elegans* that form dauer-like larvae. Dev. Biol. 126: 270–293. https://doi.org/10.1016/0012-1606(88)90138-8

Albertson D. G., and J. N. Thomson, 1976 The Pharynx of *Caenorhabditis elegans*. Philos. Trans. R. Soc. B Biol. Sci. 275: 299–325. https://doi.org/10.1098/rstb.1976.0085

American Psychological Association, 2018 *STRESS IN AMERICA ™ GENERATION Z*.

Androwski R. J., K. M. Flatt, and N. E. Schroeder, 2017 Phenotypic plasticity and remodeling in the stress-induced *Caenorhabditis elegans* dauer. Wiley Interdiscip. Rev. Dev. Biol. 6: e278. https://doi.org/10.1002/wdev.278

Apfeld J., and C. Kenyon, 1998 Cell Nonautonomy of *C. elegans* daf-2 Function in the Regulation of Diapause and Life Span. Cell 95: 199–210. https://doi.org/10.1016/S0092-8674(00)81751-1

Baba T., T. Shimizu, Y. Suzuki, M. Ogawara, K. Isono, *et al.*, 2005 Estrogen, Insulin, and Dietary Signals Cooperatively Regulate Longevity Signals to Enhance Resistance to Oxidative Stress in Mice. J. Biol. Chem. 280: 16417–16426. https://doi.org/10.1074/jbc.M500924200

Bainbridge C., A. Rodriguez, A. Schuler, M. Cisneros, and A. G. Vidal-Gadea, 2016 Magnetic orientation in *C. elegans* relies on the integrity of the villi of the AFD magnetosensory neurons. J. Physiol. 110: 76–82. https://doi.org/10.1016/j.jphysparis.2016.12.002

Bargmann C. I., and H. R. Horvitz, 1991 Chemosensory neurons with overlapping functions direct chemotaxis to multiple chemicals in *C. elegans*. Neuron 7: 729–742. https://doi.org/10.1016/0896-6273(91)90276-6

Birnby D. A., E. M. Link, J. J. Vowels, H. Tian, P. L. Colacurcio, *et al.*, 2000 A transmembrane guanylyl cyclase (DAF-11) and Hsp90 (DAF-21) regulate a common set of chemosensory behaviors in *Caenorhabditis elegans*. Genetics 155: 85–104.

Blaxter M. L., 1993 Cuticle surface proteins of wild type and mutant *Caenorhabditis elegans*. J. Biol. Chem. 268: 6600–6609.

Blelloch R., S. Santa Anna-Arriola, D. Gao, Y. Li, J. Hodgkin, *et al.*, 1999 The gon-1 Gene Is Required for Gonadal Morphogenesis in *Caenorhabditis elegans*. Dev. Biol. 382–393.

Bork P., and C. Sander, 1992 A large domain common to sperm receptors (Zp2 and Zp3) and TGF-?? type III receptor. FEBS Lett. 300: 237–240. https://doi.org/10.1016/0014-5793(92)80853-9

Bremner J. D., P. Randall, T. M. Scott, R. A. Bronen, J. P. Seibyl, *et al.*, 1995 MRI-

based measurement of hippocampal volume in patients with combat-related posttraumatic stress disorder. Am. J. Psychiatry 152: 973–81. https://doi.org/10.1176/ajp.152.7.973
Brenner S., 1974 The genetics of *Caenorhabditis elegans*. Genetics 77: 71–94.
Cassada R. C., and R. L. Russell, 1975 The dauerlarva, a post-embryonic developmental variant of the nematode *Caenorhabditis elegans*. Dev. Biol. 46: 326–342. https://doi.org/10.1016/0012-1606(75)90109-8
Celniker S. E., L. A. L. Dillon, M. B. Gerstein, K. C. Gunsalus, S. Henikoff, *et al.*, 2009 Unlocking the secrets of the genome. Nature 459: 927–30. https://doi.org/10.1038/459927a
Cinar H. N., and A. D. Chisholm, 2004 Genetic analysis of the *Caenorhabditis elegans* pax-6 locus: roles of paired domain-containing and nonpaired domain-containing isoforms. Genetics 168: 1307–22. https://doi.org/10.1534/genetics.104.031724
Clancy D. J., D. Gems, L. G. Harshman, S. Oldham, H. Stocker, *et al.*, 2001 Extension of Life-Span by Loss of CHICO, a Drosophila Insulin Receptor Substrate Protein. Science (80-.). 292: 104–106. https://doi.org/10.1126/science.1057991
Cohen J. D., K. M. Flatt, N. E. Schroeder, and M. V Sundaram, 2019 Epithelial Shaping by Diverse Apical Extracellular Matrices Requires the Nidogen Domain Protein DEX-1 in *Caenorhabditis elegans*. Genetics 211: 185–200. https://doi.org/10.1534/genetics.118.301752
Couet C., J. Delarue, T. Constans, and F. Lamisse, 1992 Age-Related Insulin Resistance; A Review. Horm. Res. 38: 46–50. https://doi.org/10.1159/000182483
Dagda R. K., S. J. Cherra, S. M. Kulich, A. Tandon, D. Park, *et al.*, 2009 Loss of PINK1 Function Promotes Mitophagy through Effects on Oxidative Stress and Mitochondrial Fission. J. Biol. Chem. 284: 13843–13855. https://doi.org/10.1074/jbc.M808515200
Dickinson D. J., and B. Goldstein, 2016 CRISPR-Based Methods for *Caenorhabditis elegans* Genome Engineering. Genetics 202: 885–901. https://doi.org/10.1534/genetics.115.182162
Dijke P. ten, M.-J. Goumans, and E. Pardali, 2008 Endoglin in angiogenesis and vascular diseases. Angiogenesis 11: 79–89. https://doi.org/10.1007/s10456-008-9101-9
Dimsdale J. E., 2008 Psychological stress and cardiovascular disease. J. Am. Coll. Cardiol. 51: 1237–46. https://doi.org/10.1016/j.jacc.2007.12.024
Dixon S. J., and P. J. Roy, 2005 Muscle arm development in *Caenorhabditis elegans*. Development 132: 3079–92. https://doi.org/10.1242/dev.01883
Dixon S. J., M. Alexander, K. K. M. Chan, and P. J. Roy, 2008 Insulin-like signaling negatively regulates muscle arm extension through DAF-12 in *Caenorhabditis elegans*. Dev. Biol. 318: 153–161. https://doi.org/10.1016/j.ydbio.2008.03.019
Doroquez D. B., C. Berciu, J. R. Anderson, P. Sengupta, and D. Nicastro, 2014 A high-resolution morphological and ultrastructural map of anterior sensory cilia and glia in *Caenorhabditis elegans*. Elife 3. https://doi.org/10.7554/eLife.01948
Egerman M. A., S. M. Cadena, J. A. Gilbert, A. Meyer, H. N. Nelson, *et al.*, 2015 GDF11 Increases with Age and Inhibits Skeletal Muscle Regeneration. Cell Metab. 22: 164–174. https://doi.org/10.1016/J.CMET.2015.05.010
Estevez M., L. Attisano, J. L. Wrana, P. S. Albert, J. Massagué, *et al.*, 1993 The daf-4

gene encodes a bone morphogenetic protein receptor controlling *C. elegans* dauer larva development. Nature 365: 644–649. https://doi.org/10.1038/365644a0
Facchini F. S., N. Hua, F. Abbasi, and G. M. Reaven, 2001 Insulin Resistance as a Predictor of Age-Related Diseases. J. Clin. Endocrinol. Metab. 86: 3574–3578. https://doi.org/10.1210/jcem.86.8.7763
Falk N., M. Lösl, N. Schröder, and A. Gießl, 2015 Specialized Cilia in Mammalian Sensory Systems. Cells 4: 500–19. https://doi.org/10.3390/cells4030500
Fedarko N. S., P. D'Avis, C. R. Frazier, M. J. Burrill, V. Fergusson, *et al.*, 2009 Cell proliferation of human fibroblasts and osteoblasts in osteogenesis imperfecta: Influence of age. J. Bone Miner. Res. 10: 1705–1712. https://doi.org/10.1002/jbmr.5650101113
Feingold K. R., 2007 Thematic review series: skin lipids. The role of epidermal lipids in cutaneous permeability barrier homeostasis. J. Lipid Res. 48: 2531–46. https://doi.org/10.1194/jlr.R700013-JLR200
Félix M. A., and C. Braendle, 2010 The natural history of *Caenorhabditis elegans*. Curr. Biol. 20.
Fielenbach N., and A. Antebi, 2008 *C. elegans* dauer formation and the molecular basis of plasticity. Genes Dev. 22: 2149–65. https://doi.org/10.1101/gad.1701508
Fire A., S. Xu, M. K. Montgomery, S. A. Kostas, S. E. Driver, *et al.*, 1998 Potent and specific genetic interference by double-stranded RNA in *Caenorhabditis elegans*. Nature 391: 806–811. https://doi.org/10.1038/35888
Flatt K. M., C. Beshers, C. Unal, J. D. Cohen, M. V Sundaram, *et al.*, 2019 Epidermal Remodeling in *Caenorhabditis elegans* Dauers Requires the Nidogen Domain Protein DEX-1. Genetics 211: 169–183. https://doi.org/10.1534/genetics.118.301557
Flibotte S., M. L. Edgley, I. Chaudhry, J. Taylor, S. E. Neil, *et al.*, 2010 Whole-Genome profiling of mutagenesis in *Caenorhabditis elegans*. Genetics. https://doi.org/10.1534/genetics.110.116616
Fujimoto D., and S. Kanaya, 1973 Cuticlin: A noncollagen structural protein from Ascaris cuticle. Arch. Biochem. Biophys. 157: 1–6. https://doi.org/10.1016/0003-9861(73)90382-2
Gaglia M. M., and C. Kenyon, 2009 Stimulation of movement in a quiescent, hibernation-like form of *Caenorhabditis elegans* by dopamine signaling. J. Neurosci. 29: 7302–14. https://doi.org/10.1523/JNEUROSCI.3429-08.2009
Gems D., A. J. Sutton, M. L. Sundermeyer, P. S. Albert, K. V King, *et al.*, 1998 *Two Pleiotropic Classes of daf-2 Mutation Affect Larval Arrest, Adult Behavior, Reproduction and Longevity in Caenorhabditis elegans*.
Gerisch B., C. Weitzel, C. Kober-Eisermann, V. Rottiers, and A. Antebi, 2001 A Hormonal Signaling Pathway Influencing *C. elegans* Metabolism, Reproductive Development, and Life Span. Dev. Cell 1: 841–851. https://doi.org/10.1016/S1534-5807(01)00085-5
Gerisch B., A. Antebi, and D. L. Riddle, 2004 Hormonal signals produced by DAF-9/cytochrome P450 regulate *C. elegans* dauer diapause in response to environmental cues. Development 131: 1765–76. https://doi.org/10.1242/dev.01068
Gill H. K., J. D. Cohen, J. Ayala-Figueroa, R. Forman-Rubinsky, C. Poggioli, *et al.*, 2016 Integrity of Narrow Epithelial Tubes in the *C. elegans* Excretory System Requires a

Transient Luminal Matrix. PLOS Genet. 12: e1006205. https://doi.org/10.1371/journal.pgen.1006205
Golden J. W., and D. L. Riddle, 1982 A pheromone influences larval development in the nematode *Caenorhabditis elegans*. Science 218: 578–80. https://doi.org/10.1126/SCIENCE.6896933
Golden J. W., and D. L. Riddle, 1984 The *Caenorhabditis elegans* dauer larva: Developmental effects of pheromone, food, and temperature. Dev. Biol. 102: 368–378. https://doi.org/10.1016/0012-1606(84)90201-X
Goldstein J. A., and E. M. McNally, 2010 Mechanisms of muscle weakness in muscular dystrophy. J. Gen. Physiol. 136: 29–34. https://doi.org/10.1085/jgp.201010436
Gottlieb S., and G. Ruvkun, 1994 daf-2, daf-16 and daf-23: genetically interacting genes controlling Dauer formation in *Caenorhabditis elegans*. Genetics 137: 107–20.
Graca L. S. da, K. K. Zimmerman, M. C. Mitchell, M. Kozhan-Gorodetska, K. Sekiewicz, *et al.*, 2004 DAF-5 is a Ski oncoprotein homolog that functions in a neuronal TGF beta pathway to regulate *C. elegans* dauer development. Development 131: 435–46. https://doi.org/10.1242/dev.00922
Greer E. R., C. L. Pérez, M. R. Van Gilst, B. H. Lee, and K. Ashrafi, 2008 Neural and molecular dissection of a *C. elegans* sensory circuit that regulates fat and feeding. Cell Metab. 8: 118–31. https://doi.org/10.1016/j.cmet.2008.06.005
Gu T., S. Orita, and M. Han, 1998 *Caenorhabditis elegans* SUR-5, a novel but conserved protein, negatively regulates LET-60 Ras activity during vulval induction. Mol. Cell. Biol. 18: 4556–4564. https://doi.org/10.1128/MCB.18.8.4556
Gunther C. V, L. L. Georgi, and D. L. Riddle, 2000 A *Caenorhabditis elegans* type I TGF beta receptor can function in the absence of type II kinase to promote larval development. Development 127: 3337–47.
Hackenbrock C. R., T. G. Rehn, E. C. Weinbach, and J. J. Lemasters, 1971 Oxidative phosphorylation and ultrastructural transformation in mitochondria in the intact ascites tumor cell. J. Cell Biol. 51: 123–37. https://doi.org/10.1083/jcb.51.1.123
Hahm J.-H., S. Kim, and Y.-K. Paik, 2009 Endogenous cGMP regulates adult longevity via the insulin signaling pathway in *Caenorhabditis elegans*. Aging Cell 8: 473–483. https://doi.org/10.1111/j.1474-9726.2009.00495.x
Hall D. H., R. Lints, and Z. Altun, 2005 Nematode Neurons: Anatomy and Anatomical Methods in *Caenorhabditis elegans*. Int. Rev. Neurobiol. 69: 1–35. https://doi.org/10.1016/S0074-7742(05)69001-0
Hall D. H., E. Hartwieg, and K. C. Q. Nguyen, 2012 *Modern Electron Microscopy Methods for C. elegans*. Elsevier Inc.
Hardy D. M., and D. L. Garbers, 1995 A sperm membrane protein that binds in a species-specific manner to the egg extracellular matrix is homologous to von Willebrand factor. J. Biol. Chem. 270: 26025–8. https://doi.org/10.1074/JBC.270.44.26025
Hedgecock E. M., and R. L. Russell, 1975 Normal and mutant thermotaxis in the nematode *Caenorhabditis elegans*. Proc. Natl. Acad. Sci. U. S. A. 72: 4061–5. https://doi.org/10.1073/pnas.72.10.4061
Hedgecock E. M., J. G. Culotti, and D. H. Hall, 1990 The unc-5, unc-6, and unc-40 genes guide circumferential migrations of pioneer axons and mesodermal cells on the epidermis in *C. elegans*. Neuron 4: 61–85. https://doi.org/10.1016/0896-

6273(90)90444-K
Heiman M. G., and S. Shaham, 2009 DEX-1 and DYF-7 Establish Sensory Dendrite Length by Anchoring Dendritic Tips during Cell Migration. Cell 137: 344–355. https://doi.org/10.1016/j.cell.2009.01.057
Hertweck M., C. Göbel, and R. Baumeister, 2004 *C. elegans* SGK-1 Is the Critical Component in the Akt/PKB Kinase Complex to Control Stress Response and Life Span. Dev. Cell 6: 577–588. https://doi.org/10.1016/S1534-5807(04)00095-4
Hills T., P. J. Brockie, and A. V Maricq, 2004 Dopamine and glutamate control area-restricted search behavior in *Caenorhabditis elegans*. J. Neurosci. 24: 1217–25. https://doi.org/10.1523/JNEUROSCI.1569-03.2004
Hinsch K. D., and E. Hinsch, 1999 The zona pellucida “receptors” ZP1, ZP2 and ZP3. Andrologia 31: 320–2.
Hochbaum D., Y. Zhang, C. Stuckenholz, P. Labhart, V. Alexiadis, *et al.*, 2011 DAF-12 Regulates a Connected Network of Genes to Ensure Robust Developmental Decisions, (S. K. Kim, Ed.). PLoS Genet. 7: e1002179. https://doi.org/10.1371/journal.pgen.1002179
Holzenberger M., J. Dupont, B. Ducos, P. Leneuve, A. Géloën, *et al.*, 2003 IGF-1 receptor regulates lifespan and resistance to oxidative stress in mice. Nature 421: 182–187. https://doi.org/10.1038/nature01298
Hughes K. J., A. Rodriguez, K. M. Flatt, S. Ray, A. Schuler, *et al.*, 2019 Physical exertion exacerbates decline in the musculature of an animal model of Duchenne muscular dystrophy. Proc. Natl. Acad. Sci. 116: 3508–3517. https://doi.org/10.1073/PNAS.1811379116
Inoue T., and J. H. Thomas, 2000 Targets of TGF-β Signaling in *Caenorhabditis elegans* Dauer Formation. Dev. Biol. 217: 192–204. https://doi.org/10.1006/dbio.1999.9545
Jia K., D. L. Riddle, D. Riddle, P. Lansdorp, F. Slack, *et al.*, 2004 The TOR pathway interacts with the insulin signaling pathway to regulate *C. elegans* larval development, metabolism and life span. Development 131: 3897–3906. https://doi.org/10.1242/dev.01255
Josso N., J. Y. Picard, R. Rey, and N. di Clemente, 2006 Testicular anti-Müllerian hormone: history, genetics, regulation and clinical applications. Pediatr. Endocrinol. Rev. 3: 347–58.
Karp X., and V. Ambros, 2012 Dauer larva quiescence alters the circuitry of microRNA pathways regulating cell fate progression in *C. elegans*. Development 139: 2177–86. https://doi.org/10.1242/dev.075986
Katsimpardi L., N. K. Litterman, P. A. Schein, C. M. Miller, F. S. Loffredo, *et al.*, 2014 Vascular and Neurogenic Rejuvenation of the Aging Mouse Brain by Young Systemic Factors. Science (80-.). 344: 630–634. https://doi.org/10.1126/science.1251141
Keane J., and L. Avery, 2003 Mechanosensory inputs influence *Caenorhabditis elegans* pharyngeal activity via ivermectin sensitivity genes. Genetics 164: 153–162. https://doi.org/10.1098/rstb.1976.0085
Kelley M., J. Yochem, M. Krieg, A. Calixto, M. G. Heiman, *et al.*, 2015 FBN-1, a fibrillin-related protein, is required for resistance of the epidermis to mechanical deformation during *C. elegans* embryogenesis. Elife 4.

https://doi.org/10.7554/eLife.06565
Kilian K. A., B. Bugarija, B. T. Lahn, and M. Mrksich, 2010 Geometric cues for directing the differentiation of mesenchymal stem cells. Proc. Natl. Acad. Sci. U. S. A. 107: 4872–7. https://doi.org/10.1073/pnas.0903269107
Kim S., and W. G. Wadsworth, 2000 Positioning of longitudinal nerves in *C. elegans* by nidogen. Science 288: 150–4. https://doi.org/10.1126/SCIENCE.288.5463.150
Kim K., K. Sato, M. Shibuya, D. M. Zeiger, R. A. Butcher, *et al.*, 2009 Two Chemoreceptors Mediate Developmental Effects of Dauer Pheromone in *C. elegans*. Science (80-.). 326: 994–998. https://doi.org/10.1126/SCIENCE.1176331
Kim E., L. Sun, C. V. Gabel, and C. Fang-Yen, 2013 Long-Term Imaging of *Caenorhabditis elegans* Using Nanoparticle-Mediated Immobilization, (A. Samuel, Ed.). PLoS One 8: e53419. https://doi.org/10.1371/journal.pone.0053419
Kimura K. D., H. A. Tissenbaum, Y. Liu, and G. Ruvkun, 1997 daf-2, an insulin receptor-like gene that regulates longevity and diapause in *Caenorhabditis elegans*. Science 277: 942–6. https://doi.org/10.1126/science.277.5328.942
Klass M., and D. Hirsh, 1976 Non-ageing developmental variant of *Caenorhabditis elegans*. Nature 260: 523–525. https://doi.org/10.1038/260523a0
Köppen M., J. S. Simske, P. A. Sims, B. L. Firestein, D. H. Hall, *et al.*, 2001 Cooperative regulation of AJM-1 controls junctional integrity in *Caenorhabditis elegans* epithelia. Nat. Cell Biol. 3: 983–991. https://doi.org/10.1038/ncb1101-983
Kramer J. M., 1997 *Extracellular Matrix*. Cold Spring Harbor Laboratory Press.
Lee R. Y. N., J. Hench, and G. Ruvkun, 2001 *Regulation of C. elegans DAF-16 and its human ortholog FKHRL1 by the daf-2 insulin-like signaling pathway*.
Lee T., T. Jarome, S.-J. Li, J. J. Kim, and F. J. Helmstetter, 2009 Chronic stress selectively reduces hippocampal volume in rats: a longitudinal magnetic resonance imaging study. Neuroreport 20: 1554–8. https://doi.org/10.1097/WNR.0b013e328332bb09
Lee H., M. Choi, D. Lee, H. Kim, H. Hwang, *et al.*, 2011 Nictation, a dispersal behavior of the nematode *Caenorhabditis elegans*, is regulated by IL2 neurons. Nat. Neurosci. 15: 107–112. https://doi.org/10.1038/nn.2975
Legan P. K., A. Rau, J. N. Keen, and G. P. Richardson, 1997 The mouse tectorins. Modular matrix proteins of the inner ear homologous to components of the sperm-egg adhesion system. J. Biol. Chem. 272: 8791–801. https://doi.org/10.1074/JBC.272.13.8791
Lehmann K., P. Seemann, J. Boergermann, G. Morin, S. Reif, *et al.*, 2006 A novel R486Q mutation in BMPR1B resulting in either a brachydactyly type C/symphalangism-like phenotype or brachydactyly type A2. Eur. J. Hum. Genet. 14: 1248–1254. https://doi.org/10.1038/sj.ejhg.5201708
Lehmann K., P. Seemann, F. Silan, T. O. Goecke, S. Irgang, *et al.*, 2007 A new subtype of brachydactyly type B caused by point mutations in the bone morphogenetic protein antagonist NOGGIN. Am. J. Hum. Genet. 81: 388–96. https://doi.org/10.1086/519697
Li W., S. G. Kennedy, and G. Ruvkun, 2003 daf-28 encodes a *C. elegans* insulin superfamily member that is regulated by environmental cues and acts in the DAF-2 signaling pathway. Genes Dev. 17: 844–58. https://doi.org/10.1101/gad.1066503
Li J., M. Tewari, M. Vidal, and S. S. Lee, 2007 The 14-3-3 protein FTT-2 regulates DAF-

16 in *Caenorhabditis elegans*. Dev. Biol. 301: 82–91. https://doi.org/10.1016/j.ydbio.2006.10.013
Libina N., J. R. Berman, and C. Kenyon, 2003 Tissue-Specific Activities of *C. elegans* DAF-16 in the Regulation of Lifespan. Cell 115: 489–502. https://doi.org/10.1016/S0092-8674(03)00889-4
Lin K., J. B. Dorman, A. Rodan, and C. Kenyon, 1997 *daf-16: An HNF-3/forkhead Family Member That Can Function to Double the Life-Span of Caenorhabditis elegans*.
Lin K., H. Hsin, N. Libina, and C. Kenyon, 2001 Regulation of the *Caenorhabditis elegans* longevity protein DAF-16 by insulin/IGF-1 and germline signaling. Nat. Genet. 28: 139–145. https://doi.org/10.1038/88850
Liu Z., and V. Ambros, 1989 Heterochronic genes control the stage-specific initiation and expression of the dauer larva developmental program in *Caenorhabditis elegans*. Genes Dev. 3: 2039–2049. https://doi.org/10.1101/gad.3.12b.2039
Liu T., K. K. Zimmerman, and G. I. Patterson, 2004 BMC Developmental Biology Regulation of signaling genes by TGFβ during entry into dauer diapause in *C. elegans*. BMC Dev. Biol. 4. https://doi.org/10.1186/1471-213X-4-11
Ludewig A. H., C. Kober-Eisermann, C. Weitzel, A. Bethke, K. Neubert, *et al.*, 2004 A novel nuclear receptor/coregulator complex controls *C. elegans* lipid metabolism, larval development, and aging. Genes Dev. 18: 2120. https://doi.org/10.1101/GAD.312604
Manning L., and J. Richmond, 2015 High-Pressure Freeze and Freeze Substitution Electron Microscopy in *C. elegans*, pp. 121–140 in *C. elegans: Methods and Applications*, edited by Biron D., Haspel G. Humana Press, Totowa, NJ.
McBeath R., D. M. Pirone, C. M. Nelson, K. Bhadriraju, and C. S. Chen, 2004 Cell shape, cytoskeletal tension, and RhoA regulate stem cell lineage commitment. Dev. Cell 6: 483–95.
McCloy R. A., S. Rogers, C. E. Caldon, T. Lorca, A. Castro, *et al.*, 2014 Partial inhibition of Cdk1 in G $_2$ phase overrides the SAC and decouples mitotic events. Cell Cycle 13: 1400–1412. https://doi.org/10.4161/cc.28401
Meléndez A., Z. Tallóczy, M. Seaman, E.-L. Eskelinen, D. H. Hall, *et al.*, 2003 Autophagy genes are essential for dauer development and life-span extension in *C. elegans*. Science 301: 1387–91. https://doi.org/10.1126/science.1087782
Mello C. C., J. M. Kramer, D. Stinchcomb, and V. Ambros, 1991 Efficient gene transfer in C.elegans: extrachromosomal maintenance and integration of transforming sequences. EMBO J. 10: 3959–70.
Michaelson L., 2000 *C. elegans*: A Practical Approach. Ian A. Hope (ed.). Oxford University Press, Oxford. 1999. Pp. 281. Price £29.95, paperback. ISBN 0 19 963738 5. Heredity (Edinb). 85: 99–99. https://doi.org/10.1046/j.1365-2540.2000.0745d.x
Mori I., and Y. Ohshima, 1995 Neural regulation of thermotaxis in *Caenorhabditis elegans*. Nature 376: 344–348. https://doi.org/10.1038/376344a0
Morris J. Z., H. A. Tissenbaum, and G. Ruvkun, 1996 A phosphatidylinositol-3-OH kinase family member regulating longevity and diapause in *Caenorhabditis elegans*. Nature 382: 536–539. https://doi.org/10.1038/382536a0
Murakami M., M. Koga, and Y. Ohshima, 2001 DAF-7/TGF-β expression required for

the normal larval development in *C. elegans* is controlled by a presumed guanylyl cyclase DAF-11. Mech. Dev. 109: 27–35. https://doi.org/10.1016/S0925-4773(01)00507-X
Muriel J. M., M. Brannan, K. Taylor, I. L. Johnstone, G. J. Lithgow, *et al.*, 2003 M142.2 (cut-6), a novel *Caenorhabditis elegans* matrix gene important for dauer body shape. Dev. Biol. 260: 339–351. https://doi.org/10.1016/S0012-1606(03)00237-9
Murphy S. L., K. D. Kochanek, J. Xu, and M. Heron, 2015 Deaths: Final Data for 2012. Natl. Vital Stat. Rep. 63: 1–117.
Naba A., K. R. Clauser, J. M. Lamar, S. A. Carr, and R. O. Hynes, 2014 Extracellular matrix signatures of human mammary carcinoma identify novel metastasis promoters. Elife 3: e01308. https://doi.org/10.7554/eLife.01308
Nass R., D. H. Hall, D. M. Miller, and R. D. Blakely, 2002 Neurotoxin-induced degeneration of dopamine neurons in *Caenorhabditis elegans*. Proc. Natl. Acad. Sci. U. S. A. 99: 3264–3269. https://doi.org/10.1073/pnas.042497999
Nguyen C. Q., D. H. Hall, Y. Yang, and D. H. A. Fitch, 1999 Morphogenesis of the*Caenorhabditis elegans*Male Tail Tip. Dev. Biol. 207: 86–106. https://doi.org/10.1006/dbio.1998.9173
Nika L., T. Gibson, R. Konkus, and X. Karp, 2016 Fluorescent Beads Are a Versatile Tool for Staging *Caenorhabditis elegans* in Different Life Histories. G3 Genes|Genomes|Genetics g3.116.030163. https://doi.org/10.1534/g3.116.030163
Obsil T., and V. Obsilova, 2008 Structure/function relationships underlying regulation of FOXO transcription factors. Oncogene 27: 2263–2275. https://doi.org/10.1038/onc.2008.20
Ogg S., S. Paradis, S. Gottlieb, G. I. Patterson, L. Lee, *et al.*, 1997 The Fork head transcription factor DAF-16 transduces insulin-like metabolic and longevity signals in *C. elegans*. Nature 389: 994–999.
Osaki M., M. Oshimura, and H. Ito, 2004 PI3K-Akt pathway: Its functions and alterations in human cancer. Apoptosis 9: 667–676. https://doi.org/10.1023/B:APPT.0000045801.15585.dd
Ouellet J., S. Li, and R. Roy, 2008 Notch signalling is required for both dauer maintenance and recovery in *C. elegans*. Development 135: 2583–92. https://doi.org/10.1242/dev.012435
Page A. P., and I. L. Johnstone, 2007 The Cuticle. Wormbook.
Paradis S., and G. Ruvkun, 1998 *Caenorhabditis elegans* Akt / PKB transduces insulin receptor-like signals from AGE-1 PI3 kinase to the DAF-16 transcription factor. 2488–2498. https://doi.org/10.1101/gad.12.16.2488
Paradis S., M. Ailion, A. Toker, J. H. Thomas, and G. Ruvkun, 1999 A PDK1 homolog is necessary and sufficient to transduce AGE-1 PI3 kinase signals that regulate diapause in *Caenorhabditis elegans*. Genes Dev. 13: 1438–52. https://doi.org/10.1101/gad.13.11.1438
Patterson G. I., A. Koweek, A. Wong, Y. Liu, and G. Ruvkun, 1997 The DAF-3 Smad protein antagonizes TGF-beta-related receptor signaling in the *Caenorhabditis elegans* dauer pathway. Genes Dev. 11: 2679–90. https://doi.org/10.1101/gad.11.20.2679
Peden E. M., and M. M. Barr, 2005 The KLP-6 Kinesin Is Required for Male Mating Behaviors and Polycystin Localization in *Caenorhabditis elegans*. Curr. Biol. 15:

394–404. https://doi.org/10.1016/J.CUB.2004.12.073
Pener M. P., and S. J. Simpson, 2009 Locust Phase Polyphenism: An Update. Adv. In Insect Phys. 36: 1–272. https://doi.org/10.1016/S0065-2806(08)36001-9
Perkins L. A., E. M. Hedgecock, J. N. Thomson, and J. G. Culotti, 1986 Mutant sensory cilia in the nematode *Caenorhabditis elegans*. Dev. Biol. 117: 456–487. https://doi.org/10.1016/0012-1606(86)90314-3
Petit C., J. Levilliers, and J.-P. Hardelin, 2001 Molecular Genetics of Hearing Loss. Annu. Rev. Genet. 35: 589–645. https://doi.org/10.1146/annurev.genet.35.102401.091224
Politz S. M., M. Philipp, M. Estevez, P. J. O'Brien, and K. J. Chin, 1990 Genes that can be mutated to unmask hidden antigenic determinants in the cuticle of the nematode *Caenorhabditis elegans*. Proc. Natl. Acad. Sci. U. S. A. 87: 2901–2905. https://doi.org/10.1073/pnas.87.8.2901
Popham J. D., and D. J. M. Webster, 1979 Aspects of the fine structure of the dauer larva of the nematode *Caenorhabditis elegans*. Can. J. Zool. 57.
Popov V. I., L. S. Bocharova, and A. G. Bragin, 1992 Repeated changes of dendritic morphology in the hippocampus of ground squirrels in the course of hibernation. Neuroscience 48: 45–51.
Priess J. R., and D. I. Hirsh, 1986 *Caenorhabditis elegans* morphogenesis: The role of the cytoskeleton in elongation of the embryo. Dev. Biol. 117: 156–173. https://doi.org/10.1016/0012-1606(86)90358-1
Reitsma S., D. W. Slaaf, H. Vink, M. A. M. J. van Zandvoort, and M. G. A. oude Egbrink, 2007 The endothelial glycocalyx: composition, functions, and visualization. Pflugers Arch. 454: 345–59. https://doi.org/10.1007/s00424-007-0212-8
Ren P., C. S. Lim, R. Johnsen, P. S. Albert, D. Pilgrim, *et al.*, 1996 Control of *C. elegans* larval development by neuronal expression of a TGF-beta homolog. Science 274: 1389–91. https://doi.org/10.1126/science.274.5291.1389
Riddle D. L., M. M. Swanson, and P. S. Albert, 1981 Interacting genes in nematode dauer larva formation. Nature 290: 668–671. https://doi.org/10.1038/290668a0
Riddle D. L., and P. S. Albert, 1997 *Genetic and Environmental Regulation of Dauer Larva Development*. Cold Spring Harbor Laboratory Press.
Robertis E. M. De, 2008 Evo-Devo: Variations on Ancestral Themes. Cell 132: 185–195. https://doi.org/10.1016/J.CELL.2008.01.003
Saltiel A. R., and C. R. Kahn, 2001 Insulin signalling and the regulation of glucose and lipid metabolism. Nature 414: 799–806. https://doi.org/10.1038/414799a
Sapio M. R., M. A. Hilliard, M. Cermola, R. Favre, and P. Bazzicalupo, 2005 The Zona Pellucida domain containing proteins, CUT-1, CUT-3 and CUT-5, play essential roles in the development of the larval alae in *Caenorhabditis elegans*. Dev. Biol. 282: 231–245. https://doi.org/10.1016/j.ydbio.2005.03.011
Sawin E. R., R. Ranganathan, and H. R. Horvitz, 2000 *C. elegans* Locomotory Rate Is Modulated by the Environment through a Dopaminergic Pathway and by Experience through a Serotonergic Pathway. Neuron 26: 619–631. https://doi.org/10.1016/S0896-6273(00)81199-X
Schackwitz W. S., T. Inoue, and J. H. Thomas, 1996 Chemosensory Neurons Function in Parallel to Mediate a Pheromone Response in *C. elegans*. Neuron 17: 719–728. https://doi.org/10.1016/S0896-6273(00)80203-2

Schmitz C., P. Kinge, and H. Hutter, 2007 Axon guidance genes identified in a large-scale RNAi screen using the RNAi-hypersensitive *Caenorhabditis elegans* strain nre-1(hd20) lin-15b(hd126). Proc. Natl. Acad. Sci. U. S. A. 104: 834–9. https://doi.org/10.1073/pnas.0510527104

Schroeder N. E., R. J. Androwski, A. Rashid, H. Lee, J. Lee, *et al.*, 2013 Dauer-specific dendrite arborization in *C. elegans* is regulated by KPC-1/furin. Curr. Biol. 23. https://doi.org/10.1016/j.cub.2013.06.058

Schroeder N. E., and K. M. Flatt, 2014 In vivo imaging of Dauer-specific neuronal remodeling in *C. elegans*. J. Vis. Exp. e51834. https://doi.org/10.3791/51834

Schultz J., F. Milpetz, P. Bork, and C. P. Ponting, 1998 SMART, a simple modular architecture research tool: Identification of signaling domains. Proc. Natl. Acad. Sci. 95: 5857–5864. https://doi.org/10.1073/pnas.95.11.5857

Sebastiano M., F. Lassandro, and P. Bazzicalupo, 1991 cut-1 a *Caenorhabditis elegans* gene coding for a dauer-specific noncollagenous component of the cuticle. Dev. Biol. 146: 519–530. https://doi.org/10.1016/0012-1606(91)90253-y

Simpson S. J., G. A. Sword, and N. Lo, 2011 Polyphenism in Insects. Curr. Biol. 21: R738–R749. https://doi.org/10.1016/J.CUB.2011.06.006

Singh R. N., and J. E. Sulston, 1978 Some Observations On Moulting in *Caenorhabditis elegans*. Nematologica 24: 63–71.

Sinha M., Y. C. Jang, J. Oh, D. Khong, E. Y. Wu, *et al.*, 2014 Restoring systemic GDF11 levels reverses age-related dysfunction in mouse skeletal muscle. Science 344: 649–52. https://doi.org/10.1126/science.1251152

Smith S. C., X. Zhang, X. Zhang, P. Gross, T. Starosta, *et al.*, 2015 GDF11 does not rescue aging-related pathological hypertrophy. Circ. Res. 117: 926–32. https://doi.org/10.1161/CIRCRESAHA.115.307527

Snyder M., W. Niu, and Z. J. Lu, 2011 Identification of Transcription Factor Binding Regions

Starich T. A., R. K. Herman, C. K. Kari, W.-H. Yeh, W. S. Schackwitz, *et al.*, Mutations Affecting the Chemosensory Neurons of *Caenorhabditis elegans*

Sulston J. E., and H. R. Horvitz, 1977 Post-embryonic cell lineages of the nematode, *Caenorhabditis elegans*. Dev. Biol. 56: 110–156. https://doi.org/10.1016/0012-1606(77)90158-0

Sulston J. E., E. Schierenberg, J. G. White, and J. N. Thomson, 1983 The embryonic cell lineage of the nematode *Caenorhabditis elegans*. Dev. Biol. 100: 64–119. https://doi.org/10.1016/0012-1606(83)90201-4

Takagi A., S. Kume, M. Kondo, J. Nakazawa, M. Chin-Kanasaki, *et al.*, 2016 Mammalian autophagy is essential for hepatic and renal ketogenesis during starvation. Sci. Rep. 6: 18944. https://doi.org/10.1038/srep18944

Tatar M., A. Kopelman, D. Epstein, M. P. Tu, C. M. Yin, *et al.*, 2001 A Mutant Drosophila Insulin Receptor Homolog That Extends Life-Span and Impairs Neuroendocrine Function. Science (80-.). 292: 107–110. https://doi.org/10.1126/science.1057987

Thomas J. H., D. A. Birnby, and J. J. Vowels, 1993 Evidence for parallel processing of sensory information controlling dauer formation in *Caenorhabditis elegans*. Genetics 134: 1105–17.

Vidal-Gadea A., K. Ward, C. Beron, N. Ghorashian, S. Gokce, *et al.*, 2015

Magnetosensitive neurons mediate geomagnetic orientation in *Caenorhabditis elegans*. Elife 4. https://doi.org/10.7554/eLife.07493
Vowels J. J., and J. H. Thomas, 1992 Genetic analysis of chemosensory control of dauer formation in *Caenorhabditis elegans*. Genetics 130: 105–123.
Vuong-Brender T. T. K., S. K. Suman, and M. Labouesse, 2017 The apical ECM preserves embryonic integrity and distributes mechanical stress during morphogenesis. Development dev.150383. https://doi.org/10.1242/dev.150383
Wang J. G., G. S. Nakhuda, M. M. Guarnaccia, M. V. Sauer, and R. A. Lobo, 2007 Müllerian inhibiting substance and disrupted folliculogenesis in polycystic ovary syndrome. Am. J. Obstet. Gynecol. 196: 77.e1-77.e5. https://doi.org/10.1016/J.AJOG.2006.07.046
Ward S., N. Thomson, J. G. White, and S. Brenner, 1975 Electron microscopical reconstruction of the anterior sensory anatomy of the nematode*Caenorhabditis elegans*. J. Comp. Neurol. 160: 313–337. https://doi.org/10.1002/cne.901600305
Wassarman P. M., 1987 The biology and chemistry of fertilization. Science 235: 553–60. https://doi.org/10.1126/science.3027891
White J. G., E. Southgate, J. N. Thomson, and S. Brenner, 1986 The structure of the nervous system of the nematode *Caenorhabditis elegans*. Philos. Trans. R. Soc. Lond. B. Biol. Sci. 314: 1-340White J. G., E. Southgate, J. N. Thomson, and. https://doi.org/10.1098/RSTB.1986.0056
White J. Q., and E. M. Jorgensen, 2012 Sensation in a single neuron pair represses male behavior in hermaphrodites. Neuron 75: 593–600. https://doi.org/10.1016/j.neuron.2012.03.044
Williams D. W., and J. W. Truman, 2004 Mechanisms of dendritic elaboration of sensory neurons in Drosophila: insights from in vivo time lapse. J. Neurosci. 24: 1541–50. https://doi.org/10.1523/JNEUROSCI.4521-03.2004
Wolkow C. A., K. D. Kimura, M. S. Lee, and G. Ruvkun, 2000 Regulation of *C. elegans* life-span by insulinlike signaling in the nervous system. Science 290: 147–50. https://doi.org/10.1126/science.290.5489.147
Wolkow C. A., and D. H. Hall, 2011 The Dauer Cuticle. WormBook.
Wolkow C. A., and D. H. Hall, 2013 The Dauer Muscle System. WormBook.
Wright K. A., and J. N. Thomson, 1981 The buccal capsule of *C. elegans* (Nematoda: Rhabditoidea): An ultrastructural study. Can. J. Zool. 59: 1952–1961. https://doi.org/doi:10.1139/z81-266
Wu G. Y., and H. T. Cline, 2003 Time-lapse in vivo imaging of the morphological development of Xenopus optic tectal interneurons. J. Comp. Neurol. 459: 392–406. https://doi.org/10.1002/cne.10618
Wu M. Y., and C. S. Hill, 2009 TGF-β Superfamily Signaling in Embryonic Development and Homeostasis. Dev. Cell 16: 329–343. https://doi.org/10.1016/J.DEVCEL.2009.02.012
Yan B., Z.-Z. Zhang, L.-Y. Huang, H.-L. Shen, and Z.-G. Han, 2012 OIT3 deficiency impairs uric acid reabsorption in renal tubule. FEBS Lett. 586: 760–765. https://doi.org/10.1016/j.febslet.2012.01.038
Yochem J., T. Gu, and M. Han, 1998 *A New Marker for Mosaic Analysis in Caenorhabditis elegans Indicates a Fusion Between hyp6 and hyp7, Two Major Components of the Hypodermis*.

Zaucke F., J. M. Boehnlein, S. Steffens, R. S. Polishchuk, L. Rampoldi, *et al.*, 2010 Uromodulin is expressed in renal primary cilia and UMOD mutations result in decreased ciliary uromodulin expression. Hum. Mol. Genet. 19: 1985–97. https://doi.org/10.1093/hmg/ddq077

Zhang Y., J. M. Foster, L. S. Nelson, D. Ma, and C. K. S. Carlow, 2005 The chitin synthase genes chs-1 and chs-2 are essential for *C. elegans* development and responsible for chitin deposition in the eggshell and pharynx, respectively. Dev. Biol. 285: 330–339. https://doi.org/10.1016/J.YDBIO.2005.06.037

Zuckerman I., B. M. Kahane, and S. Himmelhoch, 1979 *Caenorhabditis briggsae* and C . elegans : Surface Partial Characterization of Cuticle Surface Carbohydrates. 419–424.

APPENDIX A: SUPPLEMENTAL TABLE

Supplemental Table: Primers and plasmids used for this study		
PLASMID	**DESCRIPTION**	**PRIMERS (5'-3')**
pKF1	*cut-5p::DEX-1*	pMH7_Left - ATGCGCAATAGGCATGCC
		pmH7_Right - GTCGACCTGCAGGCATG
		cut-5p_Left - TTGCATGCCTGCAGGTCGAaagacgagccaattgg
		cut-5p_Right - GAAGGGCATGCCTATTGCGCATgaacaaaatctgga
pKF3	*dex-1p(5.7kbΔ)::gfp*	IRS_Left - CATTTAGCTTTCTCCGTC
		IRS_Right - ATGACAACGAAAAACCAC
pKF5	*cut-6p::DEX-1*	pMH7_Left - ATGCGCAATAGGCATGCCC
		pMH7_Right - GTCGACCTGCAGGCATGC
		cut-6p_Left - CCTGCAGGTCGACcccgaccaattgttatcagtaggag
		cut-6p_Right - GCATGVVTATTGCGCATctcatttcgcagaagaggcga
pJC15	*dex-1p::DEX-1(ecto)::sfGFP*	see Cohen *et al.*, 2019
pJC24	*dex-1p::sfGFP::DEX-1*	see Cohen *et al.*, 2019
pMH7	*dex-1p::DEX-1*	see Heiman and Shaham, 2009
pMH8	*pha-4p::DEX-1*	see Heiman and Shaham, 2009
pMH111	*dex-1p(5.7kb)::GFP*	a gift of Dr. Maxwell Heiman
pMH125	*dex-1p(2.1kb)::GFP*	a gift of Dr. Maxwell Heiman
pTG96_2	*sur-5p::GFP*	a gift of Dr. Trent Gu (Gu *et al.* 1998)